

N73-11999

NASA CONTRACTOR  
REPORT



NASA CR-2157

NASA CR-2157

CALCULATIVE TECHNIQUES FOR  
TRANSONIC FLOWS ABOUT CERTAIN CLASSES  
OF WING-BODY COMBINATIONS - PHASE II

*by Stephen S. Stahara and John R. Spreiter*

*Prepared by*  
NIELSEN ENGINEERING & RESEARCH, INC.  
Mountain View, Calif. 94040  
*for Ames Research Center*

1. Report No. <b>NASA CR-2157</b>		2. Government Accession No.		3. Recipient's Catalog No.	
4. Title and Subtitle Calculative Techniques for Transonic Flows About Certain Classes of Wing-Body Combinations - Phase II				5. Report Date <b>December 1972</b>	
				6. Performing Organization Code	
7. Author(s)  Stephen S. Stahara and John R. Spreiter				8. Performing Organization Report No.	
9. Performing Organization Name and Address  Nielsen Engineering and Research, Inc. 850 Maude Avenue Mountain View, CA 94040				10. Work Unit No.	
				11. Contract or Grant No.  NAS 2-6259	
12. Sponsoring Agency Name and Address  National Aeronautics & Space Administration Washington, D.C. 20546				13. Type of Report and Period Covered  Contractor Report	
				14. Sponsoring Agency Code	
15. Supplementary Notes					
16. Abstract  Theoretical analysis and associated computer programs were developed for predicting properties of transonic flows about certain classes of wing-body combinations. The procedures used are based on the transonic equivalence rule and employ either an arbitrarily-specified solution or the local linearization method for determining the nonlifting transonic flow about the equivalent body. The class of wind planform shapes include wings having sweptback trailing edges and finite tip chord. Theoretical results are presented for surface and flow-field pressure distributions for both nonlifting and lifting situations at Mach number one.					
17. Key Words (Suggested by Author(s))  Transonic Flow Aerodynamics Wing-Body Combinations Transonic Equivalence Rule Local Linearization			18. Distribution Statement  UNCLASSIFIED-UNLIMITED		
19. Security Classif. (of this report)  UNCLASSIFIED		20. Security Classif. (of this page)  UNCLASSIFIED		21. No. of Pages  114	22. Price*  3.00

\* For sale by the National Technical Information Service, Springfield, Virginia 22151

## CALCULATIVE TECHNIQUES FOR TRANSONIC FLOWS

### ABOUT CERTAIN CLASSES OF WING-BODY COMBINATIONS - PHASE II

By Stephen S. Stahara and John R. Spreiter\*  
Nielsen Engineering & Research, Inc.

#### SUMMARY

Theoretical analysis and the development of associated computer programs were carried out for the purpose of developing computational techniques for predicting properties of transonic flows about certain classes of wing-body combinations. The procedures used are based on the transonic equivalence rule and employ either an arbitrarily-specified solution or the local linearization method for determining the nonlifting transonic flow about the equivalent body. Theoretical results obtained by using the local linearization method are presented for surface and flow-field pressure distributions for certain members of the general classes of configurations studied, for both nonlifting and lifting situations, at  $M_\infty = 1$ .

The computational programs developed under this report are documented and presented in a general user's manual included as part of the report.

#### INTRODUCTION

Stimulated by the need for accurate prediction of transonic flows about realistic aircraft configurations, recent research is producing significant advances in the ability to predict theoretically both two and three-dimensional transonic flows about a wide variety of aerodynamic shapes. While current emphasis seems to be placed on the development of numerical techniques (refs. 1, 2, 3, 4, 5), it has become clear that, although significant accuracy limitations need not exist for advanced computer programs, these techniques do have cost limitations with regard to both accuracy and the use of alternate methods. Consequently, in

---

\*Professor, Departments of Applied Mechanics and Aeronautics and Astronautics, Stanford University, Stanford, California. (Consultant at Nielsen Engineering & Research, Inc.)

order to enhance these computational efforts, the parallel development of proven analytical and analytic/numeric methods to provide accurate first approximations, for example, in the systematic study of a large number of configurations, is clearly warranted.

Previous investigations by Nielsen Engineering & Research, Inc. (NEAR) in reference 6, where the local linearization method and the transonic equivalence rule were applied to predict surface and flow-field properties of several general classes of axisymmetric and nonaxisymmetric bodies for both lifting and nonlifting situations, and in reference 7, where those results were extended to include several classes of wing-body combinations, have demonstrated the effectiveness of such a combined approach.

While the ultimate goal of the present investigation is to develop computational techniques for the prediction of the flow field, pressure distribution, and aerodynamic characteristics of three-dimensional, lifting, wing-body combinations, the purposes of this study are to extend the results of reference 7 to include a more general class of wing planform shapes, specifically, wings having (1) sweptback trailing edges, and (2) finite tip chords. In addition, the computer programs developed in reference 7 were to be further enhanced with regard to minimization of computational time and applicability to wider classes of equivalent body shapes and equivalent body transonic solutions.

#### LIST OF SYMBOLS

a	major axis of elliptic cross section of indented body
$a_{sb}$	major axis of elliptic cross section of smooth (non-indented) body
AR	aspect ratio
b	minor axis of elliptic cross section of indented body
c	equal to $\sqrt{a^2 - b^2}$
$c_w$	wing chord
C	Euler's constant

$C_{D_{eb}}$	drag coefficient of equivalent body of revolution, $D_{eb}/q_{\infty}S_m$ eq. (22)
$C_{D_t}$	total drag coefficient, $D_t/q_{\infty}S_m$
$C_{D_{\alpha=0}}$	drag coefficient at zero lift, $D_{\alpha=0}/q_{\infty}S_m$
$C_L$	lift coefficient, $L/q_{\infty}S_m$
$C_p$	pressure coefficient, $(p - p_{\infty})/\frac{1}{2} \rho_{\infty}U_{\infty}^2$
$C_{P_{eb}}$	pressure coefficient due to equivalent body of revolution
$C_m$	pitching moment coefficient about nose, $M_y/q_{\infty}S_m l$ (positive nose-up)
$C_{tip}$	wing tip chord
$C_{R_t}$	wing root chord
$D$	maximum diameter of equivalent body of revolution
$D_{eb}$	drag of equivalent body of revolution
$D_i$	drag due to lift
$D_t$	total drag
$D_{\alpha=0}$	total drag at zero lift
$k$	equal to $M_{\infty}^2(\gamma + 1)/U_{\infty}$
$K$	complete elliptic integral of first kind
$l$	complete body length
$L$	lift
$m$	exponent describing wing ordinates, eqs. (8), (9)
$M_{cr,l}$	lower critical Mach number on equivalent body of revolution
$M_{cr,u}$	upper critical Mach number on equivalent body of revolution
$M_y$	pitching moment about nose, positive nose-up

$M_\infty$	free-stream Mach number
$n$	exponent describing equivalent body ordinates and related to location of point of maximum thickness, eqs. (11), (12), (13), (14)
$P_\infty$	free-stream pressure
$q_1, q_2, q_3$ $q_4, q_5, q_6$	quantities defined by eqs. (55), (56), (57)
$q_\infty$	free-stream dynamic pressure
$r$	radial distance in crossflow plane, $\sqrt{y^2 + z^2}$
$R_b$	radius of indented body of revolution
$R_{eb}$	radius of equivalent body of revolution
$R_1$	radius of circular body in transformed ( $\sigma_1$ ) plane, eq. (33)
$s$	semispan of wing which, depending on axial location, represents either leading ( $s = s_\ell$ ) or trailing ( $s = s_t$ ) edge
$s_\ell$	semispan of wing leading edge
$s_t$	semispan of wing trailing edge
$s_1$	semispan of wing in transformed ( $\sigma_1$ ) plane, eq. (34)
$s_{1\ell}$	semispan of wing leading edge in transformed ( $\sigma_1$ ) plane
$s_{1t}$	semispan of wing trailing edge in transformed ( $\sigma_1$ ) plane
$S_b$	area distribution of indented body of revolution
$S_{eb}$	area distribution of equivalent body of revolution
$S_m$	maximum area distribution of equivalent body of revolution, $\pi D^2/4$
$TR$	wing planform taper ratio, $C_{tip}/C_{R_t}$
$u, v, w$	perturbation velocity components parallel to the $x, y, z$ axes, respectively

$u_B, v_B, w_B$	perturbation velocity components associated with solution for transonic flow about equivalent body of revolution
$u_{2,B}, v_{2,B}, w_{2,B}$	perturbation velocity components associated with two-dimensional incompressible solution of expansion or contraction of equivalent cross section in crossflow plane
$u_{2,t}, v_{2,t}, w_{2,t}$	perturbation velocity components associated with two-dimensional incompressible solution of expanding or contracting cross section in crossflow plane
$u_{2,\alpha}, v_{2,\alpha}, w_{2,\alpha}$	perturbation velocity components associated with two-dimensional incompressible solution of translating cross section in crossflow plane
$U_\infty$	free-stream velocity
$w_{2,t}$	complex potential describing two-dimensional incompressible flow about expanding or contracting cross section in crossflow plane
$w_{2,\alpha}$	complex potential describing two-dimensional incompressible flow about translating cross section in crossflow plane
$x, y, z$	body-fixed Cartesian coordinate system with $x$ axis direction rearward and aligned with longitudinal axis of body, $y$ axis directed to the right facing forward, and $z$ axis directed vertically upward
$x_s$	location of point closest to origin where $S''_{eb}(x) = 0$
$x_b$	axial location of body base
$x_{rle}$	axial location of wing leading edge root chord
$x_{rle_1}$	axial location of point where wing leading edge pierces body surface
$x_{rte}$	axial location of wing trailing-edge root chord
$x_{rte_1}$	axial location of point where wing trailing edge pierces body surface
$x_{sm_1}$	axial location of wing tip chord leading edge
$x_{sm_2}$	axial location of wing tip chord trailing edge
$\bar{x}$	axial distance from wing leading edge

$\bar{y}$	lateral distance from wing leading edge
$z_w$	wing ordinates, eqs. (8), (9)
$\alpha$	angle of attack
$\beta_{le}$	wing leading-edge sweep angle
$\beta_{te}$	wing trailing-edge sweep angle
$\gamma$	ratio of specific heats
$\theta$	polar angle in crossflow plane
$\lambda$	ratio of major to minor axes of elliptic cross section, a/b
$\xi, \xi_1$	dummy variables
$\rho_\infty$	free-stream density
$\sigma$	complex variable in crossflow plane, $y + iz$
$\sigma_1$	complex variable in transformed crossflow plane, $Y_1 + iz_1$
$\tau_{eb}$	thickness ratio of equivalent body of revolution, $D/\ell$
$\tau_w$	thickness-to-chord ratio of wing profile, eq. (10)
$\phi$	perturbation velocity potential
$\phi_B$	perturbation velocity potential associated with transonic flow about equivalent body of revolution
$\phi_2$	perturbation velocity potential associated with two-dimensional incompressible solutions to translation and growth of cross section in crossflow plane
$\phi_{2,B}$	perturbation velocity potential associated with two-dimensional incompressible solution for expansion or contraction of equivalent cross section in crossflow plane
$\phi_{2,t}$	perturbation velocity potential associated with two-dimensional incompressible solution for expansion or contraction of cross section in crossflow plane
$\phi_{2,\alpha}$	perturbation velocity potential associated with two-dimensional incompressible solution for translation of cross section in crossflow plane



## ANALYSIS

### General Considerations

Because the current work is an extension of that of reference 7, the basic theory and equations used are discussed in depth in that reference and their derivation will not be repeated here. For convenience, however, those points relevant to the present work will be outlined.

The coordinate system used for all of the three-dimensional flows considered herein is a body-fixed Cartesian system centered at the body nose with the  $x$  axis directed rearward and aligned with the longitudinal axis of the body, the  $y$  axis directed to the right, facing forward, and the  $z$  axis directed vertically upward, as shown in figure 1. For lifting situations, the free-stream direction is taken to be inclined at any arbitrary small angle  $\alpha$  to the  $x$  axis and confined to the  $x$ - $z$  plane so that there is no sideslip. The governing partial differential equation for the perturbation potential  $\phi$  is given by

$$(1 - M_\infty^2)\phi_{xx} + \phi_{yy} + \phi_{zz} = \frac{M_\infty^2(\gamma + 1)}{U_\infty} \phi_x \phi_{xx} \quad (1)$$

where  $M_\infty$  is the free-stream Mach number,  $\gamma$  the ratio of specific heats, and  $U_\infty$  the free-stream velocity. The pressure coefficient  $C_p$  in the above reference frame is given by

$$C_p = -\frac{2}{U_\infty} (\phi_x + \alpha\phi_z) - \frac{1}{U_\infty^2} (\phi_y^2 + \phi_z^2) \quad (2)$$

The transonic equivalence rule enables the perturbation potential  $\phi$  to be expressed in the form

$$\phi = \phi_{2,\alpha} + \phi_{2,t} - \phi_{2,B} + \phi_B \quad (3)$$

where each of the individual components has the meaning indicated in figure 1. Since  $\phi_{2,\alpha}$ ,  $\phi_{2,t}$ , and  $\phi_{2,B}$  satisfy the two dimensional incompressible Laplace equation

$$(\phi_{2,i})_{yy} + (\phi_{2,i})_{zz} = 0 \quad (4)$$

(where the subscript  $i$  depends upon the particular potential in question), they are independent of Mach number. Hence, the only portion of the solution dependent upon  $M_\infty$  is  $\phi_B$  and this term represents the solution to the full transonic equation (1) for the nonlifting flow about the equivalent body of revolution. Because the equivalence rule places no essential restrictions on the methods of calculating  $\phi_B$ , its solution may be determined in a variety of ways. For example, it can be given by an exact numerical solution, by experimental data, by an approximate analytic solution, or by a combined analytic/numeric solution such as the local linearization method. One of the tasks of the present work is to extend the applicability of the computer programs developed in reference 7 to include general, arbitrarily-specified solutions for  $\phi_B$ , and the method of doing this is detailed in the user's manual. If the local linearization method is used to determine  $\phi_B$ , or more conveniently,  $u_B = (\phi_B)_x$ , then one of the following set of three first-order nonlinear differential equations must be integrated according to whether  $M_\infty \approx 1$ ,  $M_\infty < M_{cr,l}$ , or  $M_{cr,u} < M_\infty$ , where  $M_{cr,l}$ ,  $M_{cr,u}$  are the lower and upper critical Mach numbers, respectively.

Thus, for accelerating flows with  $M_\infty \approx 1$

$$\frac{d}{dx} \left( \frac{u_B}{U_\infty} \right) = \frac{S'_{eb}(x) S''_{eb}(x)}{4\pi S_{eb}(x)} + \exp \left\{ \frac{4\pi}{S''_{eb}(x)} \left[ \frac{u_B}{U_\infty} + \frac{M_\infty^2 - 1}{M_\infty^2(\gamma + 1)} \right. \right. \\ \left. \left. - \frac{S''_{eb}(x)}{4\pi} \ln \frac{M_\infty^2(\gamma + 1) S_{eb}(x) e^C}{4\pi x} - \frac{1}{4\pi} \int_0^x \frac{S''_{eb}(x) - S''_{eb}(\xi)}{x - \xi} d\xi \right] \right\} \quad (5)$$

for purely subsonic flows ( $M_\infty < M_{cr,l}$ )

$$\frac{d}{dx} \left( \frac{u_B}{U_\infty} \right) = \frac{S_{eb}'''(x)}{4\pi} \ln (1 - M_\infty^2 - k u_B) + \frac{d}{dx} \left[ \frac{S_{eb}''(x)}{4\pi} \ln \frac{S_{eb}(x)}{4\pi x(\ell - x)} + \frac{1}{4\pi} \int_0^\ell \frac{S_{eb}''(x) - S_{eb}''(\xi)}{|x - \xi|} d\xi \right] \quad (6)$$

and for purely supersonic flows ( $M_{cr,u} < M_\infty$ )

$$\frac{d}{dx} \left( \frac{u_B}{U_\infty} \right) = \frac{S_{eb}'''(x)}{4\pi} \ln (M_\infty^2 - 1 + k u_B) + \frac{d}{dx} \left[ \frac{S_{eb}''(x)}{4\pi} \ln \frac{S_{eb}(x)}{4\pi x^2} + \frac{1}{2\pi} \int_0^x \frac{S_{eb}''(x) - S_{eb}''(\xi)}{x - \xi} d\xi \right] \quad (7)$$

where  $C$  in equation (5) is Euler's constant  $\approx 0.577$ ,  $k$  in equations (6) and (7) is equal to  $M_\infty^2(\gamma + 1)/U_\infty$ ,  $S_{eb}(x)$  represents the area distribution of the equivalent body, and primes indicate differentiation with respect to the appropriate variable. These differential equations have been programmed for computation in reference 6 where details regarding starting conditions, numerical techniques, accuracy, limitations, etc. are provided.

## Wing and Body Geometry

The classes of wing-body configurations examined in reference 7 and in this study are composed of finite thickness wing and either circular or elliptic cross-sectional bodies in which the bodies are area-rule indented along the wing-body junction in such a manner that the total cross-sectional area distribution (body plus wing) remains identical to that of a smooth body having a certain specified profile. The general class of wings considered have symmetric planforms consisting of straight leading and trailing edges, swept at arbitrary angles  $\beta_{le}$  and  $\beta_{te}$  respectively, to the  $y$  axis. In reference 7, the planform shapes were restricted to wings having either straight or sweptforward trailing edges and zero taper ratio. This work extends that class to wings with sweptback trailing edges and taper ratio between zero and one, as shown in figures 2 and 3. The wing profiles are represented by expressions of the form

$$\frac{z_w}{c_w} = \frac{\tau_w^{m(m/m-1)}}{2(m-1)} \left( \frac{\bar{x}}{c_w} - \left( \frac{\bar{x}}{c_w} \right)^m \right) \quad (8)$$

or

$$\frac{z_w}{c_w} = \frac{\tau_w^{m(m/m-1)}}{2(m-1)} \left( 1 - \frac{\bar{x}}{c_w} - \left( 1 - \frac{\bar{x}}{c_w} \right)^m \right) \quad (9)$$

where  $c_w$  is the local chord,  $\bar{x}$  the distance from the leading edge,  $m$  is a constant  $\geq 2$ , and  $\tau_w$  is the wing thickness-to-chord ratio. In addition, the wings are assumed to maintain a constant thickness-to-chord ratio across the span, with the consequence that the wing profiles at all spanwise locations are geometrically similar. Thus,

$$\frac{\tau_w}{2} = \frac{(z_w(x,y))_{\max}}{c_w(y)} = \frac{(z_w(x,0))_{\max}}{C_{R_t}} \quad (10)$$

where  $C_{R_t}$  is the wing root chord.

Two categories of body shape are considered. Figure 2(a) and (b), illustrates two members of the first category which have indented bodies that are circular in cross section, while figure 3(a) and (b) illustrates two members of the second category which have indented bodies that are elliptic in cross section and that maintain a constant ratio  $\lambda(=a/b)$  of semimajor to semiminor axis along the entire body length. In reference 7, the profiles of the equivalent bodies of revolution of the wing-circular body combinations are described by the expressions

$$\frac{R_{eb}}{\ell} = \frac{\tau_{eb} n^{n/(n-1)}}{2(n-1)} \left[ \frac{x}{\ell} - \left( \frac{x}{\ell} \right)^n \right] \quad (11)$$

where the exponent  $n$  is given in terms of the location of maximum radius by

$$\left( \frac{x}{\ell} \right)_{R_{max}} = \left( \frac{1}{n} \right)^{1/(n-1)} \quad (12)$$

or

$$\frac{R_{eb}}{\ell} = \frac{\tau_{eb} n^{n/(n-1)}}{2(n-1)} \left[ 1 - \frac{x}{\ell} - \left( 1 - \frac{x}{\ell} \right)^n \right] \quad (13)$$

where

$$\left( \frac{x}{\ell} \right)_{R_{max}} = 1 - \left( \frac{1}{n} \right)^{1/(n-1)} \quad (14)$$

while the equivalent bodies of the wing-elliptic body combinations are parabolic-arc bodies, i.e. equations (11) or (13) with  $n = 2$ . This work extends the class of equivalent body profiles for both the circular and elliptic body shapes to include arbitrarily specified functions subject to certain closure and continuity restrictions on the derivatives that are discussed in the appropriate section of the included user's manual.

Straight or Sweptforward Trailing  
Edge Planforms

Circular bodies. - For finite thickness wing-circular body combinations having wings with finite tip chords and trailing edges that are either straight or sweptforward, the complex potentials,  $W_{2,\alpha}$ ,  $W_{2,t}$ , and  $W_{2,B}$  can be readily determined from the work of reference 7.

$$W_{2,\alpha} = -iU_\infty\alpha \left\{ \left[ \left( \sigma + \frac{R_b^2}{\sigma} \right)^2 - \left( s + \frac{R_b^2}{s} \right)^2 \right]^{1/2} - \sigma \right\} \quad (15)$$

$$\begin{aligned} \frac{W_{2,t}}{U_\infty} &= \frac{1}{\pi} \int_{R_b}^s \frac{dZ_w(x,\xi)}{dx} \ln \left[ \frac{(\sigma^2 - \xi^2) \left( \sigma^2 - \frac{R_b^4}{\xi^2} \right)}{\sigma^4} \right] d\xi \\ &+ \frac{1}{2\pi} \left[ S'_{eb}(x) + 4 Z_w(x, R_b) \frac{dR_b}{dx} \right] \ln \sigma \end{aligned} \quad (16)$$

$$\frac{W_{2,B}}{U_\infty} = \frac{S'_{eb}(x)}{2\pi} \ln \sigma \quad (17)$$

where  $\sigma$  is the complex variable in the crossflow plane

$$\sigma = y + iz \quad (18)$$

$R_b$  is the indented body radius,  $s$  - depending upon axial location - represents the local wing semispan of either the leading ( $s = s_t$ ) or trailing ( $s = s_\tau$ ) edge, and  $Z_w$  represents the wing ordinates. The velocity components associated with these potentials can be found by substituting those expressions into the general formulas:

$$u_{2,i} = \frac{\partial \phi_{2,i}}{\partial x} = \text{R.P.} \frac{\partial W_{2,i}}{\partial x} \quad (19)$$

$$(v - w)_{2,i} = (\phi_y - i\phi_z)_{2,i} = \frac{dW_{2,i}}{d\sigma} \quad (20)$$

where the subscript  $i$  depends upon the particular potential in question and R.P. signifies the real part of a complex quantity.

These operations have been carried out and the resulting expressions, which are quite lengthy, are given in reference 7. It should be noted that, in the evaluation of the velocity components associated with the thickness problem ( $W_{2,t}$ ), different sets of expressions are necessary depending on whether the point of interest is (1) at a general location, (2) on the wing surface, or (3) at the wing-body junction. These distinctions are required in order to account properly for the Cauchy singularities which appear in several of the integrals associated with the thickness velocity components. No such distinctions are required for the lifting ( $W_{2,\alpha}$ ) or equivalent thickness ( $W_{2,B}$ ) problems.

Because of the symmetry of the class of wing-body combinations considered, nonlifting flows will produce no lateral forces or moments. The only force will be the longitudinal drag force which can be determined through the general formula,

$$D_{\alpha=0} = D_{eb} - \frac{\rho_{\infty}}{2} \left( \oint_{C_t} \phi_{2,t} \frac{\partial \phi_{2,t}}{\partial n} d\sigma_t - \oint_{C_B} \phi_{2,B} \frac{\partial \phi_{2,B}}{\partial n} d\sigma_B \right) \quad (21)$$

where  $D_{eb}$  represents the drag of the equivalent body while the other two terms involve the line integral along their respective contours ( $C_t$  is the contour defined by the cross section of the wing-body combination while  $C_B$  is the contour about the equivalent area circular cylinder) of the product of the appropriate velocity potential and the normal velocity associated with it. We note that the drag indicated by equation (21) refers to the inviscid drag of the configuration minus the base pressure drag. As pointed out in reference 8, there exist many shapes of aerodynamic interest for which the two integrals involved cancel. In particular, we note that if the equivalent body and the original body have the same shape and surface slope at the base, as is the case for configurations studied here, then since both integrals are carried out over the same contour along which  $\phi_{2,t} = \phi_{2,B}$  and  $\partial \phi_{2,t} / \partial n = \partial \phi_{2,B} / \partial n$ , the integrals cancel and  $D_{\alpha=0} = D_{eb}$ . If we define a drag coefficient  $C_D$  based upon the maximum cross-sectional area of the equivalent body,  $S_m$ , then

$$C_{D_{\alpha=0}} = C_{D_{eb}} = \frac{D_{eb}}{\frac{\rho_{\infty}}{2} U_{\infty}^2 S_m} = \frac{1}{S_m} \int_0^{X_b} C_{P_{eb}} S'_{eb}(x) dx \quad (22)$$

where  $X_b$  is the axial location of the body base and  $C_{P_{eb}}$  is the pressure coefficient on the surface of the nonlifting equivalent body and is equal to

$$C_{P_{eb}} = -2 \frac{u_B}{U_{\infty}} - \left( \frac{dR_{eb}(x)}{dx} \right)^2 \quad (23)$$

For the lifting situation, an exact analysis of the aerodynamic forces and moments, even within the framework of small disturbance theory, is quite formidable. The general formulas for determining the coefficients of lift, pitching moment, and drag are given by

$$C_L = \frac{L}{S_m q_{\infty}} = -\frac{2}{U_{\infty}} \oint_C \phi_{2,\alpha} d\sigma_C \quad (24)$$

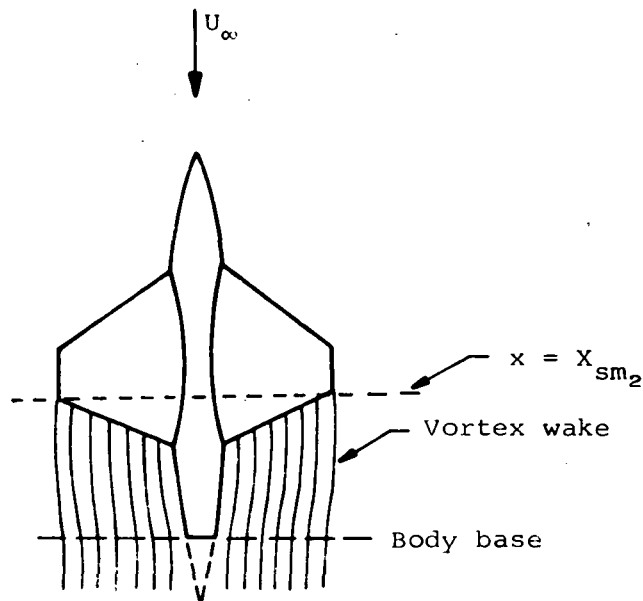
$$C_m = \frac{M_y}{q_{\infty} \cdot S_m \cdot l} = \frac{-1}{q_{\infty} \cdot S_m \cdot l} \int_0^x \xi \frac{dL(\xi)}{d\xi} d\xi \quad (25)$$

$$C_{D_t} = \frac{D_t}{q_{\infty} S_m} = \frac{D_{eb}}{q_{\infty} S_m} - \frac{1}{S_m U_{\infty}^2} \left( \oint_C \phi_{2,\alpha} \frac{\partial \phi_{2,\alpha}}{\partial n} d\sigma_C + \oint_C \phi_{2,t} \frac{\partial \phi_{2,t}}{\partial n} d\sigma_t - \oint_B \phi_{2,B} \frac{\partial \phi_{2,B}}{\partial n} d\sigma_B \right) \quad (26)$$

where now the contour  $C$ , while still taken at the base of the body, must now account for the vortex wake which springs from the wing trailing edge and, as before, the drag given by equation (26) represents the inviscid drag minus the base pressure drag. Because the vortex lines near the body surface must follow the streamlines of the flow around the body, the vortex wake will not proceed parallel to the  $x$  axis,



in general, as it does in many simpler cases considered in slender body theory; but will move away from or toward the body axis to follow the lateral expansion or contraction of the flow field near the body as shown below.



The resulting flow at the body base is influenced by the wake and, consequently, is no longer independent of the flow at cross sections preceding it. The solution of problems of this type is discussed briefly in reference 9. In general, they are quite difficult to solve and since they are by no means unique to transonic slender body flows, their exact solution is clearly beyond the scope of the present investigation. Because the analysis presented here, however, remains valid up to the axial location of the wing tip trailing edge  $x = X_{sm2}$  (i.e. as long as the edge of the wing remains a leading edge) an estimate can be made of these quantities by making the assumption that beyond that point the vortex sheet remains parallel to the  $x$  axis and does not vary with  $x$ . With this premise in mind, we can proceed to evaluate equations (24), (25), and (26). Carrying through the indicated operations (see ref. 7 for details), we arrive at the result that the coefficients of lift, drag, and pitching moment are given by

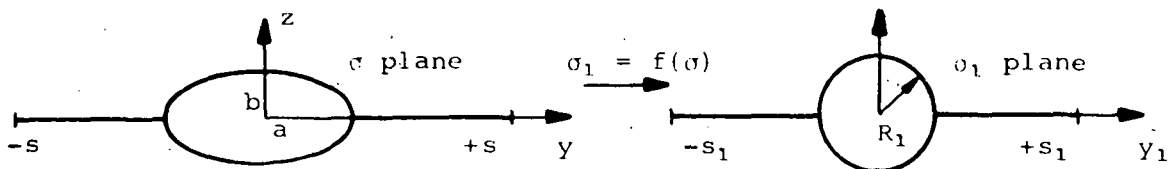
$$C_L = \frac{2\pi\alpha}{S_m} \left( s_l^2 + \frac{R_b^4}{s_l^2} - R_{eb}^2 \right) \Big|_{x = X_{sm_2}} \quad (27)$$

$$C_{D_t} = C_{D_{\alpha=0}} + \frac{\alpha}{2} C_L \quad (28)$$

$$C_m = \frac{2\pi\alpha}{S_m \cdot l} \left[ -x \left( s_l^2 + \frac{R_b^4}{s_l^2} - R_{eb}^2 \right) \Big|_{x = X_{sm_2}} + \int_0^{X_{rle_1}} R_{eb}^2 d\xi \right. \\ \left. + \int_{X_{rle_1}}^{X_{sm_2}} \left( s_l^2 + \frac{R_b^4}{s_l^2} - R_{eb}^2 \right) d\xi \right] \quad (29)$$

where the drag coefficient at zero lift  $C_{D_{\alpha=0}}$  is given by equation (22) and  $X_{rle_1}$  is the axial location of the point where the wing leading edge pierces the body surface.

Elliptic bodies.— The basic analysis of wing-body combinations composed of wings having finite tip chords with trailing edges that are either straight or sweptforward and bodies having indented elliptic cross sections such that the total cross-sectional area distribution equals the area of the original smooth body with elliptic cross section proceeds in a manner analogous to that used for the circular body shapes. Apparently, the most direct approach consists of reducing the elliptic cross section to a circular one by use of the appropriate Joukowski transformation and then applying the methods used for the circular shapes. The transformation required to take the ellipse into the circle shown below



is given by

$$\sigma_1 = \frac{\sigma + \sqrt{\sigma^2 - c^2}}{2} \quad (30)$$

where

$$c^2 = a^2 - b^2 \quad (31)$$

and

$$\sigma_1 = y_1 + iz_1 \quad (32)$$

This takes the ellipse into a circle of radius

$$R_1 = \frac{(a + b)}{2} \quad (33)$$

and the semispan  $s$  into the shortened semispan

$$s_1 = \frac{s + \sqrt{s^2 - c^2}}{2} \quad (34)$$

The potentials  $W_{2,\alpha}$ ,  $W_{2,t}$ , and  $W_{2,B}$  are then given by

$$\frac{W_{2,\alpha}}{U_\infty} = -i\alpha \left\{ \left[ \left( \sigma_1 + \frac{R_1^2}{\sigma_1} \right)^2 - \left( s_1 + \frac{R_1^2}{s_1} \right)^2 \right]^{1/2} - 0 \right\} \quad (35)$$

$$\begin{aligned} \frac{W_{2,t}}{U_\infty} = & \frac{1}{\pi} \int_{R_1}^{s_1} \frac{dZ_w(x, \xi_1 + \frac{c^2}{4\xi_1^2})}{dx} \ln \left[ \frac{(\sigma_1^2 - \xi_1^2)(\sigma_1^2 - \frac{R_1^4}{\xi_1^2})}{\sigma_1^4} \right] \left( 1 - \frac{c^2}{4\xi_1^2} \right) d\xi_1 \\ & + \left( \frac{S'_{eb}(x)}{2\pi} + 2 Z_w(x, a) \frac{da}{dx} \right) \ln \sigma_1 \end{aligned} \quad (36)$$

$$\frac{W_{2,B}}{U_\infty} = \frac{S'_{eb}(x)}{2\pi} \ln \sigma \quad (37)$$

The velocity components associated with these potentials are found through the operations

$$u_{2,i} = \text{R.P.} \frac{\partial w_{2,i}}{\partial x} \quad (38)$$

$$(v - w)_{2,i} = \frac{dw_{2,i}}{d\sigma_1} \frac{d\sigma_1}{d\sigma} \quad (39)$$

These have been carried out and are given in reference 7 where it must be remembered in those formulas that depending upon axial location  $s_1$  represents either the leading ( $s_1 = s_{1\ell}$ ) or trailing ( $s_1 = s_{1t}$ ) edge in the transformed plane. For the case of nonlifting flows about these classes of symmetric configurations, no lateral forces or moments exist so that the only force present is the longitudinal drag force. This can be determined through the use of equation (21) where now the contributions of the two line integrals do not cancel since the contour over which the product  $\phi_{2,t} \partial\phi_{2,t}/\partial n$  is evaluated is the elliptic cross section at the base of the body whereas the contour for evaluating  $\phi_{2,B} \partial\phi_{2,B}/\partial n$  is the circular cross section of the equivalent body. Carrying out the indicated operations, we find that the drag coefficient of this general class of nonlifting elliptic wing-body combinations is

$$C_{D_{t=0}} = C_{D_{eb}} - \frac{1}{S_m} \left( \frac{S'_{eb}(x)}{2\pi} \right)^2 2 \left[ \frac{2}{\lambda} \ln \left( \frac{a(\lambda + 1)}{2\lambda} \right) K \left( \frac{\sqrt{\lambda^4 - 1}}{\lambda^2} \right) - \pi \ln R_{eb} \right] \quad (40)$$

where  $C_{D_{eb}}$  is the drag coefficient of the nonlifting equivalent body and is given by equation (22), and  $K(\xi)$  is the complete elliptic integral of the first kind.

For lifting flows at small angles of attack about these configurations, if we apply the same assumptions regarding the trailing vortex wake as were made for the circular body case, then the evaluation of equations (24), (25), and (26) provides the following results for the lift, pitching moment, and drag coefficients.

$$C_L = \frac{2\pi\alpha}{S_m} \left\{ \left( \frac{s_l + \sqrt{s_l^2 - c^2}}{2} \right)^2 \left[ 1 + \frac{2c^2}{(s_l + \sqrt{s_l^2 - c^2})^2} + \left( \frac{a+b}{s_l + \sqrt{s_l^2 - c^2}} \right)^4 \right] - R_{eb}^2 \right\} \Big|_{x=X_{sm_2}} \quad (41)$$

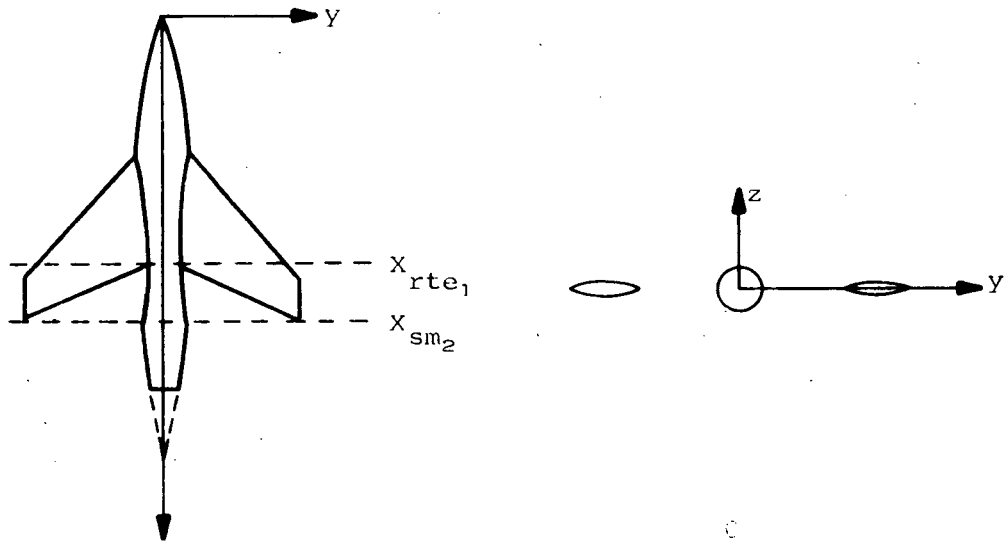
$$C_m = \frac{2\pi\alpha}{S_m \cdot l} \left( -x \left\{ \left( \frac{s_l + \sqrt{s_l^2 - c^2}}{2} \right)^2 \left[ 1 + \frac{2c^2}{(s_l + \sqrt{s_l^2 - c^2})^2} + \left( \frac{a+b}{s_l + \sqrt{s_l^2 - c^2}} \right)^4 \right] - R_{eb}^2 \right\} \Big|_{x=X_{sm_2}} + \lambda \int_0^{X_{rle_1}} R_{eb}^2(x) dx + \int_{X_{rle_1}}^{X_{sm_2}} \left\{ \left( \frac{s_l + \sqrt{s_l^2 - c^2}}{2} \right)^2 \left[ 1 + \frac{2c^2}{(s_l + \sqrt{s_l^2 - c^2})^2} + \left( \frac{a+b}{s_l + \sqrt{s_l^2 - c^2}} \right)^4 \right] - R_{eb}^2 \right\} dx \right) \quad (42)$$

$$C_{D_t} = C_{D_{\alpha=0}} + \frac{\alpha}{2} C_L \quad (43)$$

where  $C_{D_{\alpha=0}}$  is the drag coefficient at zero lift and is given by equation (40).

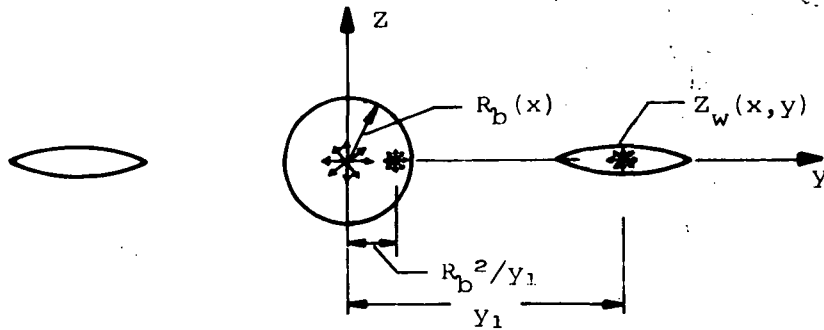
### Sweptback Trailing Edge Planforms

Circular bodies.- For finite thickness wing-indented circular body combinations having sweptback trailing edges, as illustrated below,



new potential solutions are required to account for the gap between wing and body cross sections which appear in the crossflow plane between the axial locations  $x = X_{rte_1}$  and  $x = X_{sm_2}$ . For lifting flows, the analysis is complicated even with the previously made assumption that the vortex sheet emanating from the trailing edge remains parallel to the  $x$  axis beyond the point  $x = X_{sm_2}$ . This is due to the presence of the vortex sheet in the gap between the wing and body from  $X_{rte_1}$  to  $X_{sm_2}$ . Consequently, the flow at any axial station beyond  $X_{rte_1}$  is influenced by the wake ahead of it and is no longer independent of the flow at preceding cross sections. Thus, the simplified analysis which was valid for lifting flows about wings with straight or sweptforward trailing edges - i.e. for cases where the edge of the wing always remained a leading edge - does not apply here. A new potential solution for  $W_2, \alpha'$  is required and this is beyond the work scope of the present investigation.

One of the primary goals of this study, however, is to determine the potential  $W_{2,t}$  associated with the thickness problem for configurations of this type. For  $x < X_{rte_1}$ , equation (16) is valid. For  $X_{rte_1} < x < X_{sm_2}$ , a new potential must be developed to account for the gap between the wing and body. This is accomplished by using an extension of the method developed by Stocker in reference 10. That method is based upon the method of singularities and models the wing thickness by placing a continuous distribution of two-dimensional incompressible sources (or sinks) along the wing chordal plane together with their appropriate images within the body. The body itself is represented by a source (or sink) at the origin. Although originally developed for a wing attached to a body, this method can accommodate such a wing body as shown below



by distributing sources (or sinks) only along the wing and appropriately imaging them within the body. This method thus provides the following expression for the complex potential  $W_{2,t}(x,y,z)$ :

$$\frac{W_{2,t}}{U_\infty} = \frac{1}{\pi} \int_{s_t}^{s_l} \frac{dZ_w(x,\xi)}{dx} \ln \left[ \frac{(\sigma^2 - \xi^2)(\sigma^2 - \frac{R_b^4}{\xi^2})}{\sigma^2} \right] d\xi + \frac{S'_b(x)}{2\pi} \ln \sigma$$

( $X_{rte_1} < x < X_{sm_2}$ ) (44)

Since for sweptback trailing edges with  $X_{rte_1} < x < X_{sm_2}$ , the equivalent body area distribution and actual body area distribution are related through the expression

$$S_{eb}(x) = S_b(x) + 4 \int_{s_t}^{s_l} z_w(x,y) dy \quad (45)$$

we can write the alternate form

$$\frac{w_{z,t}}{U_\infty} = \frac{1}{\pi} \int_{s_t}^{s_l} \frac{dZ_w(x,\xi)}{dx} \ln \left[ \frac{(\sigma^2 - \xi^2) (\sigma^2 - \frac{R_b^4}{\xi^2})}{\sigma^4} \right] d\xi + \frac{S'_{eb}(x)}{2\pi} \ln \sigma$$

( $X_{rte_1} < x < X_{sm_2}$ ) (46)

The velocity components associated with this potential are determined through equations (19) and (20). As in the case of straight or sweptforward trailing edges, proper account must be taken of the familiar Cauchy singularity which appears in several of the integrals associated with these velocity components on the wing surface. If, because of the symmetry of these configurations, we restrict attention to the first quadrant of the crossflow plane ( $y \geq 0, z \geq 0$ ), the following results are obtained. For points at any general location but not on the wing surface,



$$\begin{aligned}
\frac{u_{z,t}}{U_\infty} = & \frac{1}{2\pi} \left( \int_{s_t}^{s_\ell} \frac{d^2 Z_w(x, \xi)}{dx^2} \times \right. \\
& \ln \left\{ \frac{[z^2 + (y - \xi)^2] [z^2 + (y + \xi)^2] [z^2 + (y - \frac{R_b^2}{\xi})^2] [z^2 + (y + \frac{R_b^2}{\xi})^2]}{(z^2 + y^2)^4} \right\} d\xi \\
& + 4R_b \frac{dR_b}{dx} \int_{s_t}^{s_\ell} \frac{dZ_w(x, \xi)}{dx} \frac{1}{\xi} \left[ \frac{y + \frac{R_b^2}{\xi}}{z^2 + (y + \frac{R_b^2}{\xi})^2} - \frac{y - \frac{R_b^2}{\xi}}{z^2 + (y - \frac{R_b^2}{\xi})^2} \right] d\xi \\
& + \frac{dZ_w(x, s_\ell)}{dx} \frac{ds_\ell}{dx} \times \\
& \ln \left\{ \frac{[z^2 + (y - s_\ell)^2] [z^2 + (y + s_\ell)^2] [z^2 + (y - \frac{R_b^2}{s_\ell})^2] [z^2 + (y + \frac{R_b^2}{s_\ell})^2]}{(z^2 + y^2)^4} \right\} \\
& - \frac{dZ_w(x, s_t)}{dx} \frac{ds_t}{dx} \times \\
& \ln \left\{ \frac{[z^2 + (y - s_t)^2] [z^2 + (y + s_t)^2] [z^2 + (y - \frac{R_b^2}{s_t})^2] [z^2 + (y + \frac{R_b^2}{s_t})^2]}{(z^2 + y^2)^4} \right\} \\
& + \frac{S_{eb}''(x)}{2} \ln [z^2 + y^2] \Big) \tag{47}
\end{aligned}$$

$$\frac{v_{2,t}}{U_\infty} = \frac{1}{\pi} \left\{ \int_{s_t}^{s_\ell} \frac{dZ_w(x, \xi)}{dx} \left[ \frac{y - \xi}{z^2 + (y - \xi)^2} + \frac{y + \xi}{z^2 + (y + \xi)^2} + \frac{y - \frac{R_b^2}{\xi}}{z^2 + \left(y - \frac{R_b^2}{\xi}\right)^2} \right. \right. \\ \left. \left. + \frac{y + \frac{R_b^2}{\xi}}{z^2 + \left(y + \frac{R_b^2}{\xi}\right)^2} \right] d\xi + \frac{y}{z^2 + y^2} \left( -4 \int_{s_t}^{s_\ell} \frac{dZ_w(x, \xi)}{dx} d\xi + \frac{S'_{eb}(x)}{2} \right) \right\} \quad (48)$$

$$\frac{w_{2,t}}{U_\infty} = \frac{1}{\pi} \left\{ z \int_{s_t}^{s_\ell} \frac{dZ_w(x, \xi)}{dx} \left[ \frac{1}{z^2 + (y - z)^2} + \frac{1}{z^2 + (y + \xi)^2} + \frac{1}{z^2 + \left(y - \frac{R_b^2}{\xi}\right)^2} \right. \right. \\ \left. \left. + \frac{1}{z^2 + \left(y + \frac{R_b^2}{\xi}\right)^2} \right] d\xi + \frac{z}{z^2 + y^2} \left( -4 \int_{R_b}^s \frac{dZ_w(x, \xi)}{dx} d\xi + \frac{S'_{eb}(x)}{2} \right) \right\} \quad (49)$$

For points on the wing surface, i.e.  $z = 0$ ,  $s_t < y < s_\ell$ :

$$\frac{u_{2,t}}{U_\infty} = \frac{1}{2\pi} \left\{ \int_{s_t}^{s_\ell} \frac{d^2Z_w(x, \xi)}{dx^2} \ln \left[ \frac{(y + \xi)^2 (y + \frac{R_b^2}{\xi})^2 (y - \frac{R_b^2}{\xi})^2}{y^4} \right] d\xi \right. \\ \left. + \int_{s_t}^{s_\ell} \left( \frac{d^2Z_w(x, \xi)}{dx^2} - \frac{d^2Z_w(x, y)}{dx^2} \right) \ln \left[ \left( \frac{y - \xi}{y} \right)^2 \right] d\xi \right. \\ \left. + 4R_b \frac{dR_b}{dx} \frac{1}{y} \int_{s_t}^{s_\ell} \frac{dZ_w(x, \xi)}{dx} \left[ \frac{1}{\xi + \frac{R_b^2}{y}} - \frac{1}{\xi - \frac{R_b^2}{y}} \right] d\xi \right. \\ \left. + 2 \frac{d^2Z_w(x, y)}{dx^2} \left\{ (s_\ell - y) \left[ \ln \left( \frac{s_\ell - y}{y} \right) - 1 \right] + (y - s_t) \left[ \ln \left( \frac{y - s_t}{y} \right) - 1 \right] \right\} \right\}$$

(Continued on next page)

$$\begin{aligned}
& + \frac{dZ_w(x, s_l)}{dx} \frac{ds_l}{dx} \ln \left[ \frac{(s_l - y)^2 (s_l + y)^2 \left(y - \frac{R_b^2}{s_l}\right)^2 \left(y + \frac{R_b^2}{s_l}\right)^2}{y^8} \right] \\
& - \frac{dZ_w(x, s_t)}{dx} \frac{ds_t}{dx} \ln \left[ \frac{(y - s_t)^2 (y + s_t)^2 \left(y - \frac{R_b^2}{s_t}\right)^2 \left(y + \frac{R_b^2}{s_t}\right)^2}{y^8} \right] \\
& + \left. \frac{S''_{eb}(x)}{2} \ln(y^2) \right\} \tag{50}
\end{aligned}$$

$$\begin{aligned}
\frac{v_{z,t}}{U_\infty} &= \frac{1}{\pi} \left[ \int_{s_t}^{s_l} \frac{dZ_w(x, \xi)}{dx} \left( \frac{1}{y + \xi} + \frac{1}{y + \frac{R_b^2}{\xi}} + \frac{1}{y - \frac{R_b^2}{\xi}} \right) d\xi \right. \\
& - \int_{s_t}^{s_l} \frac{\left( \frac{dZ_w(x, \xi)}{dx} - \frac{dZ_w(x, y)}{dx} \right)}{\xi - y} d\xi - \frac{dZ_w(x, y)}{dx} \ln \left( \frac{s_l - y}{y - s_t} \right) \\
& \left. + \frac{1}{y} \left( -4 \int_{s_t}^{s_l} \frac{dZ_w(x, \xi)}{dx} d\xi + \frac{S'_{eb}(x)}{2} \right) \right] \tag{51}
\end{aligned}$$

$$\frac{w_{z,t}}{U_\infty} = \frac{dZ_w(x, y)}{dx} \tag{52}$$

We note that in this case no singularities occur on the body surface or in the gap between the wing and body. At the leading and trailing edges of the wing, however, the characteristic logarithmic singularity associated with two-dimensional incompressible flow at a sharp edge appears.

As before, the thickness potential for the equivalent body cross section  $w_{2,B}$  is given by equation (17). Because of the symmetry of these configurations, nonlifting flows will produce no lateral forces or

moments but only a longitudinal drag force. Since, as is the usual case of realistic wing-body combinations, the configurations considered herein have the body base located aft of the trailing edge of the wing tip chord (i.e.  $X_b > X_{sm_2}$ ), the drag coefficient at zero lift is given by

$$C_{D_{\alpha=0}} = C_{D_{eb}} \quad (53)$$

where  $C_{D_{eb}}$  is the drag coefficient of the equivalent body of revolution and is given by equation (22).

Elliptic bodies.- For the wing-body combinations with indented elliptic cross section and sweptback trailing edges, equation (36) for  $W_{2,t}$  applies for  $x < X_{rte_1}$ . For  $X_{rte_1} < x < X_{sm_2}$ , use of the Joukowski transformation, equation (30), provides the result that

$$\begin{aligned} \frac{W_{2,t}(\sigma_1)}{U_\infty} = & \frac{1}{\pi} \int_{S_{1t}}^{S_{1l}} \frac{dz_w(x, \xi_1 + \frac{c^2}{4\xi_1^2})}{dx} \ln \left[ \frac{(\sigma_1^2 - \xi_1^2)(\sigma_1^2 - \frac{R_1^4}{\xi_1^2})}{\sigma_1^4} \right] \left( 1 - \frac{c^2}{4\xi_1^2} \right) d\xi_1 \\ & + \frac{S'_{eb}(x)}{2\pi} \ln \sigma_1 \end{aligned} \quad (54)$$

If we define the following quantities

$$q_1 + iq_2 = \frac{1}{\sigma_1^2 - \frac{c^2}{4}} \quad (55)$$

$$q_3 + iq_4 = \frac{\sigma_1}{\sigma_1^2 - \frac{c^2}{4}} \quad (56)$$

$$q_5 + iq_6 = \frac{\sigma_1^2}{\sigma_1^2 - \frac{c^2}{4}} \quad (57)$$

and again restrict attention to the first quadrant of the crossflow plane, equations (38) and (39) provide the following results for the velocity components. For a point at general location but not on the wing surface,

$$\frac{u_{z,t}}{U_\infty} = \frac{1}{2\pi} \left( \int_{s_{1t}}^{s_{1l}} \frac{d^2 z_w(x, \xi + \frac{c^2}{4\xi_1})}{dx^2} \right) \times$$

$$\ln \left\{ \frac{[z_1^2 + (y_1 - z_1)^2][z_1^2 + (y_1 + z_1)^2][z_1^2 + (y_1 - \frac{R_1^2}{\xi_1})^2][z_1^2 + (y_1 + \frac{R_1^2}{\xi_1})^2]}{(z_1^2 + y_1^2)^4} \right\} \times$$

$$\left(1 - \frac{c^2}{4\xi_1^2}\right) d\xi_1$$

$$+ \left(\frac{\lambda^2 - 1}{\lambda^2}\right) a \frac{da}{dx} \left(-2 q_1 \int_{s_t}^{s_l} \frac{dz_w(x, \xi)}{dx} d\xi\right)$$

$$+ \left(\frac{\lambda + 1}{\lambda - 1}\right) \left[-q_5 \int_{s_{1t}}^{s_{1l}} \frac{dz_w(x, \xi_1 + \frac{c^2}{4\xi_1})}{dx} \frac{1}{\xi_1} \frac{(y_1 - \frac{R_1^2}{\xi_1})}{z_1^2 + (y_1^2 - \frac{R_1^2}{\xi_1})^2} d\xi_1\right]$$

$$- q_6 z_1 \int_{s_{1t}}^{s_{1l}} \frac{dz_w(x, \xi_1 + \frac{c^2}{4\xi_1})}{dx} \frac{1}{\xi_1} \frac{d\xi_1}{z_1^2 + (y_1 - \frac{R_1^2}{\xi_1})^2}$$

$$+ q_5 \int_{s_{1t}}^{s_{1l}} \frac{dz_w(x, \xi_1 + \frac{c^2}{4\xi_1})}{dx} \frac{1}{\xi_1} \frac{y_1 + \frac{R_1^2}{\xi_1}}{z_1^2 + (y_1 + \frac{R_1^2}{\xi_1})^2} d\xi_1$$

$$+ q_6 z_1 \int_{s_{1t}}^{s_{1l}} \frac{dz_w(x, \xi_1 + \frac{c^2}{4\xi_1})}{dx} \frac{1}{\xi_1} \frac{d\xi_1}{z_1^2 + (y_1 + \frac{R_1^2}{\xi_1})^2} \Big]$$

$$+ \frac{c^2}{4} \left[ q_3 \int_{s_{1t}}^{s_{1l}} \frac{dz_w(x, \xi_1 + \frac{c^2}{4\xi_1})}{dx} \frac{1}{\xi_1^2} \frac{(y_1 - \frac{R_1^2}{\xi_1})}{z_1^2 + (y_1 - \frac{R_1^2}{\xi_1})^2} d\xi_1 \right]$$

(Continued on next page)

$$\begin{aligned}
& + q_4 z_1 \int_{s_1 t}^{s_1 l} \frac{dZ_w(x, \xi_1 + \frac{c^2}{4\xi_1})}{dx} \frac{1}{\xi_1^2} \frac{d\xi_1}{z_1^2 + (y_1 - \frac{R_1^2}{\xi_1})^2} \\
& + q_3 \int_{s_1 t}^{s_1 l} \frac{dZ_w(x, \xi_1 + \frac{c^2}{4\xi_1})}{dx} \frac{1}{\xi_1^2} \frac{(y_1 + \frac{R_1^2}{\xi_1})}{z_1^2 + (y_1 + \frac{R_1^2}{\xi_1})^2} d\xi_1 \\
& + q_4 z_1 \int_{s_1 t}^{s_1 l} \frac{dZ_w(x, \xi_1 + \frac{c^2}{4\xi_1})}{dx} \frac{1}{\xi_1^2} \frac{d\xi_1}{z_1^2 + (y_1 + \frac{R_1^2}{\xi_1})^2} \Bigg) \\
& - \frac{\lambda^2 - 1}{\lambda^2} a \frac{da}{dx} q_1 \left( -4 \int_{s_t}^{s_l} \frac{dZ_w(x, \xi)}{dx} d\xi + \frac{S'_{eb}(x)}{2} \right) + \frac{dZ_w(x, s_l)}{dx} \frac{ds_l}{dx} \times \\
& \ln \left\{ \frac{[z_1^2 + (s_{1l} - y_1)^2] [z_1^2 + (s_{1l} + y_1)^2] [z_1^2 + (y_1 - \frac{R_1^2}{s_{1l}})^2] [z_1^2 + (y_1 + \frac{R_1^2}{s_{1l}})^2]}{(z_1^2 + y_1^2)^4} \right. \\
& \quad \left. - \frac{dZ_w(x, s_t)}{dx} \frac{ds_t}{dx} \times \right. \\
& \ln \left\{ \frac{[z_1^2 + (y_1 - s_{1t})^2] [z_1^2 + (y_1 + s_{1t})^2] [z_1^2 + (y_1 - \frac{R_1^2}{s_{1t}})^2] [z_1^2 + (y_1 + \frac{R_1^2}{s_{1t}})^2]}{(z_1^2 + y_1^2)^4} \right. \\
& \quad \left. + \frac{S''_{eb}(x)}{2} \ln(z_1^2 + y_1^2) \right) \tag{58}
\end{aligned}$$

$$\begin{aligned}
\frac{v_{2,t}}{U_\infty} = & \frac{1}{\pi} \left\{ q_5 \int_{s_1}^{s_1 \ell} \frac{dZ_w(x, \xi_1 + \frac{c^2}{4\xi_1})}{dx} \left[ \frac{Y_1 - \xi_1}{z_1^2 + (Y_1 - \xi_1)^2} + \frac{Y_1 + \xi_1}{z_1^2 + (Y_1 + \xi_1)^2} \right. \right. \\
& + \left. \frac{Y_1 - \frac{R_1^2}{\xi_1}}{z_1^2 + (Y_1 - \frac{R_1^2}{\xi_1})^2} + \frac{Y_1 + \frac{R_1^2}{\xi_1}}{z_1^2 + (Y_1 + \frac{R_1^2}{\xi_1})^2} \right] \left( 1 - \frac{c^2}{4\xi_1^2} \right) d\xi_1 \\
& + q_6 z_1 \int_{s_1}^{s_1 \ell} \frac{dZ_w(x, \xi_1 + \frac{c^2}{4\xi_1})}{dx} \left[ \frac{1}{z_1^2 + (Y_1 - \xi_1)^2} + \frac{1}{z_1^2 + (Y_1 + \xi_1)^2} \right. \\
& + \left. \frac{1}{z_1^2 + (Y_1 - \frac{R_1^2}{\xi_1})^2} + \frac{1}{z_1^2 + (Y_1 + \frac{R_1^2}{\xi_1})^2} \right] \left( 1 - \frac{c^2}{4\xi_1^2} \right) d\xi_1 \\
& + \left. \frac{q_5 Y_1 + q_6 z_1}{z_1^2 + Y_1^2} \left( -4 \int_{s_t}^{s_\ell} \frac{dZ_w(x, \xi)}{dx} d\xi + \frac{S'_{eb}(x)}{2} \right) \right\} \quad (59)
\end{aligned}$$

$$\begin{aligned}
\frac{w_{2,t}}{U_\infty} = & \frac{1}{\pi} \left\{ -q_6 \int_{s_1}^{s_1 \ell} \frac{dZ_w(x, \xi_1 + \frac{c^2}{4\xi_1})}{dx} \left[ \frac{Y_1 - \xi_1}{z_1^2 + (Y_1 - \xi_1)^2} + \frac{Y_1 + \xi_1}{z_1^2 + (Y_1 + \xi_1)^2} \right. \right. \\
& + \left. \frac{Y_1 - \frac{R_1^2}{\xi_1}}{z_1^2 + (Y_1 - \frac{R_1^2}{\xi_1})^2} + \frac{Y_1 + \frac{R_1^2}{\xi_1}}{z_1^2 + (Y_1 + \frac{R_1^2}{\xi_1})^2} \right] \left( 1 - \frac{c^2}{4\xi_1^2} \right) d\xi_1 \\
& + q_5 z_1 \int_{s_1}^{s_1 \ell} \frac{dZ_w(x, \xi_1 + \frac{c^2}{4\xi_1})}{dx} \left[ \frac{1}{z_1^2 + (Y_1 - \xi_1)^2} + \frac{1}{z_1^2 + (Y_1 + \xi_1)^2} \right.
\end{aligned}$$

(Continued on next page)

$$\begin{aligned}
& + \frac{1}{z_1^2 + (Y_1 - \frac{R_1^2}{\xi_1})^2} + \frac{1}{z_1^2 + (Y_1 + \frac{R_1^2}{\xi_1})^2} \left] \left(1 - \frac{c^2}{4\xi_1^2}\right) d\xi_1 \\
& + \frac{q_5 z_1 - q_6 Y_1}{z_1^2 + Y_1^2} \left( -4 \int_{s_t}^{s_l} \frac{dZ_w(x, \xi)}{dx} d\xi + \frac{S'_{eb}(x)}{2} \right) \quad (60)
\end{aligned}$$

For points on the wing surface, i.e.,  $z = 0$ ,  $s_t < y < s_l$  (or equivalently  $z_1 = 0$ ,  $s_{1t} < Y_1 < s_{1l}$ ),

$$\begin{aligned}
\frac{u_{2,t}}{U_\infty} = & \frac{1}{2\pi} \left\{ \int_{s_{1t}}^{s_{1l}} \frac{d^2 Z_w(x, \xi_1 + \frac{c^2}{4\xi_1})}{dx^2} \ln \left[ \frac{(Y_1 + \xi_1)^2 (Y_1 + \frac{R_1^2}{\xi_1})^2 (Y_1 - \frac{R_1^2}{\xi_1})^2}{Y_1^6} \right] \left(1 - \frac{c^2}{4\xi_1^2}\right) d\xi_1 \right. \\
& + \int_{s_{1t}}^{s_{1l}} \left( \frac{d^2 Z_w(x, \xi_1 + \frac{c^2}{4\xi_1})}{dx^2} - \frac{d^2 Z_w(x, Y_1 + \frac{c^2}{4Y_1})}{dx^2} \right) \ln \left[ \left( \frac{Y_1 - \xi_1}{Y_1} \right)^2 \right] \left(1 - \frac{c^2}{4\xi_1^2}\right) d\xi_1 \\
& + \frac{d^2 Z_w(x, Y_1 + \frac{c^2}{4Y_1})}{dx^2} 2 (s_{1l} - Y_1) \left[ \ln \left( \frac{s_{1l} - Y_1}{Y_1} \right) - 1 \right] + (Y_1 - s_{1t}) \left[ \ln \left( \frac{Y_1 - s_{1t}}{Y_1} \right) - 1 \right] \\
& - \frac{c^2}{4} \frac{1}{Y_1} \left[ \left( \frac{s_{1l} - Y_1}{s_{1l}} \right) \ln \left( \frac{s_{1l} - Y_1}{Y_1} \right) + \left( \frac{Y_1 - s_{1t}}{s_{1t}} \right) \ln \left( \frac{Y_1 - s_{1t}}{Y_1} \right) - \ln \left( \frac{s_{1l}}{s_{1t}} \right) \right] \\
& + \left( \frac{\lambda^2 - 1}{\lambda^2} \right) a \frac{da}{dx} \left[ -2 q_1 \int_{s_t}^{s_l} \frac{dZ_w(x, \xi)}{dx} d\xi - q_1 \left( -4 \int_{s_t}^{s_l} \frac{dZ_w(x, \xi)}{dx} d\xi + \frac{S'_{eb}(x)}{2} \right) \right]
\end{aligned}$$

(Continued on next page)



$$\begin{aligned}
& + \left( \frac{\lambda + 1}{\lambda - 1} \right) \frac{q_5}{Y_1} \left[ - \int_{s_{1t}}^{s_{1l}} \frac{dZ_w(x, \xi_1 + \frac{c^2}{4\xi_1})}{\xi_1 - \frac{R_1^2}{Y_1}} dx d\xi_1 + \int_{s_{1t}}^{s_{1l}} \frac{dZ_w(x, \xi_1 + \frac{c^2}{4\xi_1})}{\xi_1 + \frac{R_1^2}{Y_1}} dx d\xi_1 \right] \\
& + \frac{c^2}{4} \frac{q_3}{Y_1} \left[ \int_{s_{1t}}^{s_{1l}} \frac{dZ_w(x, \xi_1 + \frac{c^2}{4\xi_1})}{\xi_1 (\xi_1 - \frac{R_1^2}{Y_1})} dx d\xi_1 + \int_{s_{1t}}^{s_{1l}} \frac{dZ_w(x, \xi_1 + \frac{c^2}{4\xi_1})}{\xi_1 (\xi_1 + \frac{R_1^2}{Y_1})} dx d\xi_1 \right] \\
& + \frac{dZ_w(x, s_l)}{dx} \frac{ds_l}{dx} \ln \left[ \frac{(s_{1l} - Y_1)^2 (s_{1l} + Y_1)^2 (Y_1 - \frac{R_1^2}{s_{1l}})^2 (Y_1 + \frac{R_1^2}{s_{1l}})^2}{Y_1^8} \right] \\
& - \frac{dZ_w(x, s_t)}{dx} \frac{ds_t}{dx} \ln \left[ \frac{(Y_1 - s_{1t})^2 (Y_1 + s_{1t})^2 (Y_1 - \frac{R_1^2}{s_{1t}})^2 (Y_1 + \frac{R_1^2}{s_{1t}})^2}{Y_1^8} \right] \\
& + \frac{s''_{eb}(x)}{2} \ln (Y_1^2) \left. \right\} \tag{61}
\end{aligned}$$

$$\begin{aligned}
\frac{v_{2,t}}{U_\infty} &= \frac{q_s}{\pi} \left[ \int_{s_{1,t}}^{s_{1,l}} \frac{dZ_w(x, \xi_1 + \frac{c^2}{4\xi_1})}{dx} \left( \frac{1}{Y_1 + \xi_1} + \frac{1}{Y_1 + \frac{R_1^2}{\xi_1}} + \frac{1}{Y - \frac{R_1^2}{\xi_1}} \right) \left( 1 - \frac{c^2}{4\xi_1^2} \right) d\xi_1 \right. \\
&\quad - \int_{s_{1,t}}^{s_{1,l}} \frac{\left( \frac{dZ_w(x, \xi_1 + \frac{c^2}{4\xi_1})}{dx} - \frac{dZ_w(x, Y_1 + \frac{c^2}{4Y_1})}{dx} \right)}{\xi_1 - Y_1} \left( 1 - \frac{c^2}{4\xi_1^2} \right) d\xi_1 \\
&\quad - \frac{dZ_w(x, Y_1 + \frac{c^2}{4Y_1})}{dx} \left\{ \ln \left( \frac{s_{1,l} - Y_1}{Y_1 - s_{1,t}} \right) + \frac{c^2}{4} \left[ \frac{1}{Y_1^2} \left[ \ln \left( \frac{s_{1,l}}{s_{1,t}} \right) \right. \right. \right. \\
&\quad \left. \left. \left. - \ln \left( \frac{s_{1,l} - Y_1}{Y_1 - s_{1,t}} \right) \right] + \frac{1}{Y_1} \left( \frac{s_{1,l} - s_{1,t}}{s_{1,l} \cdot s_{1,t}} \right) \right] \right\} \\
&\quad + \left( -4 \int_{s_t}^{s_l} \frac{dZ_w(x, \xi)}{dx} d\xi + \frac{S'_{eb}(x)}{2} \frac{1}{Y_1} \right) \quad (62)
\end{aligned}$$

$$\frac{w_{2,t}}{U_\infty} = \frac{dZ_w(x, Y)}{dx} \quad (63)$$

The drag coefficient at zero lift  $C_{D_{\alpha=0}}$  of this class of configurations is given by equation (40).

## RESULTS AND DISCUSSION

While experimental verification of the theory is considered essential, particularly at this stage of development, there is not available at the present time experimental data for transonic flows about wing-indented body combinations suitable for comparison with theory developed here. Although a parallel experimental program was originally considered for a typical member of the class of configurations described herein, that program has, unfortunately, been delayed. Consequently, experimental verification of the theory, particularly for pressure distribution comparisons which are vital in assessing the validity of the assumptions of the theory within the various regions (body surface, wing surface, wing-body junction, wing leading and trailing edges, etc.) of the near flow field of these configurations will have to be deferred.

In order to illustrate the general behavior of the theoretical results for transonic flows about the slender wing-body combinations considered here, the surface and flow field pressure distributions for several typical members of the classes of configurations described previously are given in figures 4 through 7. For example, in figure 4 pressure distributions are presented for a finite thickness wing-indented circular body combination with a nonzero taper ratio and straight trailing edge in which the equivalent body is a parabolic-arc of thickness ratio  $D/l = 0.1$ , the wing is a truncated delta wing with aspect ratio  $AR = 1.7$ , and taper ratio  $TR = 0.2$  (so that  $\beta_{le} = 58^\circ$ ,  $\beta_{te} = 0$ ), and has parabolic-arc profiles of thickness/chord ratio  $t/c_w = 0.04$ . The wing root chord is half the body length, i.e.,  $C_{RT}/l = 0.5$ , the root chord leading edge is located at  $X_{rle}/l = 0.25$ , and the body base is at  $X_{b/l} = 0.86$ . The longitudinal pressure distributions given in figure 4 are for the free-stream conditions  $M_\infty = 1$ ,  $\alpha = 0^\circ$  and are presented at the two angular positions  $\theta = 0^\circ, 90^\circ$  in the crossflow plane and at locations on the body surface and also along lines parallel to the body axis but removed laterally from it by distances of 1, 2, and 4 times the maximum equivalent body diameter  $D$ . Thus, the pressure distributions given for  $\theta = 0^\circ$  and  $r/D = 1, 2$  cut across the wing surface, intersecting the leading edge at the axial positions  $x/l = 0.410$  and  $0.570$ , respectively.

The wing-body surface pressure distributions shown in the first plot of figure 4, when compared to the pressure distribution on the equivalent body alone, demonstrate the large effect that the wing has upon the body pressure distribution. Moreover, it clearly shows the rapid variation of the pressure distributions caused by the singularities at the points ( $x/l = 0.320, 0.75$ ) where the wing leading and trailing edges pierce the body surface and also at  $x/l = 0.65$  where the leading edge of the wing tip chord is. The discontinuities at the points where the leading and trailing edges intersect the body surface are related to the characteristic logarithmic singularity associated with the two-dimensional thickness problem (i.e.,  $\phi_{p,t}$ ) of flow at a sharp edge. The discontinuity at the leading edge of the wing tip chord is due to the discontinuity in slope of the indented body at that point. This discontinuity occurs since in order that the equivalent body area distribution and its derivatives remain smooth, it is necessary for the indented body to have a slope discontinuity at  $x/l = 0.65$  to compensate for the one due to the wing. This discontinuity also occurs at the trailing edge of the wing tip chord and would be evident if the trailing edge were swept forward, so that the point ( $x = X_{sm_1}$ ) would be separate and distinct from the axial location where the trailing edge pierces the body surface ( $x = X_{rte_1}$ ). For the case of a straight trailing edge as in figure 4, those points, of course, coincide so that only one singularity is evident. The flow field distributions shown at  $r/D = 1, 2,$  and  $4$  illustrate several interesting features. The most prominent is the propagation into the flow field of the singularities which occur in the surface pressure distribution at the three points discussed above. This is a direct consequence of using the transonic equivalence rule to provide flow-field information based upon knowledge of flow properties at the body surface. Also evident in the distributions along the lines  $r/D = 1, 2, \theta = 0^\circ$  are the logarithmic singularities at  $x/l = 0.410$  and  $0.570$ , respectively, as those lines cross the wing leading edge. The longitudinal flow field pressure distributions provide insight into the rapidity with which the flow field becomes axisymmetric and equal to that about the equivalent body. At the lateral distance  $r/D = 4$ , the pressure distributions at  $\theta = 0^\circ, 90^\circ$  at points ahead of the leading edge of the wing tip chord ( $X_{sm_2}/l = 0.65$ ) are virtually indistinguishable from that about the equivalent body - except for the exponentially small region of influence of the logarithmic

singularity propagating out from the body surface at the point where the leading edge pierces the body surface. However, within the axial region corresponding to the wing tip chord,  $0.65 < x/l < 0.75$ , the pressure distribution still shows some effect of the wing, although it is clearly diminishing. This is not surprising and could have been anticipated from the results from the delta wing with zero taper ratio given in figure 4 of reference 7 which also indicate that the effect of the wing on the flow field at lateral distances of several maximum body radii is negligible at all axial locations except those in the near vicinity of the wing maximum span. Knowledge of the region in which the flow about geometrically complex configurations of this type can be considered axisymmetric and equal to that about the equivalent body is quite significant and can provide, for example, useful information for a completely numerical finite difference solution in applying the far-field boundary condition. The drag coefficient for this configuration, which is provided by evaluating numerically the integral in equation (22), is found to be  $C_{Dt} = 0.1044$ .

Analogous results are given in figure 5 for a lifting flow about this same configuration for the free-stream conditions  $M_\infty = 1$  and  $\alpha = 2^\circ$ . We note again that the singularities discussed with regard to the nonlifting case also appear here. Moreover, due to the nature of lifting flows near a sharp edge, the logarithmic singularities associated with the thickness problem are further reinforced by the inverse square root behavior associated with the two-dimensional lifting problem (i.e.,  $\phi_{2,\alpha}$ ) of flow around a sharp edge. The net result is the more rapid variation of pressure evident in those regions. Nevertheless, the flow field distributions again display the strong tendency to return to those generated by the equivalent body alone, as is most apparent in the flow field distributions at  $r/D = 4$ . At this angle of attack, equations (27), (28), and (29) provide the following results for the aerodynamic coefficients:

$$C_L = 1.7070; \quad C_{Dt} = 0.1342, \quad C_m = -0.8906$$

In order to demonstrate the pressure distribution behavior typical of the wing-body combinations considered here having swept-back trailing edges and non-zero taper ratios, results are given in figure 6 for a finite

thickness wing-indented circular body combination in which the equivalent body is a parabolic-arc of thickness ratio  $D/l = 0.10$ , the wings have parabolic-arc profiles of thickness ratio  $t/c_w = 0.04$ , planform aspect ratio  $AR = 2.8$ , taper ratio  $TR = 0.4$ , root chord  $C_{RT}/l = 0.3$ , with the root chord leading edge at  $X_{rle}/l = 0.25$  (so that  $\beta_{le} = 45^\circ$ ,  $\beta_{te} = 23.75^\circ$ ). Analogous results are presented in figure 7 for a finite thickness wing-indented elliptic body combination composed of a parabolic-arc body of semimajor to semiminor axes  $\lambda = 3$  and a wing essentially identical to the one described above for the circular body except that the trailing edge is swept at the angle  $\beta_{te} = 25.05^\circ$ . The trailing edge sweep angles of these configurations are such that the axial locations of leading edge of the wing tip chord and the point where the trailing edge pierces the body surface coincide, i.e.,  $X_{sm_1} = X_{rte_1}$ .

In figure 6, we note that the general variation of both surface and flow field pressure distributions are essentially the same as those of the straight trailing edge configuration shown in figure 4 for points ahead of the leading edge of the wing tip chord ( $X_{sm_1}/l = 0.571$ ). However, within the axial region containing the wing tip chord ( $X_{sm_1} < x < X_{sm_2}$ ) and coincidentally, the wing trailing edge, the pressure distributions now indicate a much more rapid variation, while still exhibiting the same trend as that shown in figure 4. Apparently the gap between wing and body in the crossflow plane within this region influences the behavior of the surface pressures to a greater degree than in the case when there is no gap, and consequently an unbroken lateral distribution of sources along the wing from body to wing tip. The flow field distributions within the near flow field of this region maintain this rapid variation, with the distributions of  $C_p$  at  $\theta = 0^\circ$ ,  $r/D = 1, 2$  also exhibiting the characteristic influence of the logarithmic singularities at the points where these lines cross the trailing edge. Nevertheless, beyond the wing tip the flow still displays the characteristic tendency to return to that of the axisymmetric flow about the equivalent body, as is evident in the distribution at  $r/D = 4$ , a distance which is only slightly beyond the point of maximum span,  $r/D = 3.2$ .

The surface and flow field pressure distributions shown in figure 7 for the wing-indented elliptic body combination described above are essentially similar in behavior to those in figure 6 for the corresponding

circular body and do not exhibit any new characteristic features. We note that the asymmetry introduced by ellipticity of the cross section alone (excluding the influence of the wing), while being evident at the body surface, rapidly dies out. In reference 6, it was shown that for a smooth elliptic body alone having a semimajor to semiminor axis ratio  $\lambda = 3$  the flow field becomes essentially axisymmetric at  $r/D = 1$ .

Perhaps the most notable feature of the theoretical results presented here (and in ref. 7) for transonic flows about the classes of wing-indented body combinations being considered is the behavior of the pressure distributions caused by the singularities which occur at the following axial locations:

- $X_{rle_1}$  -- leading edge pierces body surface
- $X_{rte_1}$  -- trailing edge pierces body surface
- $X_{sm_1}$  -- leading edge of wing tip chord
- $X_{sm_2}$  -- trailing edge of wing tip chord

Although the singularities at general locations along the leading and trailing edges, for either nonlifting or lifting situations, could be included here, they are not, both since their character and origin are well known and also because they are local phenomena and, consequently, of restricted influence unlike the singularities delineated above.

It is important to realize that the basis of these singularities is essentially geometric in character, with the difficulty arising from either a discontinuity in first (at  $x = X_{sm_1}, X_{sm_2}$ ) or second (at  $x = X_{rle_1}, X_{rte_1}$ ) derivative of the indented body area distribution, which causes, in turn, discontinuities in the surface velocity components. Then, because the transonic equivalence rule is used to provide flow field information based upon knowledge of flow properties on the body surface, these discontinuities are propagated laterally into the flow field making their presence even more evident. A direct method of alleviating this problem, while at the same time providing both a more general and realistic approximation would be to smooth these junction points with monotonically varying fillets. It appears, however, that a simple functional representation of fairing curves of this nature is not possible. Analytic (i.e., cubic), trigonometric, or exponential curves, while

satisfying the end conditions of matching slope and ordinate at two points, fail to be continuously monotonic under boundary conditions typical of the configurations considered here. Thus, a wiggle would result in the faired curve and this is unacceptable. A means of eliminating this problem would be with piecewise continuous spline-fit functions. In any case, by whatever means the smoothing is accomplished, the result would be a more accurate representation of the actual solution in the vicinity of these points.

#### CONCLUDING REMARKS

Theoretical analysis and development of associated computer programs have been conducted in order to develop calculative techniques for predicting properties of transonic flows about certain classes of slender wing-body combinations. The theoretical analysis is based upon a combination of the transonic equivalence rule and uses either an arbitrarily specified solution or the local linearization method for determining the nonlifting transonic flow about the equivalent body.

Computational programs, which are documented in a general user's manual and included as part of this report, have been developed for finite thickness wing-body combinations in which the bodies are area-rule indented in such a manner that the resultant equivalent bodies remain smooth. The equivalent body profiles are either user-supplied subject to certain continuity and closure restrictions or program-supplied in which case the radius is of the general class  $R \sim x/l - (x/l)^n$  or  $1 - x/l - (1 - x/l)^n$ . In addition, the body cross sectional shapes are either (1) circular or (2) elliptic and such that a constant ratio  $\lambda$  of semimajor to semiminor axes is maintained along the entire body length.

A general class of wings is considered which are symmetric in plan-form about the azimuthal body meridian ( $x$ - $z$  plane) and consist of straight leading and trailing edges swept at arbitrary angles. The positions of the leading and trailing edges of the root chord are located at arbitrary locations on the body axis, and the profiles are described by  $Z_w \sim \bar{x}/c_w - (\bar{x}/c_w)^m$  or  $1 - \bar{x}/c_w - (1 - \bar{x}/c_w)^m$  where  $\bar{x}$  is the axial distance from the leading edge and  $c_w$  is the local chord.



These programs provide longitudinal pressure distributions for both nonlifting and lifting situations, at arbitrary angular positions in the crossflow plane at points along the body and wing surface and also along lines parallel to the body axis but removed at arbitrarily specified lateral distances from it. In addition to the pressure distributions, the aerodynamic characteristics of lift, drag, and pitching moment are also provided.

The theoretical pressure distributions predicted by these programs for certain members of the class of configurations described above indicate quantitatively the relatively large effects of wing thickness and lift on both the body and flow field pressures, and also serve to point out the singularities inherent to the theory as it is presently constituted. In addition, they demonstrate the large influence that sweeping the trailing edge and introducing a finite tip chord has upon the pressure distributions.

In conclusion, we emphasize that the techniques employed here are quite fundamental and possess great generality so as to allow extension to even more complex configurations. Moreover, since the solutions to the various two-dimensional crossflow problems are independent of Mach number, they can be calculated once and for all once the geometry of the configuration is fixed and then combined with any one of a possible variety of solutions (experimental, numerical, etc.) for the transonic flow about the nonlifting equivalent body. We suggest, furthermore, that experimental work be conducted to determine surface and flow-field pressure distributions on selected wing-body combinations in order to define more clearly the extent to which the theory applies to configurations of this nature and, also, that consideration be given to developing methods to smooth the solutions in the vicinity of the various discontinuities in the area derivatives of the indented body shapes.

Nielsen Engineering & Research, Inc.  
Mountain View, California  
July 13, 1972

## APPENDIX A

### COMPUTER PROGRAM USER'S MANUAL

#### SUMMARY

An operating manual is given for the computer program developed in conjunction with the theoretical work presented in this report. The program computes the transonic surface and flow field pressure distributions and aerodynamic characteristics for various classes of wing-body combinations considered herein. Use is made of the transonic equivalence rule and either the local linearization method or a user-supplied solution for flow about the nonlifting equivalent body.

A description of the general operating procedure of the program is given, together with instructions for the preparation of input data, sample output of test cases, and a listing. The program is written in FORTRAM IV programming language and prepared specifically for use on an IBM 360/67 series computer. Typical running times are approximately 30 to 45 seconds for the equivalent body calculations using the local linearization method and about 2 minutes for the crossflow solution calculations involving approximately 1000 points located typically along the wing, wing-body junction, and flow field.

#### DESCRIPTION OF PROGRAM

The computer program presented here is applicable to several classes of finite thickness wing-body combinations discussed in the preceding report in which the bodies are area-rule indented along the wing-body junction in such a manner that the total cross-sectional area distribution is identical to that of a smooth body having a specified profile. The programs compute the surface and flow field pressure distributions, for both nonlifting and lifting situations for straight or swept forward trailing edge planforms and for nonlifting situations for swept back trailing edge planforms, at arbitrarily specified angular positions in the crossflow plane, at points along the body and wing surface, and also along lines parallel to the body axis but removed from it at specified lateral distances. In addition, the aerodynamic characteristics of lift, drag, and pitching moment are computed.

## Wing and Body Geometry

The wing and body geometries of the configurations programmed are shown schematically in figures 2 and 3. Figure 2 illustrates two members of the class of wing-body combinations which have indented bodies that are circular in cross section, while figure 3 shows the corresponding members of the class having indented bodies with elliptic cross section.

Program-supplied equivalent body profiles.- Unless the user specifies to the contrary, the class of equivalent bodies of revolution of both types of the above configurations consist of profiles described by the equations

$$\frac{R_{eb}}{l} = \frac{\tau_{eb} n^{n/(n-1)}}{2(n-1)} \left[ \frac{x}{l} - \left( \frac{x}{l} \right)^n \right] \quad (64)$$

or

$$\frac{R_{eb}}{l} = \frac{\tau_{eb} n^{n/(n-1)}}{2(n-1)} \left[ 1 - \frac{x}{l} - \left( 1 - \frac{x}{l} \right)^n \right] \quad (65)$$

with  $n = \text{constant} \geq 2$ . In reference 7, the profiles of the elliptic bodies were restricted to parabolic arcs, i.e. equations (64) or (65) with  $n = 2$ . Thus, this work extends the elliptic body category to include the entire class of equivalent body profiles used for the case of the circular bodies.

User-supplied equivalent body profiles.- At the user's option, an arbitrarily specified equivalent body profile may be substituted in lieu of the above class of profiles. The modifications necessary to the program are detailed in the PROGRAM INPUT section. The restrictions on these profiles depend, in part, on the method used to calculate the solution for the nonlifting flow about the equivalent body, i.e.  $u_B$ . If the local linearization method, as presently constituted, is used to calculate  $u_B$  (see eqs. (5), (6), and (7)), then it is necessary that the profiles be closed, have sharp tips, and have continuous derivatives through the fourth. On the other hand, if the solution for  $u_B$  is user-supplied, then the requirement from the other portions of

APPENDIX A

the solution, i.e.  $\phi_{2,\alpha}$ ,  $\phi_{2,t}$ , and  $\phi_{2,B}$ , is that the equivalent body profiles have continuous derivatives through the second.

Indented-body profiles.- The ordinates of the indented body profiles are fixed once the equivalent body profile and wing profile are specified. For circular bodies with straight/sweptforward trailing edge planforms, the indented body radius  $R_b$  is found through a Newton-Raphson iteration procedure on the expression

$$\pi R_{eb}^2 = \pi R_b^2 + 4 \int_{R_b}^s Z_w(x, \xi) d\xi \quad (66)$$

while the derivatives  $dR_b/dx$  and  $d^2R_b/dx^2$  are calculated by using an appropriate five-point difference formula. For sweptback trailing edge planforms, the above method applies up to  $x = X_{rte1}$ . For  $X_{rte1} < x < X_{sm2}$ ,  $R_b$  is found without iteration from the expression

$$\pi R_{eb}^2 = \pi R_b^2 + 4 \int_{s_t}^{s_l} Z_w(x, \xi) d\xi \quad (67)$$

Analogously, for elliptic bodies with straight/sweptforward trailing edges the semimajor axis  $a$  of the indented elliptic cross section is found by iteration on

$$\pi R_{eb}^2 = \frac{\pi a^2}{\lambda} + 4 \int_a^s Z_w(x, \xi) d\xi \quad (68)$$

with the derivatives  $da/dx$  and  $d^2a/dx^2$  being evaluated numerically by using the appropriate five-point difference formula. For sweptback trailing edge planforms with  $X_{rte1} < x < X_{sm2}$ ,  $a$  is found directly from the expression

$$\pi R_{eb}^2 = \frac{\pi a^2}{\lambda} + 4 \int_{s_t}^{s_l} Z_w(x, \xi) d\xi \quad (69)$$

The general class of wings considered for both types of body shapes described above have wing planforms that consist of symmetric straight leading and trailing edges, swept at arbitrary angles  $\beta_{le}$  and  $\beta_{te}$ , respectively, to the  $y$  axis. Both  $\beta_{le}$  and  $\beta_{te}$ , are measured positive clockwise; thus, for  $\beta_{te}$  less than, equal to, or greater than zero, the trailing edge is correspondingly swept forward, straight, or swept back. The position of the leading edge of the wing root chord  $X_{rle}$  and its length  $C_{Rt}$  are arbitrary. The wing profiles are represented by expressions of the form

$$\frac{z_w}{c_w} = \frac{\tau_w m^{(m/m-1)}}{2(m-1)} \left( \frac{\bar{x}}{c_w} - \left( \frac{\bar{x}}{c_w} \right)^m \right) \quad (70)$$

or

$$\frac{z_w}{c_w} = \frac{\tau_w m^{(m/m-1)}}{2(m-1)} \left( 1 - \frac{\bar{x}}{c_w} - \left( 1 - \frac{\bar{x}}{c_w} \right)^m \right) \quad (71)$$

where  $c_w$  is the local chord,  $\bar{x}$  the distance from the leading edge,  $m$  is a constant  $\geq 2$ , and  $\tau_w$  is the wing thickness-to-chord ratio. The wings are assumed to maintain a constant thickness-to-chord ratio across the span, with the consequence that the wing profiles at all spanwise locations are geometrically similar so that

$$\frac{\tau_w}{2} = \frac{(z_w(x,y))_{\max}}{c_w(y)} = \frac{(z_w(x,0))_{\max}}{C_{Rt}} \quad (72)$$

#### General

The coordinate system used in the program is a body-fixed Cartesian system centered at the body nose with the  $x$  axis directed rearward and aligned with the longitudinal axis of the body, the  $y$  axis directed to the right facing forward, and the  $z$  axis directed vertically upward, as shown in figure 1. Because the transonic equivalence rule allows the perturbation potential  $\phi$  to be expressed in the form

$$\phi = \phi_{2,\alpha} + \phi_{2,t} - \phi_{2,B} + \phi_B \quad (73)$$

where each of the components has the meaning indicated in figure 1, and since  $\phi_{2,\alpha}$ ,  $\phi_{2,t}$ , and  $\phi_{2,B}$  satisfy the two-dimensional Laplace equation

$$(\phi_{2,i})_{yy} + (\phi_{2,i})_{zz} = 0 \quad (74)$$

they are independent of Mach number. Consequently, once the geometry of the configuration is fixed they can be calculated once and for all, stored, and used, for example, in a comparative study of a certain wing-body combination as the Mach number is varied systematically throughout the transonic range. An option for doing this is available and is discussed in the PROGRAM INPUT section. The only portion of the solution dependent upon  $M_\infty$  is  $\phi_B$  and this term represents the solution to the full transonic equation (1) for flow about the nonlifting equivalent body.

Local linearization solution of  $u_B$ . - If the local linearization method is used to determine the solution for  $\phi_B$ , or more conveniently,  $u_B = (\phi_B)_x$ , then according to whether  $M_\infty$  is near one, below the lower critical, or above the upper critical, equation (5), (6), or (7) must be integrated. Since these are all first order ordinary nonlinear differential equations, appropriate initial conditions are required. These are given at the point  $x_S$ , which is the positive root of the equation

$$S''_{eb}(x) = 0 \quad (75)$$

that is closest to the origin. The values of  $u_B/U_\infty$  at this point are, for accelerating transonic flows with  $M_\infty \approx 1$  (eq. (5))

$$\frac{u_B}{U_\infty} = \frac{1 - M_\infty^2}{M_\infty^2(\gamma + 1)} + \frac{1}{4\pi} \int_0^x \frac{S''_{eb}(x) - S''_{eb}(\xi)}{x - \xi} d\xi \quad (76)$$

for purely subsonic flow (eq. (6))

$$\frac{u_B}{U_\infty} = \frac{1}{4\pi} \int_0^{\ell} \frac{S''_{eb}(x) - S''_{eb}(\xi)}{|x - \xi|} d\xi \quad (77)$$

and for purely subsonic flow (eq. (7))

$$\frac{u_B}{U_\infty} = \frac{1}{2\pi} \int_0^x \frac{S''_{eb}(x) - S''_{eb}(\xi)}{x - \xi} d\xi \quad (78)$$

The integrations start at  $x_s$ , proceed to a specified point near the nose, and upon reaching that point, return to  $x_s$ , restart the integration procedure, and then continue toward the tail. In each of these programs, the differential equations are integrated by using Hamming's modified predictor-corrector method described in the Scientific Subroutine Package (SSP) available from the IBM Corporation. The integrals involved in those differential equations are evaluated by using Simpson's rule.

User-supplied solution for  $u_B$ . - At the user's option, an arbitrarily-specified solution for  $u_B$  can be used in lieu of the local linearization solution. This solution can involve mixed transonic flows with imbedded shocks and can be determined in any of a variety of ways (numerical, experimental, etc.). Details regarding the manner of inputting this information to the program are discussed in the PROGRAM INPUT section.

#### Crossflow Potentials and Aerodynamic Characteristics

This section assembles for user convenience, the crossflow potentials and aerodynamic characteristics of all of the configurations considered in this report.

Straight/Sweptforward trailing-edge planforms. - For the classes of finite thickness wing-circular body combinations considered herein which have straight/sweptforward trailing edge planforms, (see fig. 2(a)), the following results are provided for  $W_{2,\alpha}$ ,  $W_{2,t}$ , and  $W_{2,B}$  at the indicated axial locations:

$$\frac{W_{2,\alpha}}{U_\infty} = \frac{i\alpha R_{eb}^2}{\sigma} \quad (0 < x < X_{rle_1}) \quad (79)$$

$$\frac{W_{2,\alpha}}{U_\infty} = -i\alpha \left\{ \left[ \left( \sigma + \frac{R_b^2}{\sigma} \right)^2 - \left( s_\ell + \frac{R_b^2}{s_\ell} \right)^2 \right]^{1/2} - 0 \right\}$$

$$(X_{rle_1} < x < X_{sm_2}) \quad (80)$$

$$\frac{W_{2,t}}{U_\infty} = \frac{S'_{eb}(x)}{2\pi} \ln \sigma \quad \begin{pmatrix} 0 < x < X_{rle_1} \\ X_{rte_1} < x < \ell \end{pmatrix} \quad (81)$$

$$\frac{W_{2,t}}{U_\infty} = \frac{1}{\pi} \int_{R_b}^s \frac{dZ_w(x, \xi)}{dx} \ln \left[ \frac{(\sigma^2 - \xi^2) \left( \sigma^2 - \frac{R_b^4}{\xi^2} \right)}{\sigma^4} \right] d\xi$$

$$+ \frac{1}{2\pi} \left[ S'_{eb}(x) + 4Z_w(x, R_b) \frac{dR_b}{dx} \right] \ln \sigma \quad (X_{rle_1} < x < X_{rte_1}) \quad (82)$$

$$\frac{W_{2,B}}{U_\infty} = \frac{S'_{eb}(x)}{2\pi} \ln \sigma \quad (0 < x < \ell) \quad (83)$$

where  $s$  in equation (82) denotes either the leading ( $s = s_\ell$ ) or trailing ( $s = s_t$ ) edge, depending upon the axial location. We note that for all of the configurations considered in this report, the solution for  $W_{2,B}$  is given by equation (83).

The aerodynamic characteristics of this class of configurations are given as follows. The drag coefficient at zero lift is found through a numerical integration of the expression



$$C_{D_{\alpha=0}} = C_{D_{eb}} = \frac{1}{S_m} \int_0^{X_b} C_{p_{eb}} \frac{dS_{eb}(x)}{dx} dx \quad (84)$$

where  $C_{D_{eb}}$  is the drag coefficient of the equivalent body alone,  $S_m$  is the maximum area of the equivalent body, and  $C_{p_{eb}}$  is the pressure coefficient on the surface of the nonlifting equivalent body and is equal to

$$C_{p_{eb}} = -2 \frac{u_B}{U_\infty} - \left( \frac{dR_{eb}(x)}{dx} \right)^2 \quad (85)$$

Because of the symmetry of these configurations no lateral forces or moments exist at  $\alpha = 0$ . For the lifting situation, the coefficients of lift, drag, and pitching moment are given by

$$C_L = \frac{2\pi\alpha}{S_m} \left( s_l^2 + \frac{R_b^4}{s_l^2} - R_{eb}^2 \right) \Big|_{x = X_{sm_2}} \quad (86)$$

$$C_{D_t} = C_{D_{\alpha=0}} + \frac{\alpha}{2} C_L \quad (87)$$

$$C_m = \frac{2\pi\alpha}{S_m \cdot l} \left[ -x \left( s_l^2 + \frac{R_b^4}{s_l^2} - R_{eb}^2 \right) \Big|_{x = X_{sm_2}} + \int_0^{X_{rle_1}} R_{eb}^2 d\xi \right. \\ \left. + \int_{X_{rle_1}}^{X_{sm_2}} \left( s_l^2 + \frac{R_b^4}{s_l^2} - R_{eb}^2 \right) d\xi \right] \quad (88)$$

where  $X_{sm_2}$  and  $X_{rle_1}$  are the axial locations, respectively, of the trailing edge of the wing tip-chord and the point where the wing leading

APPENDIX A

edge pierces the body surface. The integrals involved in evaluating the pitching moment are calculated by using Simpson's rule.

The corresponding results for the wing-elliptic body combinations (see fig. 3(a)) are for  $W_{2,\alpha}$ ,  $W_{2,t}$ :

$$\frac{W_{2,\alpha}}{U_\infty} = i\alpha \left\{ \sigma_1 - \frac{R_1^2}{\sigma_1} - \sigma \right\} \quad (0 < x < X_{rle_1}) \quad (89)$$

$$\frac{W_{2,\alpha}}{U_\infty} = -i\alpha \left\{ \left[ \left( \sigma_1 + \frac{R_1^2}{\sigma_1} \right)^2 - \left( s_1 + \frac{R_1^2}{s_1} \right)^2 \right]^{1/2} - \sigma \right\} \\ (X_{rle_1} < x < X_{sm_2}) \quad (90)$$

$$\frac{W_{2,t}}{U_\infty} = \frac{S'_{eb}(x)}{2\pi} \ln \sigma_1 \quad \left( \begin{array}{l} 0 < x < X_{rle_1} \\ X_{rte_1} < x < l \end{array} \right) \quad (91)$$

$$\frac{W_{2,t}}{U_\infty} = \frac{1}{\pi} \int_{R_1}^{s_1} \frac{dz_w(x, \xi_1 + \frac{c^2}{4\xi_1^2})}{dx} \ln \left[ \frac{(\sigma_1^2 - \xi_1)(\sigma_1^2 - \frac{R_1^4}{\xi_1^2})}{\sigma_1^4} \right] \left( 1 - \frac{c^2}{4\xi_1^2} \right) d\xi_1 \\ + \left( \frac{S'_{eb}(x)}{2\pi} + 2Z_w(x, a) \frac{da}{dx} \right) \ln \sigma_1 \quad (X_{rle_1} < x < X_{rte_1}) \quad (92)$$

where  $s_1$  in equation (92) denotes either the leading ( $s_1 = s_{1l}$ ) or trailing ( $s_1 = s_{1t}$ ) edge in the transformed  $\sigma_1$  plane.

The aerodynamic characteristics of these elliptic body configurations are given, for nonlifting flows, by

$$C_{D_{\alpha=0}} = C_{D_{eb}} - \frac{1}{S_m} \left( \frac{S'_{eb}(x)}{2\pi} \right)^2 2 \left[ \frac{2}{\lambda} \ln \left( \frac{a(\lambda + 1)}{2\lambda} \right) K \left( \frac{\sqrt{\lambda^4 - 1}}{\lambda^2} \right) - \pi \ln R_{eb} \right] \quad (93)$$

where  $C_{D_{eb}}$  is given by equation (84) and  $K(\cdot)$  is the complete elliptic integral of the first kind; and for lifting flows by

$$C_L = \frac{2\pi\alpha}{S_m} \left\{ \left( \frac{s_l + \sqrt{s_l^2 - c^2}}{2} \right)^2 \left[ 1 + \frac{2c^2}{(s_l + \sqrt{s_l^2 - c^2})^2} + \left( \frac{a+b}{(s_l + \sqrt{s_l^2 - c^2})} \right)^4 \right] - R_{eb}^2 \right\} \Big|_{x=X_{sm_2}} \quad (94)$$

$$C_{D_t} = C_{D_{\alpha=0}} + \frac{\alpha}{2} C_L \quad (95)$$

$$C_m = \frac{2\pi\alpha}{S_m \cdot l} \left( -x \left\{ \left( \frac{s_l + \sqrt{s_l^2 - c^2}}{2} \right)^2 \left[ 1 + \frac{2c^2}{(s_l + \sqrt{s_l^2 - c^2})^2} + \left( \frac{a+b}{s_l + \sqrt{s_l^2 - c^2}} \right)^4 \right] - R_{eb}^2 \right\} \Big|_{x=X_{sm_2}} + \lambda \int_0^{X_{rle_1}} R_{eb}^2(x) dx + \int_{X_{rle_1}}^{X_{sm_2}} \left\{ \left( \frac{s_l + \sqrt{s_l^2 - c^2}}{2} \right)^2 \left[ 1 + \frac{2c^2}{(s_l + \sqrt{s_l^2 - c^2})^2} + \left( \frac{a+b}{s_l + \sqrt{s_l^2 - c^2}} \right)^4 \right] - R_{eb}^2 \right\} dx \right) \quad (96)$$

where the integrals involved in evaluating the pitching moment are calculated by using Simpson's rule.

Sweptback trailing edge planforms.— For the classes of finite thickness wing-circular body combinations having sweptback trailing edge planforms considered here (see fig. 2(b)), the following results for  $W_{2,t}$  are provided:

APPENDIX A

$$\frac{W_{2,t}}{U_\infty} = \frac{S'_{eb}(x)}{2\pi} \ln \sigma \quad \left( \begin{array}{l} 0 < x < X_{rle_1} \\ X_{sm_2} < x < l \end{array} \right) \quad (97)$$

$$\begin{aligned} \frac{W_{2,t}}{U_\infty} = & \frac{1}{\pi} \int_{R_b}^s l \frac{dZ_w(x, \xi)}{dx} \ln \left[ \frac{(\sigma^2 - \xi^2) \left( \sigma^2 - \frac{R_b^4}{\xi^2} \right)}{\sigma^4} \right] d\xi \\ & + \frac{1}{2\pi} \left[ S'_{eb}(x) + 4Z_w(x, R_b) \frac{dR_b}{dx} \right] \ln \sigma \quad (X_{rle_1} < x < X_{rte_1}) \end{aligned} \quad (98)$$

$$\begin{aligned} \frac{W_{2,t}}{U_\infty} = & \frac{1}{\pi} \int_{s_t}^s l \frac{dZ_w(x, \xi)}{dx} \ln \left[ \frac{(\sigma^2 - \xi^2) \left( \sigma^2 - \frac{R_b^4}{\xi^2} \right)}{\sigma^4} \right] d\xi + \frac{S'_{eb}(x)}{2\pi} \ln \sigma \\ & (X_{rte_1} < x < X_{sm_2}) \end{aligned} \quad (99)$$

and the drag coefficient at zero lift is given by

$$C_{D_{\alpha=0}} = C_{D_{eb}} \quad (100)$$

where  $C_{D_{eb}}$  is given by equation (84).

The corresponding results for the wing-elliptic body combinations are

$$\frac{W_{2,t}}{U_\infty} = \frac{S'_{eb}(x)}{2\pi} \ln \sigma_1 \quad \left( \begin{array}{l} 0 < x < X_{rle_1} \\ X_{sm_2} < x < l \end{array} \right) \quad (101)$$

$$\begin{aligned} \frac{W_{2,t}}{U_\infty} = & \frac{1}{\pi} \int_{R_1}^{s_1} l \frac{dZ_w(x, \xi_1 + \frac{c^2}{4\xi_1})}{dx} \ln \left[ \frac{(\sigma_1^2 - \xi_1^2) \left( \sigma_1^2 - \frac{R_1^4}{\xi_1^2} \right)}{\sigma_1^4} \right] \left( 1 - \frac{c^2}{4\xi_1^2} \right) d\xi_1 \\ & + \left( \frac{S'_{eb}(x)}{2\pi} + 2Z_w(x, a) \frac{da}{dx} \right) \ln \sigma_1 \quad (X_{rle_1} < x < X_{rte_1}) \end{aligned} \quad (102)$$

$$\frac{W_{2,t}}{U_\infty} = \frac{1}{\pi} \int_{R_1}^{S_1 \ell} \frac{dz_w(x, \xi_1 + \frac{c^2}{4\xi_1})}{dx} \ln \left[ \frac{(\sigma_1^2 - \xi_1^2)(\sigma_1^2 - \frac{R_1^4}{\xi_1^2})}{\sigma_1^4} \right] \left(1 - \frac{c^2}{4\xi_1^2}\right) d\xi_1$$

$$+ \frac{S'_{eb}(x)}{2\pi} \ln \sigma_1 \quad (X_{rte_1} < x < X_{sm_0}) \quad (103)$$

with the drag coefficient at zero lift  $C_{D_{Q=0}}$  given by equation (93).

### Operating Procedure

The basic characteristics and general operating procedure of the computer program developed herein are straightforward and can be outlined as follows. After reading the input data (which is detailed in a subsequent section) and checking it for obvious errors, the program proceeds to calculate certain required geometrical and flow-field constants. Then, if the user selects the equivalent body profile to be of the class described by equations (64) or (65), the program proceeds to calculate the exponent  $n$  from information regarding the point of maximum thickness (see equations (12), (14)). The point  $x_s$  is next found by solving equation (75). If however, the equivalent body profile is user supplied, the calculation of  $n$  and  $x_s$  are omitted. Next, the axial locations  $X_{rle_1}$  and  $X_{rte_1}$ , which represent, respectively, the points where the wing leading and trailing edges pierce the body surface, are calculated. The exponent  $m$  describing the wing ordinates (see eqs. (70), (71)) is then calculated in a manner similar to that used to determine  $n$ . The calculation of  $n$ ,  $x_s$ ,  $X_{rle_1}$ ,  $X_{rte_1}$ , and  $m$  are all performed in an iterative fashion by using the standard Newton-Raphson iteration scheme.

With the calculation of the above parameters complete, the program prints a number of geometrical and flow-field characteristics for the case at hand. If the solution of  $u_B$  is user-supplied, the program begins at a point close to the nose ( $x/\ell = 0.005$ ) and proceeds toward the tail. If the local linearization method is used to determine  $u_B$ , then the appropriate initial value (eqs. (76), (77), or (78)) for the local linearization equation at hand (eqs. (5), (6), or (7)) is

## APPENDIX A

calculated at  $x = x_s$  and the numerical integration begun. In the case of purely sub- or supersonic (eqs. (6), (7)) flow, it is convenient to redefine the dependent variables (see eqs. (80) through (88), ref. 6) and integrate a simplified differential equation. For the  $M_\infty \approx 1$  case, it is more advantageous to integrate equation (5) as it stands. Because of the special character of that equation at  $x = x_s$ , it is necessary to use a Taylor series for  $u_B/U_\infty$  in the neighborhood of that point in order to avoid a singularity in the numerical integration. Consequently, for that case in addition to  $u_B/U_\infty$  several derivatives are also required and are calculated by the program. Details are given in reference 6. The numerical integrations then continue toward the nose and stop at a point ( $x/l = 0.005$ ) close to it. The integrations are not carried directly to the nose because, although this is possible for the purely supersonic case, the local linearization method predicts a logarithmic singularity at  $x = 0$  for a sharp-tipped body, much like that indicated by linearized theory. With the integration to the nose complete, the program returns to  $x_s$ , restarts the numerical integration, and continues toward the tail. As these calculations progress (using either a user-supplied or local linearization solution for  $u_B$ ), the surface and flow-field pressure distributions are calculated from equations (2) and (3) and the output printed at specified axial locations. Until the point  $x = X_{rle_1}$  is reached, the appropriate crossflow solutions for determining these pressure distributions are those for the smooth body alone (see eqs. (79), (81), (83), (89), (91), and (101)). Beyond  $X_{rle_1}$ , for the case of nonlifting flows, the crossflow solutions are calculated from equation (82), (83), or (92) and (83) for  $X_{rle_1} < x < X_{rte_1}$ . Beyond  $X_{rte_1}$ , for planforms with straight/sweptforward trailing edges, the crossflow solutions revert to those for the smooth body alone; while for planforms with sweptback trailing edges, the appropriate crossflow solutions for  $X_{rte_1} < x < X_{sm_2}$  are given by equations (99), (83), or (103), (83) and beyond  $X_{sm_2}$  the solutions revert to those for the smooth body alone. The calculations continue until the body base is reached, i.e.  $x = X_b$ ; the calculation then returns to the mainline program, prints the value of the drag coefficient, and reads the input data for the next case. For lifting flows about planforms with straight/sweptforward trailing edges, the calculations proceed in a similar fashion to that of the nonlifting case (with the additional

output of surface and flow-field pressure distributions at the angular locations  $\pm \theta$  rather than just  $+\theta$ ) until the axial location of the trailing edge of the wing tip chord is reached, i.e.  $x = X_{sm_2}$ . Beyond that point, for reasons given in reference 7, no further pressure distributions are given. However, the calculation of flow about the equivalent body, i.e.  $u_B$ , continues to the body base in order that the drag coefficient at zero lift  $C_{D_{\alpha=0}}$  can be determined. When  $x = X_b$ , the calculation returns to the mainline program, determines the coefficients of lift, drag, and pitching moment from equation (86), (87), and (88), or (94), (95), and (96), prints these values, and then proceeds to read the input data for the next case.

## PROGRAM INPUT

The variables that are input to the program are described in the following list:

## Dictionary of Input Variables

AL	ratio of semimajor to semiminor axis (a/b) of elliptic cross section: program default value AL = 1
ALPHA	angle of attack, in degrees; program default value, ALPHA = 0
AMACH	free-stream Mach number
ANGLE	sweep angle, in degrees, of wing leading edge (measured positive clockwise from y axis and restricted to values $0 < \text{ANGLE} < 90$ , see figures 2, 3)
CRT	wing root chord normalized by complete body length, $C_{R_t} / \ell$
ICOPY	integer index for program option for using previously-stored values of crossflow solutions; equal to 0 or 1; program default value, ICOPY = 0
MAREA	integer index for program option for using user-supplied or program-supplied subroutines for equivalent body area and derivatives, equal to 0 or 1; program default value, MAREA = 0
MOPT	integer index for program option for using user-supplied distribution for $u_B$ or program-supplied local linearization solution; equal to 1, 2, 3, or 4.

## APPENDIX A

NTHETA	integer indicating number of angular positions in crossflow plane at which output is desired; $1 \leq \text{NTHETA} \leq 5$
NXEB	integer indicating number of table entries of the user-supplied distribution of $u_B$ ; $\text{NXEB} \leq 201$
RF(I)	six-dimensional vector representing values of $r/D$ (the radial distance in the crossflow plane normalized by the maximum equivalent body diameter $D$ ) at which flow-field pressure distributions are to be calculated
SSMAX	maximum wing semispan normalized by complete body length, $s_{\text{max}}/\ell$
TAUB	thickness ratio of equivalent body, $D/\ell$
TAUW	thickness-to-chord ratio of wing (see eq. (10))
THETA(I)	NTHETA-dimensional vector representing values of the angle $\theta$ (in degrees) in the crossflow plane; $0 \leq \text{THETA}(I) \leq 90$
TR	wing planform taper ratio, $C_{\text{tip}}/C_{R_t}$ ; $0 \leq \text{TR} \leq 1$
XEB(I)	NXEB-dimensional vector representing values of the axial locations (normalized by the complete body length) where values for the user-supplied distribution $u_B$ are given
XLBASE	axial location of body base normalized by the complete body length, $X_b/\ell$
XLOUTP	interval size, as fraction of complete body length, between output stations for pressure distribution print-out
XRLE	axial location of leading edge of wing root chord normalized by complete body length, $X_{rle}/\ell$
XMTB	axial location of position of maximum thickness of equivalent body of revolution normalized by complete body length (see eqs. (12), (14))
XMTW	location, as fraction of distance from wing leading edge to local chord length ( $\bar{x}/c_w$ ), of position of wing maximum thickness (see eqs. (8), (9))
XS2EB	user-supplied value of the axial location, normalized by the complete body length, where the user-supplied equivalent body profile satisfies $S''_{\text{eb}}(x) = 0$ ; only necessary as input when user supplies equivalent body profile and also uses local linearization method to calculate $u_B$



UEB(I) NXEB-dimensional vector representing values of  $u_B/u_\infty$  for the user-supplied distribution of  $u_B$ .

### Input Format and Options

All of the input variables are entered into the program under a NAMELIST format (the one exception being the vectors UEB(I), XEB(I) which represent the ordinates and abscissas, respectively, of the user-supplied velocity distribution  $u_B$  and the format of these quantities is discussed below). The name of the NAMELIST data block is TRANIN.

Default values.- The following input variables have default values that are indicated below and unless the user wishes to change them, it is not necessary to enter them in the input data block

<u>Variable Name</u>	<u>Default Value</u>
AL	1.
ALPHA	0.
RF(I), I=1,2,3, 4,5,6	1.,2.,3.,4.,5.,6.,
NTHETA	2
THETA(I), I=1,2	0.,90.
MAREA	0
ICOPY	0
XLOUTP	.01

It is important to realize that the above variables assume their default values each time the program is run. If the user wishes any of the above variables to be different from its default value, this must be specified in the data statement for each run. All other input variables, once specified, remain unchanged by the program; thus, it is unnecessary to respecify them in subsequent runs if their values are to remain constant.

Local linearization option.- To use the local linearization method to determine  $u_B$ , it is necessary to specify in the input data the appropriate value for the integer index MOPT. Depending on the free stream Mach number, the proper value of MOPT to use the local linearization method is

APPENDIX A

<u>Free Stream Mach No.</u>	<u>MOPT</u>
$M_\infty \approx 1$ (near sonic flow)	1
$M_\infty \leq M_{cr,l}$ (below lower critical)	2
$M_{cr,u} \leq M_\infty$ (above upper critical)	3

User-supplied  $u_B$  option.- If the user wishes to supply the solution for  $u_B$ , then the program will bypass the local linearization calculations by specifying MOPT = 4. The solution for  $u_B$  is read into the program in the form of a tabular input of values of  $u_B/U_\infty$  - vs  $-x/l$  immediately after the NAMELIST input block. Provision has been made for inputting ordinate and abscissa values up to a maximum number of 201 each (UEB(201), XEB(201)), i.e. values at each half percent of the body length if equally spaced. It is assumed that a sufficient number entries are made that linear interpolation in the table is appropriate.

User-supplied equivalent body profile.- If a class of equivalent body profiles not included in equation (64) or (65) is desired, then the user must set the integer index MAREA = 1, remove the following function subroutines from the program,

- FUNCTION SEBPI(DZ)
- FUNCTION S1EBPI(DZ)
- FUNCTION S2EBPI(DZ)
- FUNCTION S3EBPI(DZ)
- FUNCTION S4EBPI(DZ)

and replace them with his own. The above subroutines which are non-dimensionalized by normalizing them with respect to the body length, are defined in the following fashion.

$$\frac{S_{eb}(x/l)}{4\pi l^2} = \text{SEBPI}(x/l)$$

$$\frac{S'_{eb}(x/l)}{4\pi l^2} = \frac{1}{4\pi l^2} \frac{dS_{eb}(x/l)}{d(x/l)} = \text{S1EBPI}(x/l)$$

$$\frac{S''_{eb}(x/l)}{4\pi l^2} = \frac{d^2 S_{eb}(x/l)}{4\pi l^2 d(x/l)^2} = S2EBPI(x/l)$$

$$\frac{S'''_{eb}(x/l)}{4\pi l^2} = \frac{1}{4\pi l^2} \frac{d^3 S_{eb}(x/l)}{d(x/l)^3} = S3EBPI(x/l)$$

$$\frac{S^{IV}_{eb}(x/l)}{4\pi l^2} = \frac{1}{4\pi l^2} \frac{d^4 S_{eb}(x/l)}{d(x/l)^4} = S4EBPI(x/l)$$

We note again the requirements that if the local linearization method is to be used with these subroutines, then the functions must be such that the complete profiles are closed, sharp-tipped, and have continuous area derivatives through the fourth. In addition, the user must supply the point  $x/l = XS2EB$ , i.e. the point closest to the origin where

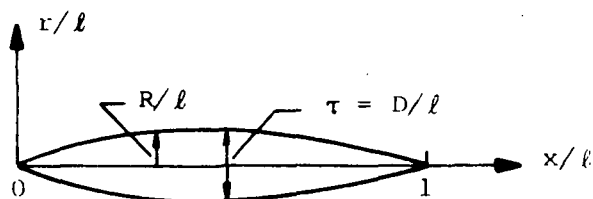
$$S''_{eb}(x/l) = 0$$

If, however, the user supplies both the equivalent body profiles and the distribution of  $u_B/U_\infty - vs - x/l$ , then it is only necessary that the equivalent body area derivatives be continuous through the second. Also, for this case, it is unnecessary to specify  $XS2EB$ . These requirements are summarized below when user-specifying the equivalent body profile:

<u>Value of MOPT</u>	<u>Requirements</u>
MOPT = 1,2,3	<ul style="list-style-type: none"> <li>① <math>S_{eb}, S'_{eb}, S''_{eb}, S'''_{eb}, S^{IV}_{eb}</math> continuous for <math>0 &lt; x &lt; l</math></li> <li>② User must input value of <math>x/l = XS2EB</math> where <math>S''_{eb}(XS2EB) = 0</math></li> <li>③ Set index MAREA = 1 in input</li> </ul>
MOPT = 4	<ul style="list-style-type: none"> <li>① <math>S_{eb}, S'_{eb}, S''_{eb}</math> continuous for <math>0 &lt; x &lt; l</math></li> <li>② Set index MAREA = 1 in input</li> </ul>

APPENDIX A

An illustrative example of a user-supplied equivalent body profile and the corresponding area and derivative subroutines to be used with, say, the local linearization method (MOPT = 1, 2, or 3) can be given as follows. Consider an equivalent body profile formed by the top half of the sinusoidal curve given by



$$\frac{R_{eb}(x/l)}{l} = \frac{\tau_{eb}}{2} \sin(\pi \frac{x}{l}) \quad \text{with say } \tau = .1$$

so that

$$\frac{S_{eb}(x/l)}{4\pi l^2} = \frac{\tau_{eb}^2}{16} (1 - \cos(2\pi(x/l)))$$

$$\frac{S'_{eb}(x/l)}{4\pi l^2} = \frac{\pi \tau_{eb}^2}{8} \sin(2\pi(x/l))$$

$$\frac{S''_{eb}(x/l)}{4\pi l^2} = \frac{\pi^2 \tau_{eb}^2}{4} \cos(2\pi(x/l))$$

$$\frac{S'''_{eb}(x/l)}{4\pi l^2} = -\frac{\pi^3 \tau_{eb}^2}{2} \sin(2\pi(x/l))$$

$$\frac{S^{IV}_{eb}(x/l)}{4\pi l^2} = -\pi^4 \tau_{eb}^2 \cos(2\pi(x/l))$$

The function subroutines for SEBPI(x/l) and SLEBPI(x/l) with  $\tau = .1$  are given by

```
FUNCTION SEBPI(DZ)
```

```
TAU = .1
```

```
PI = 3.1415927
```

```
SEBPI = TAU*TAU*(1. - COS(2.*PI*DZ))/16.
```

```

RETURN
END
FUNCTION S1EBPI(DZ)
TAU = .1
PI = 3.1415927
S1EBPI = PI*TAU*TAU*SIN (2.*PI*DZ)/8.
RETURN
END

```

The FUNCTION subroutines S2EBPI, S3EBPI, and S4EBPI are given in analogous fashion. The point where

$$S''_{eb}(x/l) = 0$$

is given by

$$XS2EB = 0.25$$

and must be included in the NAMELIST input data block.

Repetitive calculation storage option.- If the user wishes to undertake a systematic study of a wing-body configuration of the classes considered herein in which the geometry of the configuration is frozen and the Mach number and/or angle of attack are varied, a provision is included in the program whereby the velocity components associated with the crossflow solution for  $W_{2,t}$  - which is independent of  $M_\infty$  and  $\alpha$ , and is by far the most time consuming crossflow potential to calculate - is stored at the user-specified output locations for later use. These velocity components are then provided for the remainder of the cases to be run rather than recalculated unnecessarily.

In order to activate the repetitive calculation option and make use of previously-stored results from a base run, it is necessary to set the integer index ICOPY = 1. The default value for ICOPY is ICOPY = 0 and this default value instructs the program to perform the crossflow calculations at the user-indicated axial locations and then automatically store these results in anticipation of use with the next case. If it is not desired to use those stored results for the next run, (i.e. ICOPY = 0 for the next case) the program simply replaces the previously-stored results with the ones being currently calculated.

## APPENDIX A

Because for lifting situations, the crossflow calculations only proceed to  $x/l = X_{sm_2}$  (as opposed to the  $\alpha = 0$  case, which carries the calculation to  $x/l = X_b$ ) unless all of the cases in the study are for  $\alpha \neq 0$ , the initial or base run which stores the crossflow results should be made for  $\alpha = 0$ .

Finally, when using the storage option, it is necessary, because of the different starting conditions involved, to use the same method for calculating  $u_B$ , i.e. (1) local linearization or (2) user-supplied distribution of  $u_B$ .

### Data Format

The data format is most easily demonstrated by an example. Consider the case of a wing-elliptic body combination composed of a parabolic-arc equivalent body of thickness ratio 1/10, the ratio of semimajor to semiminor axis of the elliptic cross section is 3, the body base is at 85 percent of the complete body length, the wing profiles are parabolic arcs having a thickness/chord ratio of 0.04, the wing root chord is 40 percent of the complete body length with the leading edge of the wing root chord located at  $x/l = 0.3$ , the leading edge swept at 45 degrees, a taper ratio of 0.3, and a wing semispan being 28 percent of the complete body length (this implies the trailing edge is straight). The pressure distributions are required to be output at every 2 percent of the complete body length at angular locations  $\theta = 0^\circ, 45^\circ, 90^\circ$ , at radial distances  $r/D = 1, 1.5, 2, 2.5, 3$ , and 3.5 in the crossflow plane, at sonic free-stream conditions and 2 degrees angle of attack, by using the local linearization method to determine the flow about the equivalent body.

Thus, the input data cards would read (note that with a NAMELIST format, input variable sequencing is arbitrary):

CARD NO. 1

COLUMN NO.	2	9	80
	& TRANIN AL=3., AMACH=1., MOPT=1, TAUB=.1, TAUW=.04, XMTB=.5,		

CARD NO. 2

COLUMN NO.	2	80
	XMTW=.5, XRLE=.3, CRT=.4, ANGLE=45., TR=.3, SSMAX=.28, NTHETA=3,	

CARD NO. 3

COLUMN NO.	2	80
	THETA (1)=0., THETA (2)=40., THETA (3)=90., RF (1)=1., RF (2)=1.5,	

CARD NO. 4

COLUMN NO.	2	80
	RF (3)=2., RF (4)=2.5, RF (5)=3., RF (6)=3.5, ALPHA=2., XLOUTP=.02,	

CARD NO. 5

COLUMN NO.	2	80
	&END	

If for this case the user wished to supply his own distribution of  $u_B/U_\infty$  - vs. -  $x/l$ , this would have been done by specifying MOPT = 4 and also the integer NXEB representing the number (say, for example, 101) of values of  $u_B/U_\infty$  being entered (i.e. NXEB = 101) in the NAMELIST input data block. Next, all of the NXEB (101, in this example) values of  $u_B/U_\infty = UEB(I)$  would be read in under the card format 8F10.0, with each successive value of  $u_B/U_\infty$  occupying a space of 10 columns (including decimal point) with 8 values per card. Finally, the NXEB values (101, in this example) of the corresponding axial locations  $x/l = XEB(I)$  of the above values of  $u_B/U_\infty$  would be read in under the same format. Thus,

Card format for UEB(I): Format (8F10.0), decimal point required

COLUMN NO.	10	20	70	80
Data for	UEB (1)	UEB (2)		UEB (8)
	: etc.			

COLUMN NO.	10	20	30	40	50
Data for	UEB (97)	UEB (98)	UEB (99)	UEB (100)	UEB (101)

Card format for XEB(I): Format (8F10.0), decimal point required

COLUMN NO.	10	20	70	80
Data for	XEB (1)	XEB (2)		XEB (8)
	: etc.			

APPENDIX A

COLUMN NO.	10	20	30	40	50
Data for	XEB (97)	XEB (98)	XEB (99)	XEB (100)	XEB (101)

MESSAGES PRINTED BY THE PROGRAMS

This section lists the messages printed by the programs and indicates what to do when they are encountered. The first group of messages (1 to 15) are concerned with errors in input quantities and are self-explanatory.

- (1) INTERVAL SIZE FOR PRESSURE DISTRIBUTION PRINT-OUT MUST BE GREATER THAN 0 AND LESS THAN 1

This message indicates that the condition  $0 < XLOUTP/l < 1$  has been violated.

- (2) XMTB MUST BE GREATER THAN 0 AND LESS THAN 1

This message indicates that the condition  $0 < (x/l)_{R_{max}} < 1$  has been violated.

- (3) EQUIVALENT BODY THICKNESS RATIO MUST BE GREATER THAN ZERO.

This message indicates that the condition  $D/l > 0$  has been violated.

- (4) XMTW MUST BE GREATER THAN 0 AND LESS THAN 1

This message indicates that the condition  $0 < \left(\frac{x}{c_w}\right)_{z_{max}} < 1$  has been violated.

- (5) WING THICKNESS/CHORD RATIO MUST BE GREATER THAN ZERO

This message indicates that the condition  $z_{max}/c_w > 0$  has been violated.

- (6) XRLE MUST BE GREATER THAN 0 AND LESS THAN 1

This message indicates that the condition  $0 < X_{rle}/l < 1$  has been violated.

- (7) CRT MUST BE GREATER THAN 0 AND LESS THAN 1

This message indicates that the condition  $0 < C_{Rt}/l < 1$  has been violated.



## (8) XRLE MUST BE LESS THAN XRTE

This message indicates that the condition  $X_{rle} < X_{rte}$  has been violated.

## (9) ANGLE MUST BE BETWEEN 0 DEGREES AND 90 DEGREES

This message indicates that the condition  $0 < \text{ANGLE} < 90$  has been violated.

## (10) AXIAL LOCATION OF BODY BASE MUST BE AT OR BEHIND POINT WHERE WING TRAILING EDGE PIERCES BODY SURFACE

This message indicates that the condition  $X_{r/e_1} < X_b$  has been violated.

## (11) AXIAL LOCATION OF BODY BASE MUST BE AT OR BEHIND TRAILING EDGE OF WING TIP CHORD

This message indicates that the condition  $X_{sm_2} < X_b$  has been violated.

## (12) RATIO OF MAJOR TO MINOR AXIS MUST BE GREATER THAN 0

This message indicates that the condition  $\lambda (=a/b) > 0$  has been violated.

## (13) TAPER RATIO MUST BE BETWEEN 0 AND 1

This message indicates that the condition  $0 \leq TR \leq 1$  has been violated.

The following error messages, numbers (14) through (18) should not occur in the present programs. If they do, they are probably caused by an error in reproducing the source decks.

## (14) EXECUTION TERMINATED BECAUSE EXPONENT N CANNOT BE DETERMINED TO WITHIN .01 PERCENT IN 20 ITERATIONS

This message is printed by the circular body programs when the exponent  $n$  describing the equivalent body ordinates (see eqs. (11) to (14)) cannot be found accurately from information regarding the point of maximum radius (eqs. (12) or (16)) by using a Newton-Raphson procedure 20 times.

## APPENDIX A

- (15) EXECUTION TERMINATED BECAUSE POINT WHERE WING LEADING EDGE  
PIERCES BODY CANNOT BE FOUND TO WITHIN .01 PERCENT IN 20 ITERATIONS

This message is printed when the point  $X_{rle_1}/l$  cannot be found accurately by using a Newton-Raphson iteration procedure 20 times.

- (16) EXECUTION TERMINATED BECAUSE POINT WHERE WING TRAILING EDGE  
PIERCES BODY CANNOT BE FOUND TO WITHIN .01 PERCENT IN 20  
ITERATIONS

This message is printed when the point  $X_{rte_1}/l$  cannot be found accurately by using a Newton-Raphson iteration procedure 20 times.

- (17) EXECUTION TERMINATED BECAUSE  $SEB''(X)=0$  POINT CANNOT BE DETERMINED  
TO WITHIN SUFFICIENT ACCURACY IN 10 ITERATIONS

This message is printed by the circular body programs when the point  $x_s/l$  cannot be found accurately by using a Newton-Raphson iteration procedure 10 times.

- (18) INTEGRATION TERMINATED BECAUSE ACCUMULATED ERRORS HAVE CAUSED  
INTEGRATION SUBROUTINE TO BISECT ORIGINAL STEP SIZE (.001) 10  
TIMES

This message is printed when the integration subroutine used (Hamming's modified predictor-corrector scheme as described in the Scientific Subroutine Package from IBM Corporation) cannot achieve the integration accuracy (DPRMT(4)) desired even though the original step size (DPRMT(3) = 0.001) has been bisected 10 times.

- (19) PROGRAM TERMINATED BECAUSE INDENTED BODY RADIUS HAS BECOME LESS  
THAN ZERO AT  $x/l =$

This message is printed by the program when the cross-sectional area of the wing is larger than that of the equivalent body, so that the indented body radius is less than zero. A wing with smaller thickness/chord ratio or smaller span must be used.

- (20) PROGRAM TERMINATED BECAUSE INDENTED BODY MAJOR AXIS HAS BECOME  
LESS THAN ZERO AT  $x/l =$

This message is printed by the program for the same reason as message (20).

- (21) CALCULATION TERMINATED BECAUSE FLOW ABOUT EQUIVALENT BODY HAS  
BECOME SUPERSONIC AT  $x/l =$  . INPUT MACH NUMBER GREATER THAN  
LOWER CRITICAL

This message is printed when using the local linearization method for purely subsonic flow to calculate  $u_B$  and indicates that the free stream Mach number is greater than the lower critical. There exists a region of supersonic flow and the local linearization method does not apply.

- (22) CALCULATION TERMINATED BECAUSE FLOW ABOUT EQUIVALENT BODY HAS  
BECOME SUBSONIC AT  $x/l =$

This message is printed using the local linearization method for purely supersonic flow to calculate  $u_B$  and it indicates that a region of subsonic flow has been encountered. This always occurs near the tail of the equivalent bodies considered here and the phenomenon is discussed fully in reference 6. However, if this region occurs at or near the nose, the local linearization method does not apply. In this case, the following error message is also printed,

INPUT MACH NUMBER LESS THAN UPPER CRITICAL

indicating that the condition  $M_{cr,u} < M_\infty$  has been violated.

- (23) START OF SUPERSONIC CALCULATION  
SUPERSONIC CALCULATION STARTS AT  $x/l =$

This message is printed when using the local linearization method for  $M_\infty \approx 1$  flows to calculate  $u_B$  and indicates where transfer is made from the parabolic (eq. (5)) to the hyperbolic (eq. (7)) differential equation. See reference 6 for details.

- (24) START OF SUBSONIC CALCULATION  
SUBSONIC CALCULATION STARTS AT  $x/l =$

This message is printed when using the local linearization method for  $M_\infty \approx 1$  flows to calculate  $u_B$  and indicates where transfer is made from the hyperbolic (eq. (7)) to the elliptic (eq. (6)) differential equation. See reference 6 for details.

## NUMERICAL EXAMPLES

## General Description of the Output

The output format of the program developed is as follows. On the top of the first page, a heading is printed describing the Mach number range, the general class of body (circular or elliptic) and wing being considered, and the theory used. Next, the wing-body geometry and flow field characteristics are printed. Then, if the local linearization method is being used, the program prints the fact that the integrations are starting at  $x = x_s$  and proceeding to the nose. If the user supplies the distribution of  $u_B$ , this is omitted. A heading of independent and dependent variables is printed next which contains, from left to right, the axial location  $x/l$  at which output is to be given, the actual body radius  $R_b/l$  (or actual semimajor axis  $a/l$  in the case of elliptic bodies) at that axial location, the angles  $\theta$  (in degrees) in the crossflow plane at which output is desired, the surface pressure coefficient  $C_p$  (body), and six flow-field pressure coefficients  $C_p(r/D = )$  at the indicated distances  $r/D$  in the crossflow plane. For the case when the user supplies the  $u_B$  distribution, the calculation begins at a point close to the nose and proceeds toward the body base with the values of the above quantities being printed out in the indicated tabular form at specified axial locations. When the local linearization method is used to determine  $u_B$ , the calculation begins at  $x = x_s$  and proceeds to a point close to the nose, with the quantities described being printed at the specified axial locations, then, when the point close to the nose is reached, the program returns to  $x = x_s$ , prints the fact that the integration is restarting at that point and proceeding to the tail, prints the independent and dependent variable heading described above, and proceeds with the calculation to the body base. If it should happen at some point that the radial distance in the crossflow plane at which output is desired is less than the body radius (i.e. the point is inside the body), or if an output point falls on the wing leading or trailing edge, the pressure coefficient at that point is set equal to  $1.E + 6$  and the program continues. Also, because of the discontinuity in the second derivative of the indented body  $d^2R_b/dx^2$  (or  $d^2a/dx^2$ ) at the points  $x/l = X_{rle_1}$  and  $x/l = X_{rte_1}$

and the discontinuity in the slope of the wing span at the points  $x/l = X_{sm_1}$ , and  $x/l = X_{sm_2}$ , output is not printed within a band ( $\Delta x/l = 0.005$ ) of those points. When the calculations are successfully completed, the pertinent aerodynamic coefficients are calculated and printed and the program then proceeds to read the data for the next case.

#### Sample Cases

In order to provide checks on the programs, sample test cases have been run for each program and the results are provided in figures 8 through 12. In each case, the input data is provided together with the corresponding output.

Finally, we note that in order to improve their accuracy, changes have been made in the subroutines, as given in reference 6, which compute the derivatives of the indented circular and elliptic body area distributions. Consequently, the test case results that appear in reference 6 will differ slightly from the results which the current program will produce for those same wing-body geometries.











```

MAIN1049      WRITE (6+400)
MAIN1050      FORMAT (1H0,'43HMTU MUST BE GREATER THAN 0 AND LESS THAN 1 )
MAIN1051      GO TO 10
MAIN1052      WRITE (6+400)
MAIN1053      CALL UMPCG(UMPT,DT,DUERY,NUM,IMLF,FLT,OUTP,UAUX)
MAIN1054      I= (IMH-GI,I) GO TO 10
MAIN1055      GO TO 517
MAIN1056      WRITE (6+400)
MAIN1057      FORMAT (1H0,'43HARLE MUST BE GREATER THAN 0 AND LESS THAN 1 )
MAIN1058      GO TO 10
MAIN1059      WRITE (6+400)
MAIN1060      FORMAT (1H0,'42HLOT MUST BE GREATER THAN 0 AND LESS THAN 1 )
MAIN1061      GO TO 10
MAIN1062      WRITE (6+400)
MAIN1063      40R FORMAT (1H0,'27HARLE MUST BE LESS THAN XRTL )
MAIN1064      GO TO 10
MAIN1065      WRITE (6+400)
MAIN1066      40F FORMAT (1H0,'40HANGLE MUST BE BETWEEN 0 DEG5 AND 90 LF65 )
MAIN1067      GO TO 10
MAIN1068      WRITE (6+410)
MAIN1069      410 FORMAT (1H0,'35HAPR MATIU MUST BE BETWEEN 0 AND 1 )
MAIN1070      GO TO 10
MAIN1071      WRITE (6+411)
MAIN1072      411 FORMAT (1H0,'54HCRATIO OF SEMIMAJOR/SEMIMINOR AXES MUST BE GREATER
          THAN ZERO )
          GO TO 10
MAIN1073      WRITE (6+42)
MAIN1074      382 WRITE (6+482)
MAIN1075      482 FORMAT (1H0,'60HAXIAL LOCATION OF BODY BASE MUST BE AT OR BEHIND
          POINT )
          I=INT WHERE / 1X,'59HMIN TRAILING EDGE PIERCES BODY SURFACE )
          GO TO 10
MAIN1076      WRITE (6+483)
MAIN1077      563 WRITE (6+483)
MAIN1078      483 FORMAT (1H0,'62HAXIAL LOCATION OF BODY BASE MUST BE AT OR BEHIND
          TRAILING EDGE / 1X,'17HOF WING-TIP CHORD )
          GO TO 10
MAIN1081      WRITE (6+483)
MAIN1082      483 FORMAT (1H0,'62HAXIAL LOCATION OF BODY BASE MUST BE AT OR BEHIND
          TRAILING EDGE / 1X,'17HOF WING-TIP CHORD )
          GO TO 10
          END

SUBROUTINE OUTP1(IX,UY,DDERT,IMLF,NGIM,DPHMT)
DIMENSION DT(1),DUERY(1),DPHMT(S)
CALL OUTP(IX,UY,DUERY,IMLF,NGIM,DPHMT)
RETURN
END

C
C SUBROUTINE UMPCG(PRMT,YOERT,NOIM,IMLF,FCI,OUTP,UAUX)
C DIMENSION PRMT(1),Y(1),DEKY(1),AUX(1,6+1)
C COMMON /BLK5/ MH
C IMLF=0
C X=PRMT(1)
C PRMT(15)
C PRMT(19)=0
C DU=1-I-DOIM
C AUX(1,6+1)=DEKY(1)
C AUX(1,1)=1
C 1 AUX(1,1)=1
C IF((PRMT(2)-X) > .3/2+4
C
C 2 EMOR RETURN
C 3 IMLF=1
C
C
C COMPUTATION OF DEKY FOR STARTING VALUES
C CALL FCI(1,1,DEKY)
  
```

```

MAIN1577      WRITE (6+400)
MAIN1578      FORMAT (1H0,'43HMTU MUST BE GREATER THAN 0 AND LESS THAN 1 )
MAIN1579      GO TO 10
MAIN1580      WRITE (6+400)
MAIN1581      CALL UMPCG(UMPT,DT,DUERY,NUM,IMLF,FLT,OUTP,UAUX)
MAIN1582      I= (IMH-GI,I) GO TO 10
MAIN1583      GO TO 517
MAIN1584      WRITE (6+400)
MAIN1585      FORMAT (1H0,'43HARLE MUST BE GREATER THAN 0 AND LESS THAN 1 )
MAIN1586      GO TO 10
MAIN1587      WRITE (6+400)
MAIN1588      FORMAT (1H0,'42HLOT MUST BE GREATER THAN 0 AND LESS THAN 1 )
MAIN1589      GO TO 10
MAIN1590      WRITE (6+400)
MAIN1591      40R FORMAT (1H0,'27HARLE MUST BE LESS THAN XRTL )
MAIN1592      GO TO 10
MAIN1593      WRITE (6+400)
MAIN1594      40F FORMAT (1H0,'40HANGLE MUST BE BETWEEN 0 DEG5 AND 90 LF65 )
MAIN1595      GO TO 10
MAIN1596      WRITE (6+410)
MAIN1597      410 FORMAT (1H0,'35HAPR MATIU MUST BE BETWEEN 0 AND 1 )
MAIN1598      GO TO 10
MAIN1599      WRITE (6+411)
MAIN1600      411 FORMAT (1H0,'54HCRATIO OF SEMIMAJOR/SEMIMINOR AXES MUST BE GREATER
          THAN ZERO )
          GO TO 10
MAIN1601      WRITE (6+42)
MAIN1602      382 WRITE (6+482)
MAIN1603      482 FORMAT (1H0,'60HAXIAL LOCATION OF BODY BASE MUST BE AT OR BEHIND
          POINT )
          I=INT WHERE / 1X,'59HMIN TRAILING EDGE PIERCES BODY SURFACE )
          GO TO 10
MAIN1604      WRITE (6+483)
MAIN1605      563 WRITE (6+483)
MAIN1606      483 FORMAT (1H0,'62HAXIAL LOCATION OF BODY BASE MUST BE AT OR BEHIND
          TRAILING EDGE / 1X,'17HOF WING-TIP CHORD )
          GO TO 10
MAIN1607      WRITE (6+483)
MAIN1608      483 FORMAT (1H0,'62HAXIAL LOCATION OF BODY BASE MUST BE AT OR BEHIND
          TRAILING EDGE / 1X,'17HOF WING-TIP CHORD )
          GO TO 10
MAIN1611      WRITE (6+483)
MAIN1612      483 FORMAT (1H0,'62HAXIAL LOCATION OF BODY BASE MUST BE AT OR BEHIND
          TRAILING EDGE / 1X,'17HOF WING-TIP CHORD )
          GO TO 10
MAIN1613      WRITE (6+483)
MAIN1614      483 FORMAT (1H0,'62HAXIAL LOCATION OF BODY BASE MUST BE AT OR BEHIND
          TRAILING EDGE / 1X,'17HOF WING-TIP CHORD )
          GO TO 10
MAIN1615      WRITE (6+483)
MAIN1616      483 FORMAT (1H0,'62HAXIAL LOCATION OF BODY BASE MUST BE AT OR BEHIND
          TRAILING EDGE / 1X,'17HOF WING-TIP CHORD )
          GO TO 10
MAIN1617      WRITE (6+483)
MAIN1618      483 FORMAT (1H0,'62HAXIAL LOCATION OF BODY BASE MUST BE AT OR BEHIND
          TRAILING EDGE / 1X,'17HOF WING-TIP CHORD )
          GO TO 10
MAIN1619      WRITE (6+483)
MAIN1620      483 FORMAT (1H0,'62HAXIAL LOCATION OF BODY BASE MUST BE AT OR BEHIND
          TRAILING EDGE / 1X,'17HOF WING-TIP CHORD )
          GO TO 10
MAIN1621      WRITE (6+483)
MAIN1622      483 FORMAT (1H0,'62HAXIAL LOCATION OF BODY BASE MUST BE AT OR BEHIND
          TRAILING EDGE / 1X,'17HOF WING-TIP CHORD )
          GO TO 10
MAIN1623      WRITE (6+483)
MAIN1624      483 FORMAT (1H0,'62HAXIAL LOCATION OF BODY BASE MUST BE AT OR BEHIND
          TRAILING EDGE / 1X,'17HOF WING-TIP CHORD )
          GO TO 10
MAIN1625      WRITE (6+483)
MAIN1626      483 FORMAT (1H0,'62HAXIAL LOCATION OF BODY BASE MUST BE AT OR BEHIND
          TRAILING EDGE / 1X,'17HOF WING-TIP CHORD )
          GO TO 10
MAIN1627      WRITE (6+483)
MAIN1628      483 FORMAT (1H0,'62HAXIAL LOCATION OF BODY BASE MUST BE AT OR BEHIND
          TRAILING EDGE / 1X,'17HOF WING-TIP CHORD )
          GO TO 10
MAIN1629      WRITE (6+483)
MAIN1630      483 FORMAT (1H0,'62HAXIAL LOCATION OF BODY BASE MUST BE AT OR BEHIND
          TRAILING EDGE / 1X,'17HOF WING-TIP CHORD )
          GO TO 10
MAIN1631      WRITE (6+483)
MAIN1632      483 FORMAT (1H0,'62HAXIAL LOCATION OF BODY BASE MUST BE AT OR BEHIND
          TRAILING EDGE / 1X,'17HOF WING-TIP CHORD )
          GO TO 10
MAIN1633      WRITE (6+483)
MAIN1634      483 FORMAT (1H0,'62HAXIAL LOCATION OF BODY BASE MUST BE AT OR BEHIND
          TRAILING EDGE / 1X,'17HOF WING-TIP CHORD )
          GO TO 10
MAIN1635      WRITE (6+483)
MAIN1636      483 FORMAT (1H0,'62HAXIAL LOCATION OF BODY BASE MUST BE AT OR BEHIND
          TRAILING EDGE / 1X,'17HOF WING-TIP CHORD )
          GO TO 10
MAIN1637      WRITE (6+483)
MAIN1638      483 FORMAT (1H0,'62HAXIAL LOCATION OF BODY BASE MUST BE AT OR BEHIND
          TRAILING EDGE / 1X,'17HOF WING-TIP CHORD )
          GO TO 10
MAIN1639      WRITE (6+483)
MAIN1640      483 FORMAT (1H0,'62HAXIAL LOCATION OF BODY BASE MUST BE AT OR BEHIND
          TRAILING EDGE / 1X,'17HOF WING-TIP CHORD )
          GO TO 10
MAIN1641      WRITE (6+483)
MAIN1642      483 FORMAT (1H0,'62HAXIAL LOCATION OF BODY BASE MUST BE AT OR BEHIND
          TRAILING EDGE / 1X,'17HOF WING-TIP CHORD )
          GO TO 10
MAIN1643      WRITE (6+483)
MAIN1644      483 FORMAT (1H0,'62HAXIAL LOCATION OF BODY BASE MUST BE AT OR BEHIND
          TRAILING EDGE / 1X,'17HOF WING-TIP CHORD )
          GO TO 10
MAIN1645      WRITE (6+483)
MAIN1646      483 FORMAT (1H0,'62HAXIAL LOCATION OF BODY BASE MUST BE AT OR BEHIND
          TRAILING EDGE / 1X,'17HOF WING-TIP CHORD )
          GO TO 10
MAIN1647      WRITE (6+483)
MAIN1648      483 FORMAT (1H0,'62HAXIAL LOCATION OF BODY BASE MUST BE AT OR BEHIND
          TRAILING EDGE / 1X,'17HOF WING-TIP CHORD )
          GO TO 10
MAIN1649      WRITE (6+483)
MAIN1650      483 FORMAT (1H0,'62HAXIAL LOCATION OF BODY BASE MUST BE AT OR BEHIND
          TRAILING EDGE / 1X,'17HOF WING-TIP CHORD )
          GO TO 10
  
```



APPENDIX B

222 H MUST BE HALVED
223 IF (INLF=1) DELT=223.223.210
224 H=5\*H
225 ISTEP=0
DO 224 I=1,NDIM
Y(I)=.39025E-2\*(6.E1\*AUX(N-1))+135.00\*AUX(N-2)+I+.E1\*AUX(N-3)+
J\*AUX(N-4)+I)-.117875\*(AUX(N+1)-6.\*AUX(N+5))-AUX(N+4)+I)+H
AUX(N-4)+I)=.39025E-2\*(12.00\*AUX(N-1))+135.00\*AUX(N-2)+I)+
1109.00\*AUX(N-3)+AUX(N-4)+I)-.023575\*(AUX(N+6)+I)+
218.00\*AUX(N+5)+I)-9.00\*AUX(N+4)+I)+H
AUX(N-3)+I)=AUX(N-2)+I
AUX(N-4)+I)=AUX(N-5)+I
K=K+H
DELTA=(H+H)
CALL FCT(DELTA,DELTA)
IF (MM.GT.1) RETURN
DO 225 I=1,NDIM
AUX(N-2)+I)=I
AUX(N-5)+I)=QUERY(I)
225 Y(I)=AUX(N-4)+I
DELTA=DELTA\*(H+H)
CALL FCT(DELTA,DELTA)
IF (MM.GT.1) RETURN
DO 226 I=1,NDIM
DELTA=AUX(N-5)+I\*DELTA
DELTA=DELTA\*(H+H)
AUX(N-1)=2\*H\*DELTA\*(AUX(N-1)+Y(I))
AUX(N-3)=3\*I\*DELTA\*(AUX(N-3)+Y(I))
DELTA=DELTA\*(H+H)
226 AUX(N-3)+I)=QUERY(I)
GO TO 206
END

203 AUX(N+6)=AUX(N+7)
204 NET
205 N LESS THAN A CAUSES N+1 TO GET N
206 NEN=N+1
207 COMPUTATION OF NEXT VECTOR Y
DO 205 I=1,NDIM
AUX(N-1)+I)=I
205 AUX(N+6)=I\*QUERY(I)
206 ISTEP=ISTEP+1
DO 207 I=1,NDIM
DELTA=AUX(N-4)+I)+.33333333\*(AUX(N+6)+I)-AUX(N+5)+I)+AUX(N+6)+I)
1\*(N+4)+I)+AUX(N+6)+I)
DHPG6181
DHPG6182
DHPG6183
DHPG6184
DHPG6185
DHPG6186
DHPG6187
DHPG6188
DHPG6189
DHPG6190
DHPG6191
DHPG6192
DHPG6193
DHPG6194
DHPG6195
DHPG6196
DHPG6197
DHPG6198
DHPG6199
DHPG6200
DHPG6201
DHPG6202
DHPG6203
DHPG6204
DHPG6205
DHPG6206
DHPG6207
DHPG6208
DHPG6209
DHPG6210
DHPG6211
DHPG6212
DHPG6213
DHPG6214
DHPG6215
DHPG6216
DHPG6217
DHPG6218
DHPG6219
DHPG6220
DHPG6221
DHPG6222
DHPG6223
DHPG6224
DHPG6225
DHPG6226
DHPG6227
DHPG6228
DHPG6229
DHPG6230
DHPG6231
DHPG6232
DHPG6233
DHPG6234
DHPG6235
DHPG6236
DHPG6237
DHPG6238
DHPG6239
DHPG6240
DHPG6241
DHPG6242
DHPG6243
DHPG6244
DHPG6245
DHPG6246
DHPG6247
DHPG6248
DHPG6249
DHPG6250
DHPG6251
DHPG6252
DHPG6253
DHPG6254
DHPG6255
DHPG6256
DHPG6257
DHPG6258
DHPG6259
DHPG6260
DHPG6261
DHPG6262
DHPG6263
DHPG6264
DHPG6265
DHPG6266
DHPG6267
DHPG6268
DHPG6269
DHPG6270
DHPG6271

PHTKS108	VTZ=DZWAY
PHTKS109	RETURN
PHTKS110	50 VTBZ=2 *DZRN*XUL*(ALOG(XUL/R)-1.)
PHTKS111	VTFRZ=2 *DZRN*(XU*ALOG(XUL/PU)-R*ALOG(KUL/K))
PHTKS112	VX10E=0.
PHTKS113	VTKR=-4.*UZH*URUX*ALOG(Z.*XUL/R)
PHTKS114	GO TO 51
PHTKS115	33 VTYE=0.
PHTKS116	VYTBZ=XUL*2
PHTKS117	GO TO 54
PHTKS118	500 STE=SPANT(X)
PHTKS119	SLE=SPANLE(X)
PHTKS120	DSLEDRE=JSPCL(X)
PHTKS121	USTEDRE=USPTL(X)
PHTKS122	HRR=RG(X)
PHTKS123	UMDX=UMGDA(X)
PHTKS124	DZLE=DUZADA(X*SLE)
PHTKS126	DZTE=DUZADA(X*STE)
PHTKS127	VTEY
PHTKS128	ZZZZ
PHTKS129	42=RRH**2
PHTKS130	ZZZ**2
PHTKS131	ZZZ**2
PHTKS132	ZZZ**2
PHTKS133	ZZZ**2
PHTKS134	ZZZ**2
PHTKS135	ZZZ**2
PHTKS136	ZZZ**2
PHTKS137	A1=Z2*(1+R*STE)**2
PHTKS138	A2=Z2*(1+R*SLE)**2
PHTKS139	A3=Z2*(1+R*SLE)**2
PHTKS140	A4=Z2*(1+R*SLE)**2
PHTKS141	A5=Z2*(1+R*STE)**2
PHTKS142	A6=Z2*(1+R*STE)**2
PHTKS143	A7=Z2*(1+R*STE)**2
PHTKS144	A8=Z2*(1+R*STE)**2
PHTKS145	VTXMLE=UZLE+USLED*ALOG(A1+A2+A3+A4+A5+A6+A7+A8)
PHTKS146	VYXMLE=DZTE+USTEUX*ALOG(A5+A6+A7+A8/Ztn)
PHTKS147	VTFRP12=2*SLE*HP1(X)*ALOG(ZTn)
PHTKS148	CALL SIMP1(STE,SLE,NIT,NIIT,TOL,FUNX1,X,VTX)
PHTKS149	VTYZ=1-4.*VTYZ*PI2*SLE*HP1(X)/ZT2
PHTKS150	IF (ABS(Z)-LE,1-E=4) GO TO 94
PHTKS151	GO TO 96
PHTKS152	99 IF (ABS(Y)-LT,SLE-A/D,ARS(Y),GT,STE) GO TO 100
PHTKS153	94 CALL SIMP1(STE,SLE,NIT,NIIT,TOL,FUNX1,X,VTX1)
PHTKS154	CALL SIMP1(STE,SLE,NIT,NIIT,TOL,FUNX2,X,VTX2)
PHTKS155	VTKZ=4.*RRH*UMDX*VTX2
PHTKS156	VTK=(VTX1+VTX2+VTXMLE*VTXSTE+VTX1*PI2)
PHTKS157	CALL SIMP1(STE,SLE,NIT,NIIT,TOL,FUNY1,X,VTY1)
PHTKS158	VTYZ=Y*VTYZ
PHTKS159	VY=(VY+VTY+VTYZ)/PI
PHTKS160	IF (ABS(Z)-LE,1-E=4) GO TO 97
PHTKS161	CALL SIMP1(STE,SLE,NIT,NIIT,TOL,FUNZ1,X,VTZ1)
PHTKS162	VTZ1=Z*VTZ1
PHTKS163	VTZ=(VTZ1+VTZ2)/PI
PHTKS164	RETURN
PHTKS165	97 VTZ=0.
PHTKS167	100 RETURN
PHTKS168	DZWAY=DZWAY(X,Y)
PHTKS169	DZWAY=U2ZDAY(X,Y)
PHTKS170	RZYRZ/7
PHTKS171	SLEYSLE-1
PHTKS172	YSTE=STC
PHTKS173	CALL SIMP1(STE,SLE,NIT,NIIT,TOL,FUNAR,X,VTX1)
PHTKS174	CALL SIMP1(STE,SLE,NIT,NIIT,TOL,FUNAR,X,VTX4)
PHTKS175	CALL SIMP1(STE,SLE,NIT,NIIT,TOL,FUNAR,X,VTX12)
PHTKS176	VTX12=4.*RRH*UMDX*VTX12
PHTKS177	VTX12=0.2ZRN*VTK*SLE*ALOG(SLE/Y)-1.)
PHTKS178	VTK=(VTX1+VTX4+VTX12+VTX12*VTX12+VTXMLE*VTX12)/PI2

PHTKS036	VTK=Z1-Z2-ZTZ
PHTKS037	VTK=Z1-ZTZ
PHTKS038	RZSLE=AL
PHTKS039	RZSLE=AL
PHTKS040	VTEY
PHTKS041	ZZZ
PHTKS042	RZSLE=AL
PHTKS043	RZSLE=AL
PHTKS044	RZSLE=AL
PHTKS045	A1=Z2*(1+R*STE)**2
PHTKS046	A2=Z2*(1+R*STE)**2
PHTKS047	A3=Z2*(1+R*STE)**2
PHTKS048	A4=Z2*(1+R*STE)**2
PHTKS049	A5=Z2*(1+R*STE)**2
PHTKS050	A6=Z2*(1+R*STE)**2
PHTKS051	VTKMLE=UZLE+USLED*ALOG(A1+A2+A3+A4+A5+A6)
PHTKS052	VTKMLE=DZTE+USTEUX*ALOG(A5+A6/Ztn)
PHTKS053	CALL SIMP1(STE,SLE,NIT,NIIT,TOL,FUNX1,X,VTX1)
PHTKS054	VTKMLE=UZLE+USLED*ALOG(ZTn)
PHTKS055	CALL SIMP1(STE,SLE,NIT,NIIT,TOL,FUNX1,X,VTX1)
PHTKS056	CALL SIMP1(STE,SLE,NIT,NIIT,TOL,FUNX1,X,VTX1)
PHTKS057	VTKMLE=UZLE+USLED*ALOG(ZTn)
PHTKS058	VTKMLE=DZTE+USTEUX*ALOG(ZTn)
PHTKS059	CALL SIMP1(STE,SLE,NIT,NIIT,TOL,FUNX1,X,VTX1)
PHTKS060	CALL SIMP1(STE,SLE,NIT,NIIT,TOL,FUNX2,X,VTX2)
PHTKS061	VTKZ=4.*RRH*UMDX*VTX2
PHTKS062	VTK=(VTX1+VTX2+VTXMLE*VTX1*PI2)
PHTKS063	CALL SIMP1(STE,SLE,NIT,NIIT,TOL,FUNY1,X,VTY1)
PHTKS064	VTYZ=Y*VTYZ
PHTKS065	VY=(VY+VTY+VTYZ)/PI
PHTKS066	IF (ABS(Z)-LE,1-E=4) GO TO 400
PHTKS067	CALL SIMP1(STE,SLE,NIT,NIIT,TOL,FUNZ1,X,VTZ1)
PHTKS068	VTZ1=Z*VTZ1
PHTKS069	VTZ=(VTZ1+VTZ2)/PI
PHTKS070	RETURN
PHTKS071	400 VTZ=0.
PHTKS072	1 DE TURN
PHTKS073	UZWAY=UZWAY(X,Y)
PHTKS074	UZWAY=U2ZWAY(X,Y)
PHTKS075	UZWAY=U2ZWAY(X,Y)
PHTKS076	UZWAY=U2ZWAY(X,Y)
PHTKS077	UZWAY=U2ZWAY(X,Y)
PHTKS078	UZWAY=U2ZWAY(X,Y)
PHTKS079	UZWAY=U2ZWAY(X,Y)
PHTKS080	UZWAY=U2ZWAY(X,Y)
PHTKS081	UZWAY=U2ZWAY(X,Y)
PHTKS082	UZWAY=U2ZWAY(X,Y)
PHTKS083	UZWAY=U2ZWAY(X,Y)
PHTKS084	CALL SIMP1(STE,SLE,NIT,NIIT,TOL,FUNX3,X,VTX3)
PHTKS085	CALL SIMP1(STE,SLE,NIT,NIIT,TOL,FUNX4,X,VTX4)
PHTKS086	CALL SIMP1(STE,SLE,NIT,NIIT,TOL,FUNX5,X,VTX5)
PHTKS087	CALL SIMP1(STE,SLE,NIT,NIIT,TOL,FUNX6,X,VTX6)
PHTKS088	VTX6=4.*RRH*UMDX*VTX6
PHTKS089	VTK=(VTX3+VTX4+VTX5+VTX6+VTX7+VTX8+VTX9)
PHTKS090	VTX7=4.*RRH*UMDX*VTX7
PHTKS091	VTX7=4.*RRH*UMDX*VTX7
PHTKS092	IF (ABS(Y)-LT,SLE-A/D,ARS(Y)-1.)
PHTKS093	VTKZ=2.*DZRN*(XU*ALOG(SRY/Y))-1.)
PHTKS094	VTK=(VTX3+VTX4+VTX5+VTX6+VTX7+VTX8+VTX9)
PHTKS095	VTKZ=2.*DZRN*(XU*ALOG(SRY/Y))-1.)
PHTKS096	VTKZ=2.*DZRN*(XU*ALOG(SRY/Y))-1.)
PHTKS097	VTKZ=2.*DZRN*(XU*ALOG(SRY/Y))-1.)
PHTKS098	VTKZ=2.*DZRN*(XU*ALOG(SRY/Y))-1.)
PHTKS099	VTX9=4.*RRH*UMDX*VTX9
PHTKS100	VTK=(VTX3+VTX4+VTX5+VTX6+VTX7+VTX8+VTX9)
PHTKS101	VTKZ=2.*DZRN*(XU*ALOG(SRY/Y))-1.)
PHTKS102	VTX9=4.*RRH*UMDX*VTX9
PHTKS103	VTX9=4.*RRH*UMDX*VTX9
PHTKS104	VTKZ=2.*DZRN*(XU*ALOG(SRY/Y))-1.)
PHTKS105	VTKZ=2.*DZRN*(XU*ALOG(SRY/Y))-1.)
PHTKS106	VTKZ=2.*DZRN*(XU*ALOG(SRY/Y))-1.)
PHTKS107	VTKZ=2.*DZRN*(XU*ALOG(SRY/Y))-1.)





```

PHLFT064
PHLFT065
PHLFT066
PHLFT067
PHLFT068
PHLFT069
PHLFT070
PHLFT071
PHLFT072
PHLFT073
PHLFT074
PHLFT075
PHLFT076
PHLFT077
PHLFT078
PHLFT079
PHLFT080
PHLFT081
PHLFT082
PHLFT083
PHLFT084
PHLFT085
PHLFT086
PHLFT087
PHLFT088
PHLFT089
PHLFT090
PHLFT091
PHLFT092
PHLFT093
PHLFT094
PHLFT095
PHLFT096
PHLFT097
PHLFT098
PHLFT099
PHLFT100
PHLFT101
PHLFT102
PHLFT103
PHLFT104
PHLFT105
PHLFT106
PHLFT107

R1S1=K1/S1
S1R2S1=S1*R2/S1
R1S1S2=R1S1*R1S1
C=CMPLX(YI,ZI)
IF (ABS(IN2-ZI2).LE.1.E-5) GO TO 13
C1=R2/C
C2=C1/C
C3=C4C1
C4=C3+C3
C5=C1/R1
C6=C7/C+C-.25*A2H22)
CNMEL3=(1.-C2)*C6C
CENELCSORT(C4-S1R2S1*S1R2S1)
CF=CONUM/CUE4
UF1=REAL(CF)
UF2=AIMAG(CF)
D=2*E-30*0.1C+A*0A1DX
S1R2S1=S1R2S1/3.1415926535897932384626
DR1=DC*E-30*0.1C+A*0A1DX
CGNMELC*(1.-C2)*S1R2S1*(1.-R1S1S2)*0S1UX*2.*(C3+C5-S1R2S1)
R1S1I=0K1UX
C4=C6GMUM/LC4N
D4=2*AIMAG(C4)
V1=DC2
V2=DC2
V3=DF*1-1.
RETURN

14  IF (ABS(YI).LE.1.E-4) GO TO 15
    THE1=ATAN(DL*Z/Y)
16  C1=THE1*CMPLX(I0.,THE1)
    C2=CEXP(-C*THE1)
    DCOS=REAL(C2)
    IF (ABS(LUCOS).LE.1.E-4) UCOS=0.
    C1=R1+C3
    C2=CEXP(-Z*CTHET1)
    C3=2.*R.A*UCOS
    C4=C3+C3
    GO TO 14
15  THE1=PI/2.
    IF (Z.LT..0) GO TO 17
    GO TO 16
17  THE1=3.*THE1
    GO TO 16
    END
  
```

```

PHLFT001
PHLFT002
PHLFT003
PHLFT004
PHLFT005
PHLFT006
PHLFT007
PHLFT008
PHLFT009
PHLFT010
PHLFT011
PHLFT012
PHLFT013
PHLFT014
PHLFT015
PHLFT016
PHLFT017
PHLFT018
PHLFT019
PHLFT020
PHLFT021
PHLFT022
PHLFT023
PHLFT024
PHLFT025
PHLFT026
PHLFT027
PHLFT028
PHLFT029
PHLFT030
PHLFT031
PHLFT032
PHLFT033
PHLFT034
PHLFT035
PHLFT036
PHLFT037
PHLFT038
PHLFT039
PHLFT040
PHLFT041
PHLFT042
PHLFT043
PHLFT044
PHLFT045
PHLFT046
PHLFT047
PHLFT048
PHLFT049
PHLFT050
PHLFT051
PHLFT052
PHLFT053
PHLFT054
PHLFT055
PHLFT056
PHLFT057
PHLFT058
PHLFT059
PHLFT060
PHLFT061
PHLFT062
PHLFT063
PHLFT064
PHLFT065
PHLFT066
PHLFT067
PHLFT068
PHLFT069
PHLFT070
PHLFT071
PHLFT072
PHLFT073
PHLFT074
PHLFT075
PHLFT076
PHLFT077
PHLFT078
PHLFT079
PHLFT080
PHLFT081
PHLFT082
PHLFT083
PHLFT084
PHLFT085
PHLFT086
PHLFT087
PHLFT088
PHLFT089
PHLFT090
PHLFT091
PHLFT092
PHLFT093
PHLFT094
PHLFT095
PHLFT096
PHLFT097
PHLFT098
PHLFT099
PHLFT100
PHLFT101
PHLFT102
PHLFT103
PHLFT104
PHLFT105
PHLFT106
PHLFT107

SUBROUTINE PHLFTI(Y,Z,VLX,VLY,VLZ)
  IMPLICIT COMPLEX*8(C)
  COMMON /BLK4/ DL,DL2,DL3,DL4,M,MUPT,MELLPT
  IF (MUPT.EQ.1) GO TO 300
  M=2*E-30*0.1C+A*0A1DX
  C=CMPLX(YI,ZI)
  IF (ABS(IN2-ZI2).LE.1.E-5) GO TO 300
  C1=R2/C
  C2=C1/C
  C3=C4C1
  C4=C3+C3
  C5=C1/R1
  C6=C7/C+C-.25*A2H22)
  CNMEL3=(1.-C2)*C6C
  CENELCSORT(C4-S1R2S1*S1R2S1)
  CF=CONUM/CUE4
  UF1=REAL(CF)
  UF2=AIMAG(CF)
  D=2*E-30*0.1C+A*0A1DX
  S1R2S1=S1R2S1/3.1415926535897932384626
  DR1=DC*E-30*0.1C+A*0A1DX
  CGNMELC*(1.-C2)*S1R2S1*(1.-R1S1S2)*0S1UX*2.*(C3+C5-S1R2S1)
  R1S1I=0K1UX
  C4=C6GMUM/LC4N
  D4=2*AIMAG(C4)
  V1=DC2
  V2=DC2
  V3=DF*1-1.
  RETURN

11  SK2=XU*Z2/ZU
    P=XL/XU
    GN=SR2*(P+.S)*UNDA*(1.-K*S*R5)*D5DX1
    I=(ABS(ZI2-K22).LL.1.E-5) GO TO 3
    C1=CMPLX(YI,ZI)
    C1M2=Z1/S16
    C2=C1/C16
    C3=C51G+C1
    C4=C3+C3
    C5=2*E-30*0.1C+A*0A1DX
    C6=C3/C3
    C7=2*E-30*0.1C+A*0A1DX
    C8=C51G+C1
    C9=C3+C3
    C10=C3/C3
    C11=C51G+C1
    C12=C3+C3
    C13=C51G+C1
    C14=C3+C3
    C15=C51G+C1
    C16=C3+C3
    C17=C51G+C1
    C18=C3+C3
    C19=C51G+C1
    C20=C3+C3
    C21=C51G+C1
    C22=C3+C3
    C23=C51G+C1
    C24=C3+C3
    C25=C51G+C1
    C26=C3+C3
    C27=C51G+C1
    C28=C3+C3
    C29=C51G+C1
    C30=C3+C3
    C31=C51G+C1
    C32=C3+C3
    C33=C51G+C1
    C34=C3+C3
    C35=C51G+C1
    C36=C3+C3
    C37=C51G+C1
    C38=C3+C3
    C39=C51G+C1
    C40=C3+C3
    C41=C51G+C1
    C42=C3+C3
    C43=C51G+C1
    C44=C3+C3
    C45=C51G+C1
    C46=C3+C3
    C47=C51G+C1
    C48=C3+C3
    C49=C51G+C1
    C50=C3+C3
    C51=C51G+C1
    C52=C3+C3
    C53=C51G+C1
    C54=C3+C3
    C55=C51G+C1
    C56=C3+C3
    C57=C51G+C1
    C58=C3+C3
    C59=C51G+C1
    C60=C3+C3
    C61=C51G+C1
    C62=C3+C3
    C63=C51G+C1
    C64=C3+C3
    C65=C51G+C1
    C66=C3+C3
    C67=C51G+C1
    C68=C3+C3
    C69=C51G+C1
    C70=C3+C3
    C71=C51G+C1
    C72=C3+C3
    C73=C51G+C1
    C74=C3+C3
    C75=C51G+C1
    C76=C3+C3
    C77=C51G+C1
    C78=C3+C3
    C79=C51G+C1
    C80=C3+C3
    C81=C51G+C1
    C82=C3+C3
    C83=C51G+C1
    C84=C3+C3
    C85=C51G+C1
    C86=C3+C3
    C87=C51G+C1
    C88=C3+C3
    C89=C51G+C1
    C90=C3+C3
    C91=C51G+C1
    C92=C3+C3
    C93=C51G+C1
    C94=C3+C3
    C95=C51G+C1
    C96=C3+C3
    C97=C51G+C1
    C98=C3+C3
    C99=C51G+C1
    C100=C3+C3
  
```

```

OUTP0001
OUTP0002
OUTP0003
OUTP0004
OUTP0005
OUTP0006
OUTP0007
OUTP0008
OUTP0009
OUTP0010
OUTP0011
OUTP0012
OUTP0013
OUTP0014
OUTP0015
OUTP0016
OUTP0017
OUTP0018
OUTP0019
OUTP0020

SUBROUTINE OUTP(OX,DY,DDERY,IMLF,M0IN,DPRINT)
  IMPLICIT COMPLEX*8(C)
  REAL CPU,CPL,COOS
  DIMENSION D(17),DPL(17),UPMT(5)
  DIMENSION CAU(7),DPL(7),RF(7),THE1(5),THE2(5),YH(5),THE2(5),THE1(5),THE2(5),THE1(5),THE2(5),THE1(5),THE2(5)
  IZAL(1),C3(L5)
  COMMON /BLK2/ DX11,DX12,DUJ1,DUJ2,DCD,ALPHA,THETA,THE1,THE2,
  IRF,YN1,ZHL,SCS,DKMTE,MMH,MM,M11,NTHETA,IC,ICOPY
  COMMON /BLK3/ DN,UN1,UN2,XTEML,XHLE,XRTE,TBLE,TRIE,TBLNTE,XCMT,
  IRLSK1,XLSM2,SSMAX,DAIR,MTE,MTR
  COMMON /BLK4/ AL,AL12,AL1,AL2,AL3,AL4,M,MPT,MELLPT
  COMMON /BLK5/ XRLE1,XRTE1,HH,M3,MM
  COMMON /BLK6/ PI,PI2,TOL,NIT
  COMMON /BLK7/ NH
  COMMON /BLK10/ DHE,DEF
  COMMON /BLK11/ RF,II
  IF (MPT.EQ.4) GO TO 2000
  IF (M.LQ.2) OK=MOPT-EG.3) GO TO 3
  IF (M.EQ.3) OK=MOPT-EG.2) GO TO 11
  
```

```

PHLFT548
PHLFT549
PHLFT550
PHLFT551

SUBROUTINE PHLFTI(Y,Z,VLX,VLY,VLZ)
  IMPLICIT COMPLEX*8(C)
  COMMON /BLK4/ DL,DL2,DL3,DL4,M,MUPT,MELLPT
  IF (MUPT.EQ.1) GO TO 300
  M=2*E-30*0.1C+A*0A1DX
  C=CMPLX(YI,ZI)
  IF (ABS(IN2-ZI2).LE.1.E-5) GO TO 300
  C1=R2/C
  C2=C1/C
  C3=C4C1
  C4=C3+C3
  C5=C1/R1
  C6=C7/C+C-.25*A2H22)
  CNMEL3=(1.-C2)*C6C
  CENELCSORT(C4-S1R2S1*S1R2S1)
  CF=CONUM/CUE4
  UF1=REAL(CF)
  UF2=AIMAG(CF)
  D=2*E-30*0.1C+A*0A1DX
  S1R2S1=S1R2S1/3.1415926535897932384626
  DR1=DC*E-30*0.1C+A*0A1DX
  CGNMELC*(1.-C2)*S1R2S1*(1.-R1S1S2)*0S1UX*2.*(C3+C5-S1R2S1)
  R1S1I=0K1UX
  C4=C6GMUM/LC4N
  D4=2*AIMAG(C4)
  V1=DC2
  V2=DC2
  V3=DF*1-1.
  RETURN

11  SK2=XU*Z2/ZU
    P=XL/XU
    GN=SR2*(P+.S)*UNDA*(1.-K*S*R5)*D5DX1
    I=(ABS(ZI2-K22).LL.1.E-5) GO TO 3
    C1=CMPLX(YI,ZI)
    C1M2=Z1/S16
    C2=C1/C16
    C3=C51G+C1
    C4=C3+C3
    C5=2*E-30*0.1C+A*0A1DX
    C6=C3/C3
    C7=2*E-30*0.1C+A*0A1DX
    C8=C51G+C1
    C9=C3+C3
    C10=C3/C3
    C11=C51G+C1
    C12=C3+C3
    C13=C51G+C1
    C14=C3+C3
    C15=C51G+C1
    C16=C3+C3
    C17=C51G+C1
    C18=C3+C3
    C19=C51G+C1
    C20=C3+C3
    C21=C51G+C1
    C22=C3+C3
    C23=C51G+C1
    C24=C3+C3
    C25=C51G+C1
    C26=C3+C3
    C27=C51G+C1
    C28=C3+C3
    C29=C51G+C1
    C30=C3+C3
    C31=C51G+C1
    C32=C3+C3
    C33=C51G+C1
    C34=C3+C3
    C35=C51G+C1
    C36=C3+C3
    C37=C51G+C1
    C38=C3+C3
    C39=C51G+C1
    C40=C3+C3
    C41=C51G+C1
    C42=C3+C3
    C43=C51G+C1
    C44=C3+C3
    C45=C51G+C1
    C46=C3+C3
    C47=C51G+C1
    C48=C3+C3
    C49=C51G+C1
    C50=C3+C3
    C51=C51G+C1
    C52=C3+C3
    C53=C51G+C1
    C54=C3+C3
    C55=C51G+C1
    C56=C3+C3
    C57=C51G+C1
    C58=C3+C3
    C59=C51G+C1
    C60=C3+C3
    C61=C51G+C1
    C62=C3+C3
    C63=C51G+C1
    C64=C3+C3
    C65=C51G+C1
    C66=C3+C3
    C67=C51G+C1
    C68=C3+C3
    C69=C51G+C1
    C70=C3+C3
    C71=C51G+C1
    C72=C3+C3
    C73=C51G+C1
    C74=C3+C3
    C75=C51G+C1
    C76=C3+C3
    C77=C51G+C1
    C78=C3+C3
    C79=C51G+C1
    C80=C3+C3
    C81=C51G+C1
    C82=C3+C3
    C83=C51G+C1
    C84=C3+C3
    C85=C51G+C1
    C86=C3+C3
    C87=C51G+C1
    C88=C3+C3
    C89=C51G+C1
    C90=C3+C3
    C91=C51G+C1
    C92=C3+C3
    C93=C51G+C1
    C94=C3+C3
    C95=C51G+C1
    C96=C3+C3
    C97=C51G+C1
    C98=C3+C3
    C99=C51G+C1
    C100=C3+C3
  
```



```

OUTPUT0021
OUTPUT0022
OUTPUT0023
OUTPUT0024
OUTPUT0025
OUTPUT0026
OUTPUT0027
OUTPUT0028
OUTPUT0029
OUTPUT0030
OUTPUT0031
OUTPUT0032
OUTPUT0033
OUTPUT0034
OUTPUT0035
OUTPUT0036
OUTPUT0037
OUTPUT0038
OUTPUT0039
OUTPUT0040
OUTPUT0041
OUTPUT0042
OUTPUT0043
OUTPUT0044
OUTPUT0045
OUTPUT0046
OUTPUT0047
OUTPUT0048
OUTPUT0049
OUTPUT0050
OUTPUT0051
OUTPUT0052
OUTPUT0053
OUTPUT0054
OUTPUT0055
OUTPUT0056
OUTPUT0057
OUTPUT0058
OUTPUT0059
OUTPUT0060
OUTPUT0061
OUTPUT0062
OUTPUT0063
OUTPUT0064
OUTPUT0065
OUTPUT0066
OUTPUT0067
OUTPUT0068
OUTPUT0069
OUTPUT0070
OUTPUT0071
OUTPUT0072
OUTPUT0073
OUTPUT0074
OUTPUT0075
OUTPUT0076
OUTPUT0077
OUTPUT0078
OUTPUT0079
OUTPUT0080
OUTPUT0081
OUTPUT0082
OUTPUT0083
OUTPUT0084
OUTPUT0085
OUTPUT0086
OUTPUT0087
OUTPUT0088
OUTPUT0089
OUTPUT0090
OUTPUT0091
OUTPUT0092

OUTPUT0093
OUTPUT0094
OUTPUT0095
OUTPUT0096
OUTPUT0097
OUTPUT0098
OUTPUT0099
OUTPUT0100
OUTPUT0101
OUTPUT0102
OUTPUT0103
OUTPUT0104
OUTPUT0105
OUTPUT0106
OUTPUT0107
OUTPUT0108
OUTPUT0109
OUTPUT0110
OUTPUT0111
OUTPUT0112
OUTPUT0113
OUTPUT0114
OUTPUT0115
OUTPUT0116
OUTPUT0117
OUTPUT0118
OUTPUT0119
OUTPUT0120
OUTPUT0121
OUTPUT0122
OUTPUT0123
OUTPUT0124
OUTPUT0125
OUTPUT0126
OUTPUT0127
OUTPUT0128
OUTPUT0129
OUTPUT0130
OUTPUT0131
OUTPUT0132
OUTPUT0133
OUTPUT0134
OUTPUT0135
OUTPUT0136
OUTPUT0137
OUTPUT0138
OUTPUT0139
OUTPUT0140
OUTPUT0141
OUTPUT0142
OUTPUT0143
OUTPUT0144
OUTPUT0145
OUTPUT0146
OUTPUT0147
OUTPUT0148
OUTPUT0149
OUTPUT0150
OUTPUT0151
OUTPUT0152
OUTPUT0153
OUTPUT0154
OUTPUT0155
OUTPUT0156
OUTPUT0157
OUTPUT0158
OUTPUT0159
OUTPUT0160
OUTPUT0161
OUTPUT0162
OUTPUT0163
OUTPUT0164

VLXE=VLX
VLYE=VLY
CPL(I)=2-*(UB-U2B+VTA+VLX+ALPHA*(VTZ+VLZ))-*(VTY+VLY)*2-*(VTZ+VLZ)
1**2
GO TO 5
40 VLXE=0.
VLYE=0.
VLZE=0.
GO TO 4
0000 VIXTKSSTR(IC)
VIZTKSSTR(IC*1)
VIZTKSSTR(IC*2)
IC=IC+3
GO TO 19
0001 TASSSTR(IC)EVTK
TASSSTR(IC+1)=VTZ
TASSSTR(IC+2)=VIZ
IC=IC+3
GO TO 19
902 CPL(I)=999999.
CPL(I)=999999.
5 CONTINUE
IF (ABS(THETA(I))) .LE. 1.E-4 .AND. ABS(ALPHA) .GT. 1.E-4 GO TO 101
WRITE (7,100) X,R,THETA(I),CPU
100 FORMAT (1H 'F7.4',2X,F7.4,2X,IPEL1,4,7(2X,IPEL1,4))
IF (ABS(CALPHA)) .LE. 1.E-4 GO TO 500
WRITE (7,100) X,R,THETA(I),CPU
101 IF (X.LT.XMLE1) GO TO 499
WRITE (7,102) X,R,CPU
102 FORMAT (1H 'F7.4',2X,F7.4,2X,IPEL1,4,7(2X,IPEL1,4))
103 WRITE (7,103) X,R,CPU
104 FORMAT (1H 'F7.4',2X,F7.4,2X,IPEL1,4,7(2X,IPEL1,4))
499 GO TO 500
500 CONTINUE
501 WRITE (7,104)
104 FORMAT (1H '
RETURN
502 MILLI
3 DU=DU*(1)+UH
UH=DU
DX1=DX12
DX12=DX
DU1=DU12
DU12=DU
11 DU=DU*(1)+UEF
UH=DU
GO TO 21
1 WRITE (7,110)
110 FORMAT (1H0.74HINTEGRATION TERMINATED BECAUSE ACCUMULATED ERRORS MOUNTED
22E (*001) 10 TIMES )
300 A=ABS(X)
DO 1500 I=1,NTHETA
REF(I)=A/S(I)
DO 115 I=1,7
YZN(I)=6P(I)
Z=ZN(I)+REF(I)
REF(I)
REF(I)
IF (IR-REF(I)-GT-.001) GO TO 1902
IF (X.LT.XMLE1) GO TO 1900
IF (IR-EG-1-AND-X.GT.XLMS2) GO TO 1900
IF (IR-EG-1-AND-X.GT.XART1) GO TO 1900
IF (IR-EG-1) GO TO 1100
IF (X.LT.XLMS2) GO TO 1102
S=SPANTETA)
S=SPANTETA)

```

OUTP0237  
OUTP0238

GO TO 21  
END

```

R0000001
R0000002
R0000003
R0000004
R0000005
R0000006
R0000007
R0000008
R0000009
R0000010
R0000011
R0000012
R0000013
R0000014
R0000015
R0000016
R0000017
R0000018
R0000019
R0000020
R0000021
R0000022
R0000023
R0000024
R0000025
R0000026
R0000027
R0000028
R0000029
R0000030
R0000031
R0000032
R0000033
R0000034
R0000035
R0000036
R0000037
R0000038
R0000039
R0000040
R0000041
R0000042
R0000043
R0000044
R0000045
R0000046
R0000047
R0000048
R0000049

FUNCTION MH(X)
COMMON /BLK3/ DN,DM1,DM2,ATE,MLE,XRLE,XRTE,TBLE,TBTE,TCMTE,ICMT,
IXLSM1,XLSM2,SSMAX,DAIR,MTE,MTR
COMMON /BLK5/ XHLE1,XHTE1,H,H3,MW
COMMON /BLK6/ PL,P12,TOL,NIT
EXTERNAL ZM
NEI
RI=SQRT(4.*SEBP1(X))
HEGRI
IF (MNH.EQ.0) GO TO 2
IF (MTE.EQ.1) GO TO 10
IF (X.LE.XHLE1.OR.X.GE.XHTE1) GO TO 8
IF (X.LT.XLSM2) XUS=SPANLE(X)
IF (X.GT.XLSM2) XUS=SPANLE(X)
5 XLR=OLD
CALL SIMP1(XL,XU,NIT,NITI,TUL,ZM,X,ANS)
PREP1(ROLD*ROLD+HEGRI*HEGRI,ANS)
DFD=PI2*ROLD-4.*ZM*(X*ROLD)
IF (M=ROLD*FR/DFD)
PIABS(MNH*W=ROLD).LE.1.E-5) GO TO 4
ROLD=NEW
NEW=NEW
IF (M.GT.1) GO TO 4
GO TO 5
4 R0=NEW
ROLD=RB
IF (RB.LE..0) GO TO 9
RETURN
2 ROLD=HEW
NN=1
GO TO 7
8 R0=HEG
ROLD=RB
RETURN
9 WRITE (6,103) X
103 FORMAT (1H0,51MPROGRAM TERMINATED BECAUSE INDENTED BODY RADIIUS
1 / 1X,31HBELOWE LESS THAN ZERO AT X/L = ,L12.5)
STOP
10 XUS=SPANLE(X)
IF (X.LE.XHLE1.OR.X.GE.XLSM2) GO TO 6
IF (X.LE.XHTE1) GO TO 5
XLS=SPANLE(X)
CALL SIMP1(AL,XU,NIT,NITI,TUL,ZM,X,ANS)
R2=ROE*ROE-4.*ANS/PI
IF (R2H.LE.0.) GO TO 9
R0=SOHT(R2B)
ROLD=RB
RETURN
END

```

```

OUTP0165
OUTP0166
OUTP0167
OUTP0168
OUTP0169
OUTP0170
OUTP0171
OUTP0172
OUTP0173
OUTP0174
OUTP0175
OUTP0176
OUTP0177
OUTP0178
OUTP0179
OUTP0180
OUTP0181
OUTP0182
OUTP0183
OUTP0184
OUTP0185
OUTP0186
OUTP0187
OUTP0188
OUTP0189
OUTP0190
OUTP0191
OUTP0192
OUTP0193
OUTP0194
OUTP0195
OUTP0196
OUTP0197
OUTP0198
OUTP0199
OUTP0200
OUTP0201
OUTP0202
OUTP0203
OUTP0204
OUTP0205
OUTP0206
OUTP0207
OUTP0208
OUTP0209
OUTP0210
OUTP0211
OUTP0212
OUTP0213
OUTP0214
OUTP0215
OUTP0216
OUTP0217
OUTP0218
OUTP0219
OUTP0220
OUTP0221
OUTP0222
OUTP0223
OUTP0224
OUTP0225
OUTP0226
OUTP0227
OUTP0228
OUTP0229
OUTP0230
OUTP0231
OUTP0232
OUTP0233
OUTP0234
OUTP0235
OUTP0236

1100 GO TO 1111
1101 IF (X.LT.XHTE1) GO TO 1102
1102 STE=SPANLE(X)
1103 YSTE=STL
1104 IF (ABS(Z).LE.1.E-3.AND.ABS(YSTE).LE.1.E-3) GO TO 1902
1105 S=SPANLE(X)
1106 YS=Y+S
1107 IF (ABS(Z).LE.1.E-3.AND.ABS(YS).LE.1.E-3) GO TO 1902
1108 IF (ICOPY) S100=S100/6100
1109 CALL PHITAS(X,Y,Z,VTR,VLY,V17)
1110 GO TO 6101
1111 IF (ABS(AL*PHA).LE.1.E-4) GO TO 140
1112 IF (X.LT.XHLE1) GO TO 1901
1113 CALL PHILT(X,Y,Z,VLR,VLY,VLZ)
1114 VLZ=ALPHA*VLX
1115 VLY=ALPHA*VLY
1116 VLZ=ALPHA*VLZ
1117 GO TO 114
1118 CS16=CPLA(FZ)
1119 ARPHZ=ALJ+A+A
1120 CA=COS(PI*CS16*CS16-A2MR2)
1121 CI=CS16*AR1Z2
1122 CU=NC1/(1+CI)-.25*A2MR2)
1123 RI=AL+A
1124 SCRI=SI*PI(DX)
1125 C=C2*RC*RL
1126 CU=SEDI*AL*RI*(1.+URC2)*COS*(AL+1.)*(AL+1.)/(AL+C1))
1127 CF=11.*RZ21M/30*CI
1128 VLX=AL*PHASIM/3(CP)
1129 VLZ=AL*PHASIM/3(CP)
1130 VLY=AL*PHASIM/3(CP)
1131 CU(11)=2.*U1-U2B*VTR+VLX+AL*PHA*(VTR+VLZ))-((VTR+VLY)*2-(VTR+VLZ)*2)-(VTR+VLY)*2-(VTR+VLZ)*2))
1132 1902
1133 VLY=VLY
1134 VLX=VLX
1135 VLY=VLY
1136 CPL(11)=2.*U1-U2B*VTR+VLX+AL*PHA*(VTR+VLZ))-((VTR+VLY)*2-(VTR+VLZ)*2)-(VTR+VLY)*2-(VTR+VLZ)*2))
1137 1902
1138 VLX=0.
1139 VLY=0.
1140 GO TO 114
1141 VIX=TKSST1
1142 VIV=TKSST1
1143 VIZ=TKSST1
1144 IL=IC+3
1145 GO TO 115
1146 TASSTR(I) /TX
1147 TASSTR(I) /VY
1148 TASSTR(I) /VTZ
1149 IC=IC+3
1150 GO TO 11
1151 CPU(11)= 999.
1152 CPL(11)= 999.
1153 CONTINU
1154 IF (ABS(1.-ATAI(11)).LE.1.E-4.AND.ABS(AL*PHA).GT.1.E-4) GO TO 1101
1155 WRITE (6,100) X,R,T,ETA(11),CPU
1156 IF (ABS(AL*PHA).LE.1.E-4) GO TO 1500
1157 WRITE (6,100) X,R,T,ETA(11),CPL
1158 GO TO 1500
1159 WRITE (6,102) X,R,CPU
1160 WRITE (6,103) X,R,CPL
1161 GO TO 1500
1162 CONTINUE
1163 WRITE (6,104)
1164 WRITE (6,104)
1165 RETURN
1166 USE=UE*BOY(DI)
2000

```

```

FCT00046
FCT00049
FCT00050
FCT00051
FCT00052
FCT00053
FCT00054
FCT00055
FCT00056
FCT00057
FCT00058
FCT00059
FCT00060
FCT00061
FCT00062
FCT00063
FCT00064
FCT00065
FCT00066
FCT00067
FCT00068
FCT00069
FCT00070
FCT00071
FCT00072
FCT00073

11 DEF=DA2*ALOG(UA/(UX*(1.-DX)))*(DINT(UX)+DINT(DX))
DU1E=U1M*UX*(DY(1)+DEF)
IF(DU1) 24,22,21
21 DZ(1)=DA3*ALOG(UUU)
RETURN
22 MM=2
700 FORMAT (1M0.6)H,KALCULATION TEMPERATURE BECAUSE FLOW AROUND EQUIVALENT
IT BODY HAS / 1X,25HBECAUSE SURFONAL AT Y/L = *E12.5)
WRITE (0,701)
701 FORMAT (1H *SHINPUT MACH NUMBER GREATER THAN LOWER CRITICAL )
RETURN
12 DHF=DA2*ALOG(UA/(UX*(DX)))*(2.*DINT(UX))
DU1E(1)=DX*(DY(1)+DHF)
IF(DU1) 24,24,23
23 DZ(1)=DA3*ALOG(UUU)
RETURN
24 MM=3
703 FORMAT (1M0.6)H,KALCULATION TEMPERATURE BECAUSE FLOW AROUND EQUIVALENT
IT BODY HAS / 1X,25HBECAUSE SURFONAL AT Y/L = *E12.5)
IF(DX-DZ5) 31,31,31
31 WRITE (0,704)
704 FORMAT (1H *SHINPUT MACH NUMBER LESS THAN UPPER CRITICAL )
RETURN
41 END

```

```

DINT0001
DINT0002
DINT0003
DINT0004
DINT0005
DINT0006
DINT0007
DINT0008
DINT0009
DINT0010
DINT0011
DINT0012
DINT0013
DINT0014
DINT0015
DINT0016
DINT0017
DINT0018
DINT0019
DINT0020
DINT0021
DINT0022
DINT0023
DINT0024
DINT0025
DINT0026
DINT0027
DINT0028
DINT0029
DINT0030
DINT0031
DINT0032
DINT0033
DINT0034
DINT0035
DINT0036
DINT0037
DINT0038
DINT0039
DINT0040
DINT0041
DINT0042
DINT0043
DINT0044
DINT0045
DINT0046
DINT0047
DINT0048
DINT0049
DINT0050
DINT0051
DINT0052
DINT0053
DINT0054
DINT0055
DINT0056
DINT0057
DINT0058
DINT0059
DINT0060
DINT0061
DINT0062
DINT0063
DINT0064
DINT0065
DINT0066
DINT0067
DINT0068
DINT0069
DINT0070
DINT0071
DINT0072
DINT0073

FUNCTION UJINT(DZ)
EXTERNAL UFUN
COMMON /BLK9/ DTOL
COMMON /BLK17/ UW*DA2
IF(ABS(UZ)-LT.1.E-5) GO TO 25
D=UZ
DA2=S2EPI(UZ)
NITE=U
CALL SIMP(1.,DZ,NITE,NITE,DTOL,DFUN,DANS)
DINT=DANS
RETURN
25 DINT=0.
RETURN
END

FUNCTION UJINT(UZ)
EXTERNAL UFUN
COMMON /BLK9/ DTOL
COMMON /BLK17/ UW*DA2
IF(ABS(1.-DZ)-LT.1.E-5) GO TO 25
D=UZ
DA2=S2EPI(UZ)
NITE=U
CALL SIMP(1.,DZ,NITE,NITE,DTOL,DFUN,DANS)
DINT=DANS
RETURN
25 DINT=0.
RETURN
END

```

```

DINT0001
DINT0002
DINT0003
DINT0004
DINT0005
DINT0006
DINT0007
DINT0008
DINT0009
DINT0010
DINT0011
DINT0012
DINT0013
DINT0014
DINT0015
DINT0016
DINT0017
DINT0018
DINT0019
DINT0020
DINT0021
DINT0022
DINT0023
DINT0024
DINT0025
DINT0026
DINT0027
DINT0028
DINT0029
DINT0030
DINT0031
DINT0032
DINT0033
DINT0034
DINT0035
DINT0036
DINT0037
DINT0038
DINT0039
DINT0040
DINT0041
DINT0042
DINT0043
DINT0044
DINT0045
DINT0046
DINT0047
DINT0048
DINT0049
DINT0050
DINT0051
DINT0052
DINT0053
DINT0054
DINT0055
DINT0056
DINT0057
DINT0058
DINT0059
DINT0060
DINT0061
DINT0062
DINT0063
DINT0064
DINT0065
DINT0066
DINT0067
DINT0068
DINT0069
DINT0070
DINT0071
DINT0072
DINT0073

FUNCTION UJINT(DZ)
EXTERNAL UFUN
COMMON /BLK9/ DTOL
COMMON /BLK18/ UZ3*DA3
IF(ABS(UZ)-LE.1.E-5) GO TO 25
DZ3=DZ
DA3=S2EPI(UZ)
NITE=U
CALL SIMP(1.,DZ,NITE,NITE,DTOL,DFUN,DANS)
DINT=DANS
RETURN
25 DINT=0.
RETURN
END

```

```

UE00001
UE00002
UE00003
UE00004
UE00005
UE00006
UE00007
UE00008
UE00009
UE00010
UE00011
UE00012
UE00013
UE00014
UE00015
UE00016
UE00017
UE00018
UE00019
UE00020
UE00021

FUNCTION UEWDY(UX)
DIMENSION UE(20),UEB(20),UEB(20)
COMMON /BLK19/ UE,UEB,NTER,ITE5T
IF(ITE5T.EQ.0) GO TO 10
IF(UEB(NTER)-R) 1,3,13,12
10 DO 1 J=NK*NAEB
IF(UEB(J)-R) 1,2,2
1 CONTINUE
UE(UEB(J)-1)=((UEB(J)-UEB(J-1))/(UEB(J)-UEB(J-1)))*((X-UEB(J-1))
NAX=J
RETURN
10 IF((X-UEB(J-1))-GT.0) GO TO 11
ITE5T=1
K=2
GO TO 12
11 UE(NU)=UE(1)-((UE(1)-UEB(1))/(UEB(1)-UEB(1)))*((X-UEB(1)-X)
RETURN
13 UE(NU)=UE(UEB(NTER))*((UEB(NTER)-UEB(NTER-1))/(UEB(NTER)-UEB(NTER-1))
RETURN
END

```

```

FCT00001
FCT00002
FCT00003
FCT00004
FCT00005
FCT00006
FCT00007
FCT00008
FCT00009
FCT00010
FCT00011
FCT00012
FCT00013
FCT00014
FCT00015
FCT00016
FCT00017
FCT00018
FCT00019
FCT00020
FCT00021
FCT00022
FCT00023
FCT00024
FCT00025
FCT00026
FCT00027
FCT00028
FCT00029
FCT00030
FCT00031
FCT00032
FCT00033
FCT00034
FCT00035
FCT00036
FCT00037
FCT00038
FCT00039
FCT00040
FCT00041
FCT00042
FCT00043
FCT00044
FCT00045
FCT00046
FCT00047

SUBROUTINE FCT(UX,UY,UZ)
DIMENSION DT(1),DZ(1)
COMMON /BLK1/ DM,UK,DI,DM,UM,DUZ,DU1,USAD,DU,DU3,DTAU2
COMMON /BLK2/ AL,AL12,AL1,AL2,AL3,AL4,M,MPRT,MELPT
COMMON /BLK9/ MM
COMMON /BLK10/ UH,DEF
DA=S2EPI(UX)
DA2=S2EPI(UY)
DA3=S2EPI(UZ)
IF(MPT.EQ.2) GO TO 11
IF(MPT.EQ.3) GO TO 12
IF(ABS(UX-DZ5).LE.5.E-3) GO TO 10
IF(UEB(2)) GO TO 2
IF(UEB(3)) GO TO 3
IF(UEB(4)) GO TO 4
1 UJINT=UJINT(DZ)
2 UJINT=UJINT(DZ)
3 UJINT=UJINT(DZ)
4 UJINT=UJINT(DZ)
5 UJINT=UJINT(DZ)
6 UJINT=UJINT(DZ)
7 UJINT=UJINT(DZ)
8 UJINT=UJINT(DZ)
9 UJINT=UJINT(DZ)
10 UJINT=UJINT(DZ)
11 UJINT=UJINT(DZ)
12 UJINT=UJINT(DZ)
13 UJINT=UJINT(DZ)
14 UJINT=UJINT(DZ)
15 UJINT=UJINT(DZ)
16 UJINT=UJINT(DZ)
17 UJINT=UJINT(DZ)
18 UJINT=UJINT(DZ)
19 UJINT=UJINT(DZ)
20 UJINT=UJINT(DZ)
21 UJINT=UJINT(DZ)
22 UJINT=UJINT(DZ)
23 UJINT=UJINT(DZ)
24 UJINT=UJINT(DZ)
25 UJINT=UJINT(DZ)
26 UJINT=UJINT(DZ)
27 UJINT=UJINT(DZ)
28 UJINT=UJINT(DZ)
29 UJINT=UJINT(DZ)
30 UJINT=UJINT(DZ)
31 UJINT=UJINT(DZ)
32 UJINT=UJINT(DZ)
33 UJINT=UJINT(DZ)
34 UJINT=UJINT(DZ)
35 UJINT=UJINT(DZ)
36 UJINT=UJINT(DZ)
37 UJINT=UJINT(DZ)
38 UJINT=UJINT(DZ)
39 UJINT=UJINT(DZ)
40 UJINT=UJINT(DZ)
41 UJINT=UJINT(DZ)
42 UJINT=UJINT(DZ)
43 UJINT=UJINT(DZ)
44 UJINT=UJINT(DZ)
45 UJINT=UJINT(DZ)
46 UJINT=UJINT(DZ)
47 UJINT=UJINT(DZ)
48 UJINT=UJINT(DZ)
49 UJINT=UJINT(DZ)
50 UJINT=UJINT(DZ)
51 UJINT=UJINT(DZ)
52 UJINT=UJINT(DZ)
53 UJINT=UJINT(DZ)
54 UJINT=UJINT(DZ)
55 UJINT=UJINT(DZ)
56 UJINT=UJINT(DZ)
57 UJINT=UJINT(DZ)
58 UJINT=UJINT(DZ)
59 UJINT=UJINT(DZ)
60 UJINT=UJINT(DZ)
61 UJINT=UJINT(DZ)
62 UJINT=UJINT(DZ)
63 UJINT=UJINT(DZ)
64 UJINT=UJINT(DZ)
65 UJINT=UJINT(DZ)
66 UJINT=UJINT(DZ)
67 UJINT=UJINT(DZ)
68 UJINT=UJINT(DZ)
69 UJINT=UJINT(DZ)
70 UJINT=UJINT(DZ)
71 UJINT=UJINT(DZ)
72 UJINT=UJINT(DZ)
73 UJINT=UJINT(DZ)
74 UJINT=UJINT(DZ)
75 UJINT=UJINT(DZ)
76 UJINT=UJINT(DZ)
77 UJINT=UJINT(DZ)
78 UJINT=UJINT(DZ)
79 UJINT=UJINT(DZ)
80 UJINT=UJINT(DZ)
81 UJINT=UJINT(DZ)
82 UJINT=UJINT(DZ)
83 UJINT=UJINT(DZ)
84 UJINT=UJINT(DZ)
85 UJINT=UJINT(DZ)
86 UJINT=UJINT(DZ)
87 UJINT=UJINT(DZ)
88 UJINT=UJINT(DZ)
89 UJINT=UJINT(DZ)
90 UJINT=UJINT(DZ)
91 UJINT=UJINT(DZ)
92 UJINT=UJINT(DZ)
93 UJINT=UJINT(DZ)
94 UJINT=UJINT(DZ)
95 UJINT=UJINT(DZ)
96 UJINT=UJINT(DZ)
97 UJINT=UJINT(DZ)
98 UJINT=UJINT(DZ)
99 UJINT=UJINT(DZ)
100 UJINT=UJINT(DZ)

```

APPENDIX B

SEBP1001  
SEBP1002  
SEBP1003  
SEBP1004  
SEBP1005  
SEBP1006  
SEBP1007  
SEBP1008  
SEBP1009

```
FUNCTION SEBP1(DZ)
COMMON /BLK7/ DCTAU2,DN,K
IF (K.GT.0) GO TO 2
DS1=DZ*(UN-1.00)
1 SEBP1=DCTAU2*DS1*DS1/16.
RETURN
2 DS1=(1.00-UZ-(1.00-UZ)**UN
GO TO 1
END
```

SIEBP001  
SIEBP002  
SIEBP003  
SIEBP004  
SIEBP005  
SIEBP006  
SIEBP007  
SIEBP008  
SIEBP009  
SIEBP010

```
FUNCTION SIEBP1(DZ)
COMMON /BLK7/ DCTAU2,DN,K
IF (K.GT.0) GO TO 2
DS1=DZ*(UN-1.00)
1 SIEBP1=DCTAU2*DS1*(1.-(DN+1.)*US1+UN*DS1*DS1)/8.
RETURN
2 DS1=(1.00-UZ)**(UN-1.00)
SIEBP1=DCTAU2*(1.-(DN+1.)*US1+UN*DS1*DS1)/8.
RETURN
END
```

SZBP001  
SZBP002  
SZBP003  
SZBP004  
SZBP005  
SZBP006  
SZBP007  
SZBP008  
SZBP009

```
FUNCTION SZBP1(DZ)
COMMON /BLK7/ DCTAU2,UN,K
IF (K.GT.0) GO TO 2
DS1=DZ*(UN-1.00)
1 SZBP1=DCTAU2*(1.-(DN+1.)*US1+UN*DS1*DS1)/8.
RETURN
2 DS1=(1.00-UZ)**(UN-1.00)
GO TO 1
END
```

SZBP001  
SZBP002  
SZBP003  
SZBP004  
SZBP005  
SZBP006  
SZBP007  
SZBP008  
SZBP009  
SZBP010  
SZBP011

```
FUNCTION SZBP1(DZ)
COMMON /BLK7/ DCTAU2,DN,K
IF (K.GT.0) GO TO 2
DS1=DZ*(UN-2.00)
1 SZBP1=DCTAU2*DN*(DN-1.)*US1+2*(2.*DN-1.)*US2)/8.
RETURN
2 DS1=(1.00-UZ)**(UN-2.)
DS2=DS1*US1*(1.-(DN+1.)*US1+UN*DS1*DS1)/8.
GO TO 1
END
```

DFUN0001  
DFUN0002  
DFUN0003  
DFUN0004  
DFUN0005  
DFUN0006  
DFUN0007  
DFUN0008  
DFUN0009  
DFUN0010  
DFUN0011  
DFUN0012  
DFUN0013  
DFUN0014  
DFUN0015  
DFUN0016  
DFUN0017  
DFUN0018  
DFUN0019  
DFUN0020

```
FUNCTION DFUN(DZ)
COMMON /BLK17/ UM,DA2
IF (ABS(UZ-UM),LT.1.E-5) GO TO 20
DB2=SEBP1(UZ)
DFUN=DA2-UM*(1.00-UZ)
20 DFUN=SEBP1(UM)
RETURN
END
FUNCTION DFUN1(UZ)
COMMON /BLK18/ UZ3,DA3
IF (ABS(UZ-UZ3),LT.1.E-5) GO TO 20
DB3=SEBP1(UZ)
DFUN1=(DA3-UB3)/(UZ3-UZ)
RETURN
20 DFUN1=SEBP1(UZ3)
RETURN
END
```

DLIFT001  
DLIFT002  
DLIFT003  
DLIFT004  
DLIFT005  
DLIFT006  
DLIFT007  
DLIFT008  
DLIFT009  
DLIFT010  
DLIFT011  
DLIFT012  
DLIFT013  
DLIFT014  
DLIFT015  
DLIFT016  
DLIFT017  
DLIFT018  
DLIFT019  
DLIFT020  
DLIFT021

```
FUNCTION DLIFT(X)
COMMON /BLK4/ AL,AL12,AL1,AL2,AL3,AL4,M,MUPT,HELLPT
IF (HELLPT.EQ.1) GO TO 1
S=SPANL(A)
S2=S*5
RUA=RU(X)
RBA=RB(A**4)
RBEQ2=4.*SEBP1(X)
DLIFT=S2*M*H*AN/S2-RBEQ2
RETURN
1 DS=SPANLE(X)
DS2=DS*US
A=AB(X)
DC2=AL1+A*A
DSC12=DS+S*ORT(DS2-UC2)
DSC12Z=DSC1Z*USCLZ
DAPR2=.9*AL4*A
DREB2=.9*SEBP1(X)
DLIFT=.25*DSC12Z*(1.+Z.*DC2/DSC12Z*(DAPB/DSC12)**4)-DREB2
RETURN
END
```

DHORT001  
DHORT002  
DHORT003  
DHORT004  
DHORT005  
DHORT006  
DHORT007  
DHORT008  
DHORT009  
DHORT010  
DHORT011  
DHORT012

```
FUNCTION DHORT(X)
EXTERNAL DLIFT,SEBP1
COMMON /BLK4/ AL,AL12,AL1,AL2,AL3,AL4,M,MUPT,HELLPT
COMMON /BLK5/ XRL1,XRTE1,MH,H3,M*H
COMMON /BLK6/ PI,PI2,TOL,NIT
CALL SIMP(TO,XRL1,NIT,NIT1,TOL,SEBP1,ANS)
M*H2=.9*ANS
IF (HELLPT.EQ.3) ANS1=AL*ANS1
CALL SIMP(XRL1,NIT,NIT1,TOL,DLIFT,ANS)
DHORT=ANS1*ANS
RETURN
END
```

FUNK1001  
 FUNK1002  
 FUNK1003  
 FUNK1004  
 FUNK1005  
 FUNK1006  
 FUNK1007  
 FUNK1008  
 FUNK1009  
 FUNK1010  
 FUNK1011

FUNCTION FUNK1(X0,X1)  
 COMMON /BLK13/ YZ,R2,ZZ,YZ2,ZY6,R2Y,A2MB24  
 Y0=RZ/X1  
 Y1=Z2\*(Y-X1)/(Y-X1)  
 Y2=Z2\*(Y+X1)/(Y+X1)  
 Y3=Z2\*(Y-70)/(Y-70)  
 Y4=Z2\*(Y+70)/(Y+70)  
 Z1=ALOG(Y1\*Y2\*Y3\*Y4/ZY6)  
 FUNK1=Z1+JZWD(X0,X1)  
 RETURN  
 END

FUNK2001  
 FUNK2002  
 FUNK2003  
 FUNK2004  
 FUNK2005  
 FUNK2006  
 FUNK2007  
 FUNK2008  
 FUNK2009  
 FUNK2010  
 FUNK2011

FUNCTION FUNK2(X0,X1)  
 COMMON /BLK13/ YZ,R2,ZZ,YZ2,ZY6,R2Y,A2MB24  
 Y0=RZ/X1  
 Y1=Y4\*Y0  
 Y2=Y4\*Y0  
 Y3=Z2\*Y4\*Y1  
 Y4=Z2\*Y4\*Y1  
 Z1=Y2\*Y4-Y1\*Y3/X1  
 FUNK2=Z1+JZWD(X0,X1)  
 RETURN  
 END

FUNK3001  
 FUNK3002  
 FUNK3003  
 FUNK3004  
 FUNK3005  
 FUNK3006  
 FUNK3007  
 FUNK3008  
 FUNK3009

FUNCTION FUNK3(X0,X1)  
 COMMON /BLK13/ YZ,R2,ZZ,YZ2,ZY6,R2Y,A2MB24  
 Y0=RZ/X1  
 Y1=Y4\*Y0  
 Y2=Y4\*Y0  
 Z1=ALOG(Y1\*Y2\*Y3\*Y4/ZY6)  
 FUNK3=Z1+JZWD(X0,X1)  
 RETURN  
 END

FUNK4001  
 FUNK4002  
 FUNK4003  
 FUNK4004  
 FUNK4005  
 FUNK4006  
 FUNK4007  
 FUNK4008  
 FUNK4009  
 FUNK4010  
 FUNK4011  
 FUNK4012  
 FUNK4013

FUNCTION FUNK4(X0,X1)  
 COMMON /BLK13/ YZ,R2,ZZ,YZ2,ZY6,R2Y,A2MB24  
 COMMON /BLK14/ DZBXY,DZZWAY,DZFR,DZFR,DZFR,DZFR  
 Y1=Y-X1  
 IF (ABS(Y1).LE.1.E-4) GO TO 1  
 Y1=Y1/Y  
 Z1=LOG(Y1)  
 FUNK4=Z1+JZWD(X0,X1)-DZFR\*Y1  
 RETURN  
 1 FUNK4=0.  
 RETURN  
 END

S4EBP001  
 S4EBP002  
 S4EBP003  
 S4EBP004  
 S4EBP005  
 S4EBP006  
 S4EBP007  
 S4EBP008  
 S4EBP009  
 S4EBP010  
 S4EBP011  
 S4EBP012

FUNCTION S4EBP1(DZ)  
 COMMON /BLK7/ DLTAP,DUR,K  
 IF (K.GT.0) GO TO 2  
 US2=Z\*(1.-DZ)  
 US2=US2\*(1.-DZ)  
 1 S4EBP1=UC(LAU2\*US2\*(1.-DZ)+US1\*(1.-DZ)+US1\*2.\*(2.-DZ)-  
 RETURN  
 2 US1=(1.-DZ)\*(1.-DZ)  
 US2=(1.-DZ)\*(2.-DZ)  
 GO TO 1  
 END

AB000001  
 AB000002  
 AB000003  
 AB000004  
 AB000005  
 AB000006  
 AB000007  
 AB000008  
 AB000009  
 AB000010  
 AB000011  
 AB000012  
 AB000013  
 AB000014  
 AB000015  
 AB000016  
 AB000017  
 AB000018  
 AB000019  
 AB000020  
 AB000021  
 AB000022  
 AB000023  
 AB000024  
 AB000025  
 AB000026  
 AB000027  
 AB000028  
 AB000029  
 AB000030  
 AB000031  
 AB000032  
 AB000033  
 AB000034  
 AB000035  
 AB000036  
 AB000037  
 AB000038  
 AB000039  
 AB000040  
 AB000041  
 AB000042  
 AB000043  
 AB000044  
 AB000045  
 AB000046  
 AB000047  
 AB000048  
 AB000049  
 AB000050  
 AB000051  
 AB000052

FUNCTION AB001  
 COMMON /BLK3/ DN,PHI,UN2,KTE,MLE,XMLE,XPIE,IBLE,IBTE,IBLWTE,XCMT,  
 XLSM,XLSM2,SSMAX,DAIM,XTE,MTN  
 COMMON /BLK4/ DL,LL1,DL2,DL3,DL4,DL5,MUPT,MFLPT  
 COMMON /BLK5/ XMLE1,XMLE2,XMLE3,XMLE4,XMLE5  
 COMMON /BLK6/ PI,PI2,TOL,PHI  
 EXTERNAL Z  
 NE1  
 MIESORT(4,\*S4EBP1(X))  
 MIE=1  
 IF (MIE.EQ.0) GO TO 2  
 IF (XMLE.EG.1) GO TO 10  
 IF (XMLE.XMLE1.OH.A.GE.XMLE1) GO TO 8  
 IF (XMLE.XMLE2) XRESPANLE(X)  
 IF (XMLE.XMLE3) XRESPANLE(X)  
 IF (XMLE.XMLE4) XRESPANLE(X)  
 IF (XMLE.XMLE5) XRESPANLE(X)  
 5 AL=AL+DL  
 CALL SIMPICAL(XU,PHI,MTN,TOL,Z,X,X,ANS)  
 FREPI=AL+DL/2+DL\*(2.-PHI)/4+X,ANS  
 (PHI=PI2\*AL+DL-4.\*Z\*(X,AL))  
 ANE=AL-D\*PHI/UP  
 IF (ABS(ANE)-AL).LE.1.E-5) GO TO 4  
 AULD=ANE  
 NEN=1  
 IF (NEN.GT.1) GO TO 4  
 GO TO 5  
 4 AULD=NE  
 IF (G.GT.1) WRITE (6,201)  
 201 FORMAT (1H,'ANN GT 11')  
 AULD=AN  
 IF (ABS(LE..)) GO TO 10  
 AULD=PI2\*PHI  
 GO TO 7  
 8 ANE=AL2+AL  
 AULD=AN  
 RETURN  
 10 WRITE (6,11) X  
 11 FORMAT (10D,PHI,PROGRAM TERMINATED BECAUSE INDENTED BODY MAJOR AXIS  
 1 HAS BECOME LESS THAN ZERO AT X/L = .E12.5)  
 STOP  
 100 XU=SPANLE(X)  
 IF (XMLE.XMLE1.OH.A.GE.XLSM2) GO TO 6  
 IF (XMLE.XMLE1) GO TO 5  
 XU=SPANLE(X)  
 CALL SIMPICAL(XU,PHI,MTN,TOL,Z,X,X,ANS)  
 A2B=UL\*(RCQ+REG-4.\*ANS/PI)  
 IF (A2B.LE.0.) GO TO 10  
 A2=SPANTACH)  
 AULD=A2B  
 RETURN  
 END



FNX15001  
FNX15002  
FNX15003  
FNX15004  
FNX15005  
FNX15006  
FNX15007  
FNX15008  
FNX15009  
FNX15010  
FNX15011  
FNX15012  
FNX15013  
FNX15014  
FNX15015  
FNX15016

FUNCTION FUNK15(X0,X1)  
COMMON /BLK13/ Y,Z,R2,Z2,Y2,Z2,Y2,Z2,Y2,Z2,Y2,Z2  
X2=A2M24/X1  
X3=X1\*X2  
X4=X2/X1  
Y1=Y-R2/A1  
IF (ABS(Y1)-LE.1.E-4) GO TO 1  
Y1=Y1\*Y1  
Z1=(1.-X4)\*ALOG(Y2)  
X0X15=Z1\*(O2ZM0X(X0,X3)-O2Z1)  
RETURN  
1 RETURN  
END

FNX16001  
FNX16002  
FNX16003  
FNX16004  
FNX16005  
FNX16006  
FNX16007  
FNX16008

FUNCTION FUNK16(X0,X1)  
COMMON /BLK13/ Y,Z,R2,Z2,Y2,Z2,Y2,Z2,Y2,Z2,Y2,Z2  
X2=A2M24/X1  
X3=X1\*X2  
X4=X2/X1  
Y1=Y-R2/A1  
IF (ABS(Y1)-LE.1.E-4) GO TO 1  
Y1=Y1\*Y1  
Z1=(1.-X4)\*ALOG(Y2)  
X0X16=Z1\*(O2ZM0X(X0,X3)-O2Z1)  
RETURN  
1 RETURN  
END

FNX17001  
FNX17002  
FNX17003  
FNX17004  
FNX17005  
FNX17006  
FNX17007  
FNX17008  
FNX17009  
FNX17010  
FNX17011  
FNX17012  
FNX17013  
FNX17014

FUNCTION FUNK17(X0,X1)  
COMMON /BLK13/ Y,Z,R2,Z2,Y2,Z2,Y2,Z2,Y2,Z2,Y2,Z2  
X2=A2M24/X1  
X3=X1\*X2  
X4=X2/X1  
Y1=Y-R2/A1  
IF (ABS(Y1)-LE.1.E-4) GO TO 1  
Y1=Y1\*Y1  
Z1=(1.-X4)\*ALOG(Y2)  
X0X17=Z1\*(O2ZM0X(X0,X3)-O2Z1)  
RETURN  
1 RETURN  
END

FNX18001  
FNX18002  
FNX18003  
FNX18004  
FNX18005  
FNX18006  
FNX18007  
FNX18008  
FNX18009  
FNX18010  
FNX18011  
FNX18012  
FNX18013  
FNX18014

FUNCTION FUNK18(X0,X1)  
COMMON /BLK13/ Y,Z,R2,Z2,Y2,Z2,Y2,Z2,Y2,Z2,Y2,Z2  
X2=A2M24/X1  
X3=X1\*X2  
X4=X2/X1  
Y1=Y-R2/A1  
IF (ABS(Y1)-LE.1.E-4) GO TO 1  
Y1=Y1\*Y1  
Z1=(1.-X4)\*ALOG(Y2)  
X0X18=Z1\*(O2ZM0X(X0,X3)-O2Z1)  
RETURN  
1 RETURN  
END

FNX11001  
FNX11002  
FNX11003  
FNX11004  
FNX11005  
FNX11006  
FNX11007  
FNX11008  
FNX11009  
FNX11010  
FNX11011  
FNX11012  
FNX11013  
FNX11014  
FNX11015

FUNCTION FUNK11(X0,X1)  
COMMON /BLK13/ Y,Z,R2,Z2,Y2,Z2,Y2,Z2,Y2,Z2,Y2,Z2  
X2=A2M24/X1  
X3=X1\*X2  
X4=X2/X1  
Y1=Y-R2/A1  
IF (ABS(Y1)-LE.1.E-4) GO TO 1  
Y1=Y1\*Y1  
Z1=(1.-X4)\*ALOG(Y2)  
X0X11=Z1\*(O2ZM0X(X0,X3)-O2Z1)  
RETURN  
1 RETURN  
END

FNX12001  
FNX12002  
FNX12003  
FNX12004  
FNX12005  
FNX12006  
FNX12007  
FNX12008  
FNX12009  
FNX12010  
FNX12011  
FNX12012  
FNX12013  
FNX12014  
FNX12015

FUNCTION FUNK12(X0,X1)  
COMMON /BLK13/ Y,Z,R2,Z2,Y2,Z2,Y2,Z2,Y2,Z2,Y2,Z2  
X2=A2M24/X1  
X3=X1\*X2  
X4=X2/X1  
Y1=Y-R2/A1  
IF (ABS(Y1)-LE.1.E-4) GO TO 1  
Y1=Y1\*Y1  
Z1=(1.-X4)\*ALOG(Y2)  
X0X12=Z1\*(O2ZM0X(X0,X3)-O2Z1)  
RETURN  
1 RETURN  
END

FNX13001  
FNX13002  
FNX13003  
FNX13004  
FNX13005  
FNX13006  
FNX13007  
FNX13008  
FNX13009  
FNX13010  
FNX13011  
FNX13012  
FNX13013

FUNCTION FUNK13(X0,X1)  
COMMON /BLK13/ Y,Z,R2,Z2,Y2,Z2,Y2,Z2,Y2,Z2,Y2,Z2  
X2=A2M24/X1  
X3=X1\*X2  
X4=X2/X1  
Y1=Y-R2/A1  
IF (ABS(Y1)-LE.1.E-4) GO TO 1  
Y1=Y1\*Y1  
Z1=(1.-X4)\*ALOG(Y2)  
X0X13=Z1\*(O2ZM0X(X0,X3)-O2Z1)  
RETURN  
1 RETURN  
END

FNX14001  
FNX14002  
FNX14003  
FNX14004  
FNX14005  
FNX14006  
FNX14007  
FNX14008  
FNX14009  
FNX14010  
FNX14011  
FNX14012  
FNX14013  
FNX14014  
FNX14015

FUNCTION FUNK14(X0,X1)  
COMMON /BLK13/ Y,Z,R2,Z2,Y2,Z2,Y2,Z2,Y2,Z2,Y2,Z2  
X2=A2M24/X1  
X3=X1\*X2  
X4=X2/X1  
Y1=Y-R2/A1  
IF (ABS(Y1)-LE.1.E-4) GO TO 1  
Y1=Y1\*Y1  
Z1=(1.-X4)\*ALOG(Y2)  
X0X14=Z1\*(O2ZM0X(X0,X3)-O2Z1)  
RETURN  
1 RETURN  
END

APPENDIX B

FMT27001  
FMT27002  
FMT27003  
FMT27004

FMT28001  
FMT28002  
FMT28003  
FMT28004

FMT11001  
FMT11002  
FMT11003  
FMT11004  
FMT11005  
FMT11006  
FMT11007  
FMT11008  
FMT11009  
FMT11010  
FMT11011  
FMT11012  
FMT11013  
FMT11014  
FMT11015  
FMT11016  
FMT11017  
FMT11018  
FMT11019

FMT12001  
FMT12002  
FMT12003  
FMT12004  
FMT12005  
FMT12006  
FMT12007  
FMT12008  
FMT12009  
FMT12010  
FMT12011  
FMT12012  
FMT12013

FMT13001  
FMT13002  
FMT13003  
FMT13004  
FMT13005  
FMT13006  
FMT13007  
FMT13008  
FMT13009  
FMT13010  
FMT13011  
FMT13012  
FMT13013  
FMT13014

```
FUNCTION FMT27100(X1)
COMMON /BLK13/ Y,Z,RZ,ZZ,Y2B,K2Y,A2MB24
RETURN
END
```

```
FUNCTION FMT28100(X1)
COMMON /BLK13/ Y,Z,RZ,ZZ,Y2B,K2Y,A2MB24
RETURN
END
```

```
FUNCTION FMT11001(X1)
COMMON /BLK13/ Y,Z,RZ,ZZ,Y2B,K2Y,A2MB24
K3E11*Z2
K4E12*Z1
Y0E2/Z1
Y1E1*Y1
Y2E1*Y1
Y3E1*Y0
Y4E1*Y0
Y5E2*Y1*Y1
Y6E2Z2*Y2*Y1
Y7E2Z2*Y3*Y1
Y8E2Z2*Y4*Y1
Y1E1/Y5+Y2/Y6+Y3/Y7+Y4/Y8
Z1E11--R41*Z1
FUNY11=Z1*OZ*HUX(X0,X3)
RETURN
END
```

```
FUNCTION FMT12100(X1)
COMMON /BLK13/ Y,Z,RZ,ZZ,Y2B,K2Y,A2MB24
K3E11*Z2
K4E12*Z1
Y0E2/Z1
Y1E1*Y1
Z1E11/Y1+1./Y2
FUNY12=Z1*OZ*HUX(X0,X3)
RETURN
END
```

```
FUNCTION FMT13100(X1)
COMMON /BLK13/ Y,Z,RZ,ZZ,Y2B,K2Y,A2MB24
K3E11*Z2
K4E12*Z1
Y0E2/Z1
Y1E1*Y1
IF (ABS(Y11-LE-11-E-4) GO TO 1
Z1E11--R41/Y1
FUNY13=Z1*(OZ*HUX(X0,X3)-OZ*Y1)
RETURN
1 FUNY13=OZ*Y1*(1--R41*Y11--R4)
RETURN
END
```

FMT19002  
FMT19003  
FMT19004  
FMT19005  
FMT19006  
FMT19007

FMT2001  
FMT2002  
FMT2003  
FMT2004  
FMT2005  
FMT2006  
FMT2007  
FMT2008  
FMT2009  
FMT2010  
FMT2011

FMT2001  
FMT2002  
FMT2003  
FMT2004  
FMT2005  
FMT2006  
FMT2007  
FMT2008  
FMT2009  
FMT2010  
FMT2011

FMT23001  
FMT23002  
FMT23003  
FMT23004  
FMT23005  
FMT23006  
FMT23007  
FMT23008  
FMT23009  
FMT23010  
FMT23011

FMT24001  
FMT24002  
FMT24003  
FMT24004  
FMT24005  
FMT24006  
FMT24007  
FMT24008  
FMT24009  
FMT24010

FMT25001  
FMT25002  
FMT25003  
FMT25004

FMT26001  
FMT26002  
FMT26003  
FMT26004

```
FUNCTION FMT19100(X1)
COMMON /BLK13/ Y,Z,RZ,ZZ,Y2B,K2Y,A2MB24
K3E11*Z2
K4E12*Z1
Y0E2/Z1
Y1E1*Y1
FUNY19=Z1*(OZ*HUX(X0,X3)
RETURN
END
```

```
FUNCTION FMT20100(X1)
COMMON /BLK13/ Y,Z,RZ,ZZ,Y2B,K2Y,A2MB24
K3E11*Z2
K4E12*Z1
Y0E2/Z1
Y1E1*Y1
Y2E2*Y1*Y1
Y3E2*Y2*Y1
Y4E2*Y3*Y1
Y1E1/Y5+Y2/Y6+Y3/Y7+Y4/Y8
Z1E11--R41*Z1
FUNY20=Z1*OZ*HUX(X0,X3)
RETURN
END
```

```
FUNCTION FMT20100(X1)
COMMON /BLK13/ Y,Z,RZ,ZZ,Y2B,K2Y,A2MB24
K3E11*Z2
K4E12*Z1
Y0E2/Z1
Y1E1*Y1
Y2E2*Y1*Y1
Y3E2*Y2*Y1
Y4E2*Y3*Y1
Y1E1/Y5+Y2/Y6+Y3/Y7+Y4/Y8
Z1E11--R41*Z1
FUNY20=Z1*OZ*HUX(X0,X3)
RETURN
END
```

```
FUNCTION FMT23100(X1)
COMMON /BLK13/ Y,Z,RZ,ZZ,Y2B,K2Y,A2MB24
K3E11*Z2
K4E12*Z1
Y0E2/Z1
Y1E1*Y1
Y2E2*Y1*Y1
Y3E2*Y2*Y1
Y4E2*Y3*Y1
Y1E1/Y5+Y2/Y6+Y3/Y7+Y4/Y8
Z1E11--R41*Z1
FUNY23=Z1*OZ*HUX(X0,X3)
RETURN
END
```

```
FUNCTION FMT24100(X1)
COMMON /BLK13/ Y,Z,RZ,ZZ,Y2B,K2Y,A2MB24
K3E11*Z2
K4E12*Z1
Y0E2/Z1
Y1E1*Y1
IF (ABS(Y11-LE-11-E-4) GO TO 1
Z1E11--R41/Y1
FUNY24=Z1*(OZ*HUX(X0,X3)-OZ*Y1)
RETURN
1 FUNY24=OZ*Y1*(1--R41*Y11--R4)
RETURN
END
```

```
FUNCTION FMT25100(X1)
COMMON /BLK13/ Y,Z,RZ,ZZ,Y2B,K2Y,A2MB24
K3E11*Z2
K4E12*Z1
Y0E2/Z1
Y1E1*Y1
IF (ABS(Y11-LE-11-E-4) GO TO 1
Z1E11--R41/Y1
FUNY25=Z1*(OZ*HUX(X0,X3)-OZ*Y1)
RETURN
1 FUNY25=OZ*Y1*(1--R41*Y11--R4)
RETURN
END
```

```
FUNCTION FMT26100(X1)
COMMON /BLK13/ Y,Z,RZ,ZZ,Y2B,K2Y,A2MB24
K3E11*Z2
K4E12*Z1
Y0E2/Z1
Y1E1*Y1
IF (ABS(Y11-LE-11-E-4) GO TO 1
Z1E11--R41/Y1
FUNY26=Z1*(OZ*HUX(X0,X3)-OZ*Y1)
RETURN
1 FUNY26=OZ*Y1*(1--R41*Y11--R4)
RETURN
END
```



SPNTE001  
 SPNTE002  
 SPNTE003  
 SPNTE004  
 SPNTE005  
 SPNTE006

```
FUNCTION SPNTE(X)
COMMON /BLK3/ DN,DU1,UM2,AT,MLF,XMLL,XPTE,TBLE,IBTE,TBLMTE,XCMT,
1XLSM1,XLSM2,SSMAX,DAIR,ATE,MTR
SPNTE=1-(XTE)/TBLE
RETURN
END
```

DSPLE001  
 DSPLE002  
 DSPLE003  
 DSPLF004  
 DSPLF005  
 DSPLF006  
 DSPLF007  
 DSPLF008  
 DSPLF009  
 DSPLE010  
 DSPLE011  
 DSPLE012

```
FUNCTION DSPL(X)
COMMON /BLK3/ DN,DU1,UM2,AT,MLF,XMLL,XPTE,TBLE,IBTE,TBLMTE,XCMT,
1XLSM1,XLSM2,SSMAX,DAIR,ATE,MTR
IF (MTR.EQ.1) GO TO 1
DSPLE=1./TBLE
RETURN
1 IF (X.GE.XLSM1) GO TO 2
DSPLE=1./TBLE
RETURN
2 DSPLF0.
RETURN
END
```

DSPT001  
 DSPT002  
 DSPT003  
 DSPT004  
 DSPT005  
 DSPT006

```
FUNCTION DSPT(X)
COMMON /BLK3/ DN,DU1,UM2,AT,MLF,XMLL,XPTE,TBLE,IBTE,TBLMTE,XCMT,
1XLSM1,XLSM2,SSMAX,DAIR,ATE,MTR
DSPT=1./TBLE
RETURN
END
```

Z#000001  
 Z#000002  
 Z#000003  
 Z#000004  
 Z#000005  
 Z#000006  
 Z#000007  
 Z#000008  
 Z#000009  
 Z#000010  
 Z#000011  
 Z#000012  
 Z#000013  
 Z#000014  
 Z#000015  
 Z#000016  
 Z#000017  
 Z#000018  
 Z#000019  
 Z#000020  
 Z#000021  
 Z#000022  
 Z#000023  
 Z#000024  
 Z#000025  
 Z#000026  
 Z#000027  
 Z#000028  
 Z#000029

```
FUNCTION ZM(X,Y)
COMMON /BLK3/ DN,DU1,UM2,AT,MLF,XMLL,XPTE,TBLE,IBTE,TBLMTE,XCMT,
1XLSM1,XLSM2,SSMAX,DAIR,ATE,MTR
COMMON /BLK3/ XMLL,XPTE,TBLE,IBTE,MTR,MH3,NHN
IF (XTE.EQ.1) GO TO 100
SSPALE=1.
Z#000001
Z#000002
Z#000003
Z#000004
Z#000005
Z#000006
Z#000007
Z#000008
Z#000009
Z#000010
Z#000011
Z#000012
Z#000013
Z#000014
Z#000015
Z#000016
Z#000017
Z#000018
Z#000019
Z#000020
Z#000021
Z#000022
Z#000023
Z#000024
Z#000025
Z#000026
Z#000027
Z#000028
Z#000029
```

FNY1001  
 FNY1002  
 FNY1003  
 FNY1004  
 FNY1005  
 FNY1006  
 FNY1007  
 FNY1008  
 FNY1009  
 FNY1010  
 FNY1011  
 FNY1012  
 FNY1013  
 FNY1014

```
FUNCTION FNY(X)
COMMON /BLK13/ YZ,HR2,ZZ,YZ,AT,MLF,XMLL,XPTE,TBLE,IBTE,TBLMTE,XCMT,
1XLSM1,XLSM2,SSMAX,DAIR,ATE,MTR
FNY=1-(XTE)/TBLE
RETURN
END
```

FNY1501  
 FNY1502  
 FNY1503  
 FNY1504  
 FNY1505  
 FNY1506  
 FNY1507  
 FNY1508  
 FNY1509  
 FNY1510  
 FNY1511  
 FNY1512  
 FNY1513  
 FNY1514

```
FUNCTION FNY15(X)
COMMON /BLK13/ YZ,HR2,ZZ,YZ,AT,MLF,XMLL,XPTE,TBLE,IBTE,TBLMTE,XCMT,
1XLSM1,XLSM2,SSMAX,DAIR,ATE,MTR
XZ=2*YZ/X
YZ=X1+X2
Y1=X1-Y
IF (ABS(Y1)-LE,1.E-4) GO TO 1
Z1=(1.-X4)/11
FNY15=Z1*(UZ*DX(X0,X3)-DZ*XY)
RETURN
1 FNY15=UZ*YV*(1.-X4)*(1.-X4)
RETURN
END
```

FNZ11001  
 FNZ11002  
 FNZ11003  
 FNZ11004  
 FNZ11005  
 FNZ11006  
 FNZ11007  
 FNZ11008  
 FNZ11009  
 FNZ11010  
 FNZ11011  
 FNZ11012  
 FNZ11013  
 FNZ11014  
 FNZ11015

```
FUNCTION FNZ(X)
COMMON /BLK13/ YZ,HR2,ZZ,YZ,AT,MLF,XMLL,XPTE,TBLE,IBTE,TBLMTE,XCMT,
1XLSM1,XLSM2,SSMAX,DAIR,ATE,MTR
XZ=2*YZ/X
YZ=X1+X2
Y1=X1-Y
IF (ABS(Y1)-LE,1.E-4) GO TO 1
Z1=(1.-X4)/11
FNZ15=Z1*(UZ*DX(X0,X3)-DZ*XY)
RETURN
1 FNZ15=UZ*YV*(1.-X4)*(1.-X4)
RETURN
END
```

SPNLE001  
 SPNLE002  
 SPNLE003  
 SPNLE004  
 SPNLE005  
 SPNLE006  
 SPNLE007  
 SPNLE008  
 SPNLE009  
 SPNLE010  
 SPNLE011  
 SPNLE012

```
FUNCTION SPNLE(X)
COMMON /BLK3/ DN,DU1,UM2,AT,MLF,XMLL,XPTE,TBLE,IBTE,TBLMTE,XCMT,
1XLSM1,XLSM2,SSMAX,DAIR,ATE,MTR
IF (MTR.EQ.1) GO TO 1
SPNLE=1-(XTE)/TBLE
RETURN
1 IF (X.GE.XLSM1) GO TO 2
SPNLE=1-(XTE)/TBLE
RETURN
2 SPNLE=SSMAX
RETURN
END
```

```

FUNCTION UZDXY(X,Y)
COMMON /BLK3/ DN,DNI,DN2,ATE,MLE,XHLE,XRTE,TBLE,TBTE,TBLMTE,XCNT,
XLSM1,XLSM2,SSMAX,DAIR,MTE,ATH
CL=XTMLE-TBLMTE*Y
XLE=XHLE-TBLE*Y
XC=XBL/CL
FAC=DAIR*DN*(1--XC)*TBLE*XC*TRTF/CL
IF(XCNT.LT.5) GO TO 1
IF(AHS(XC).LE.1.E-4) GO TO 2
XN2=XC**XN2
DZDXY=FA*ACN2
RETURN
2 IF(ABS(LN-2.)).LE.1.E-4) GO TO 4
DZDXY=0.
RETURN
4 DZDXY=+AL
RETURN
1 XC=1--XC
XN2=XC**XN2
DZDXY=FA*ACN2
RETURN
3 DZDXY=0.
RETURN
END
    
```

```

DZDXY001
DZDXY002
DZDXY003
DZDXY004
DZDXY005
DZDXY006
DZDXY007
DZDXY008
DZDXY009
DZDXY010
DZDXY011
DZDXY012
DZDXY013
DZDXY014
DZDXY015
DZDXY016
DZDXY017
DZDXY018
DZDXY019
DZDXY020
DZDXY021
DZDXY022
DZDXY023
DZDXY024
DZDXY025
    
```

```

FUNCTION UZDXY(X,Y)
COMMON /BLK3/ DN,DNI,DN2,ATE,MLE,XHLE,XRTE,TBLE,TBTE,TBLMTE,XCNT,
XLSM1,XLSM2,SSMAX,DAIR,MTE,ATH
CL=XTMLE-TBLMTE*Y
XLE=XHLE-TBLE*Y
XC=XBL/CL
FAC=DAIR*DN*(1--XC)*TBLE*XC*TRTF/CL
IF(XCNT.LT.5) GO TO 1
IF(AHS(XC).LE.1.E-4) GO TO 2
XN2=XC**XN2
DZDXY=FA*ACN2
RETURN
2 IF(ABS(LN-2.)).LE.1.E-4) GO TO 4
DZDXY=0.
RETURN
4 DZDXY=+AL
RETURN
1 XC=1--XC
XN2=XC**XN2
DZDXY=FA*ACN2
RETURN
3 DZDXY=0.
RETURN
END
    
```

```

SUBROUTINE CELI(RLS,AK,IER)
IER=0
GLO=1--AK*AK
IF(GEO)I=2*3
1 IER=1
RETURN
2 IER=1.E75
RETURN
3 GLO=SSRT(GEO)
AHT=1
AARI=ARI
TEST=AARI*1.E-4
AHI=GLO*ARI
IF(AARI-GLO-TEST).GT.6*5
AHI=0.5*ARI
GO TO 4
6 RES=3.14159265/ARI
RETURN
END
    
```

```

CELI0001
CELI0002
CELI0003
CELI0004
CELI0005
CELI0006
CELI0007
CELI0008
CELI0009
CELI0010
CELI0011
CELI0012
CELI0013
CELI0014
CELI0015
CELI0016
CELI0017
CELI0018
CELI0019
CELI0020
    
```

```

FUNCTION UZDXY(X,Y)
COMMON /BLK3/ DN,DNI,DN2,ATE,MLE,XHLE,XRTE,TBLE,TBTE,TBLMTE,XCNT,
XLSM1,XLSM2,SSMAX,DAIR,MTE,ATH
CL=XTMLE-TBLMTE*Y
XLE=XHLE-TBLE*Y
XC=XBL/CL
FAC=DAIR*DN*(1--XC)*TBLE*XC*TRTF/CL
IF(XCNT.LT.5) GO TO 1
IF(AHS(XC).LE.1.E-4) GO TO 2
XN2=XC**XN2
DZDXY=FA*ACN2
RETURN
2 IF(ABS(LN-2.)).LE.1.E-4) GO TO 4
DZDXY=0.
RETURN
4 DZDXY=+AL
RETURN
1 XC=1--XC
XN2=XC**XN2
DZDXY=FA*ACN2
RETURN
3 DZDXY=0.
RETURN
END
    
```

```

SUBROUTINE CELI(RLS,AK,IER)
IER=0
GLO=1--AK*AK
IF(GEO)I=2*3
1 IER=1
RETURN
2 IER=1.E75
RETURN
3 GLO=SSRT(GEO)
AHT=1
AARI=ARI
TEST=AARI*1.E-4
AHI=GLO*ARI
IF(AARI-GLO-TEST).GT.6*5
AHI=0.5*ARI
GO TO 4
6 RES=3.14159265/ARI
RETURN
END
    
```

```

SUBROUTINE CELI(RLS,AK,IER)
IER=0
GLO=1--AK*AK
IF(GEO)I=2*3
1 IER=1
RETURN
2 IER=1.E75
RETURN
3 GLO=SSRT(GEO)
AHT=1
AARI=ARI
TEST=AARI*1.E-4
AHI=GLO*ARI
IF(AARI-GLO-TEST).GT.6*5
AHI=0.5*ARI
GO TO 4
6 RES=3.14159265/ARI
RETURN
END
    
```

```

SUBROUTINE SIMP(DXL,DKU,NIT,NIT1,UTOL,DFUN,DANS)
NIT=10
DH=(DXU-DAL)/2.
IF(ABS(LM).LT.1.E-5) GO TO *
DSUM1=DFUN(DXL)*DKU(DXU)
DSUM2=DFUN(DXL)*DH
DANS=SUM(DSUM1+4.*DSUM2)/3.
N=2
DO 3 I=1,NIT
DANS1=DANS
N=N+2
D=DH/2.
DSUM3=0.
MLRN=1
DO 1 N=1,MLRN-1
DF=K
1 DSUM3=DSUM3+DFUN(DXL+D)*DSUM3/3.
    
```

```

SUBROUTINE SIMP(DXL,DKU,NIT,NIT1,UTOL,DFUN,DANS)
NIT=10
DH=(DXU-DAL)/2.
IF(ABS(LM).LT.1.E-5) GO TO *
DSUM1=DFUN(DXL)*DKU(DXU)
DSUM2=DFUN(DXL)*DH
DANS=SUM(DSUM1+4.*DSUM2)/3.
N=2
DO 3 I=1,NIT
DANS1=DANS
N=N+2
D=DH/2.
DSUM3=0.
MLRN=1
DO 1 N=1,MLRN-1
DF=K
1 DSUM3=DSUM3+DFUN(DXL+D)*DSUM3/3.
    
```

```

SIMP0001
SIMP0002
SIMP0003
SIMP0004
SIMP0005
SIMP0006
SIMP0007
SIMP0008
SIMP0009
SIMP0010
SIMP0011
SIMP0012
SIMP0013
SIMP0014
SIMP0015
SIMP0016
SIMP0017
SIMP0018
SIMP0019
SIMP0020
    
```

```

D2ADX001
D2ADX002
D2ADX003
D2ADX004
D2ADX005
D2ADX006
D2ADX007
D2ADX008
D2ADX009
D2ADX010
D2ADX011
D2ADX012
D2ADX013
D2ADX014
D2ADX015
D2ADX016
D2ADX017
D2ADX018
D2ADX019
D2ADX020
D2ADX021
D2ADX022
D2ADX023
D2ADX024
D2ADX025

FUNCTION U2ADIX(X)
DOUBLE PRECISION K14,RR3,RR2,RR1,RR0,RF1,RF2,RF3,RF4,UNUM
COMMON /BLK3/ DN,UN1,UN2,XT,MLE,XHLE,XRTE,TBLE,TBTE,TBLMTE,XCMT,
XLSM1,XLSM2,SSMAX,DAI,MTE,MTR
COMMON /BLK5/ XHLE1,XHTE1,H3,MNN
IF(X.LT.XHLE1) GO TO 4
IF(MTE.LG.1.AND.X.GT.XLSM2) GO TO 4
IF(MTE.NE.1.AND.X.GT.XRTE1) GO TO 4
RR3=RR1*(X-3.*H)
RR2=RR0*(X-2.*H)
RR1=RR0*(X-H)
RR0=RR0*(X)
RF1=RR1*(X+H)
RF2=RR2*(X+2.*H)
RF3=RR3*(X+3.*H)
RF4=RR4*(X+4.*H)
UNUM=XI*(4+H)*RR3+H*RR2-H*RR1-UN1*RR0+RF4,RF3,RF2,RF1+H*RF4
RETURN
END
4 RESORT(4,5,CMP1(X))
INDX=2*SIZEPI(X)/I
D2ADJ=12*SIZEPI(X)-JPIX*DNDX1/P
RETURN
END

```

```

D4ADY001
D4ADY002
D4ADY003
D4ADY004
D4ADY005
D4ADY006
D4ADY007
D4ADY008
D4ADY009
D4ADY010
D4ADY011
D4ADY012
D4ADY013
D4ADY014
D4ADY015
D4ADY016
D4ADY017
D4ADY018
D4ADY019
D4ADY020
D4ADY021
D4ADY022
D4ADY023
D4ADY024
D4ADY025

FUNCTION U4ADY(X)
DOUBLE PRECISION K12,K11,RF1,RF2,UNUM
COMMON /BLK3/ DN,UN1,UN2,XT,MLE,XHLE,XRTE,TBLE,TBTE,TBLMTE,XCMT,
XLSM1,XLSM2,SSMAX,DAI,MTE,MTR
COMMON /BLK5/ XHLE1,XHTE1,H3,MNN
IF(X.LT.XHLE1) GO TO 4
IF(MTE.LG.1.AND.X.GT.XLSM2) GO TO 4
IF(MTE.NE.1.AND.X.GT.XRTE1) GO TO 4
RR2=RR1*(X-2.*H)
RR1=RR0*(X+H)
RF1=RR1*(X+H)
RF2=RR2*(X+2.*H)
RF3=RR3*(X+3.*H)
RF4=RR4*(X+4.*H)
UNUM=XI*(4+H)*RR3+H*RR2-H*RR1-UN1*RR0+RF4,RF3,RF2,RF1+H*RF4
RETURN
END
4 RESORT(4,5,CMP1(X))
INDX=2*SIZEPI(X)/I
D4ADJ=12*SIZEPI(X)-JPIX*DNDX1/P
RETURN
END

```

```

D2ADY001
D2ADY002
D2ADY003
D2ADY004
D2ADY005
D2ADY006
D2ADY007
D2ADY008
D2ADY009
D2ADY010
D2ADY011
D2ADY012
D2ADY013
D2ADY014
D2ADY015
D2ADY016
D2ADY017
D2ADY018
D2ADY019
D2ADY020
D2ADY021
D2ADY022
D2ADY023
D2ADY024
D2ADY025

FUNCTION U2ADY(X)
DOUBLE PRECISION K14,RR3,RR2,RR1,RR0,RF1,RF2,RF3,RF4,UNUM
COMMON /BLK3/ DN,UN1,UN2,XT,MLE,XHLE,XRTE,TBLE,TBTE,TBLMTE,XCMT,
XLSM1,XLSM2,SSMAX,DAI,MTE,MTR
COMMON /BLK5/ XHLE1,XHTE1,H3,MNN
IF(X.LT.XHLE1) GO TO 4
IF(MTE.LG.1.AND.X.GT.XLSM2) GO TO 4
IF(MTE.NE.1.AND.X.GT.XRTE1) GO TO 4
RR3=RR1*(X-3.*H)
RR2=RR0*(X-2.*H)
RR1=RR0*(X+H)
RR0=RR0*(X)
RF1=RR1*(X+H)
RF2=RR2*(X+2.*H)
RF3=RR3*(X+3.*H)
RF4=RR4*(X+4.*H)
UNUM=XI*(4+H)*RR3+H*RR2-H*RR1-UN1*RR0+RF4,RF3,RF2,RF1+H*RF4
RETURN
END
4 RESORT(4,5,CMP1(X))
INDX=2*SIZEPI(X)/I
D2ADJ=12*SIZEPI(X)-JPIX*DNDX1/P
RETURN
END

```

```

SIMP0019
SIMP0020
SIMP0021
SIMP0022
SIMP0023
SIMP0024
SIMP0025
SIMP0026
SIMP0027
SIMP0028
SIMP0029
SIMP0030
SIMP0031

SIMP1001
SIMP1002
SIMP1003
SIMP1004
SIMP1005
SIMP1006
SIMP1007
SIMP1008
SIMP1009
SIMP1010
SIMP1011
SIMP1012
SIMP1013
SIMP1014
SIMP1015
SIMP1016
SIMP1017
SIMP1018
SIMP1019
SIMP1020
SIMP1021
SIMP1022
SIMP1023
SIMP1024
SIMP1025
SIMP1026
SIMP1027
SIMP1028
SIMP1029
SIMP1030
SIMP1031
SIMP1032
SIMP1033

FUNCTION U2ADY(X)
DOUBLE PRECISION K14,RR3,RR2,RR1,RR0,RF1,RF2,RF3,RF4,UNUM
COMMON /BLK3/ DN,UN1,UN2,XT,MLE,XHLE,XRTE,TBLE,TBTE,TBLMTE,XCMT,
XLSM1,XLSM2,SSMAX,DAI,MTE,MTR
COMMON /BLK5/ XHLE1,XHTE1,H3,MNN
IF(X.LT.XHLE1) GO TO 4
IF(MTE.LG.1.AND.X.GT.XLSM2) GO TO 4
IF(MTE.NE.1.AND.X.GT.XRTE1) GO TO 4
RR3=RR1*(X-3.*H)
RR2=RR0*(X-2.*H)
RR1=RR0*(X+H)
RR0=RR0*(X)
RF1=RR1*(X+H)
RF2=RR2*(X+2.*H)
RF3=RR3*(X+3.*H)
RF4=RR4*(X+4.*H)
UNUM=XI*(4+H)*RR3+H*RR2-H*RR1-UN1*RR0+RF4,RF3,RF2,RF1+H*RF4
RETURN
END
4 RESORT(4,5,CMP1(X))
INDX=2*SIZEPI(X)/I
D2ADJ=12*SIZEPI(X)-JPIX*DNDX1/P
RETURN
END

```

```

D4ADY001
D4ADY002
D4ADY003
D4ADY004
D4ADY005
D4ADY006
D4ADY007
D4ADY008
D4ADY009
D4ADY010
D4ADY011
D4ADY012
D4ADY013
D4ADY014
D4ADY015
D4ADY016
D4ADY017
D4ADY018
D4ADY019

SIMP2001
SIMP2002
SIMP2003
SIMP2004
SIMP2005
SIMP2006
SIMP2007
SIMP2008
SIMP2009
SIMP2010
SIMP2011
SIMP2012
SIMP2013
SIMP2014
SIMP2015
SIMP2016
SIMP2017
SIMP2018
SIMP2019
SIMP2020
SIMP2021
SIMP2022
SIMP2023
SIMP2024
SIMP2025
SIMP2026
SIMP2027
SIMP2028
SIMP2029
SIMP2030
SIMP2031
SIMP2032
SIMP2033

FUNCTION U4ADY(X)
DOUBLE PRECISION K12,K11,RF1,RF2,UNUM
COMMON /BLK3/ DN,UN1,UN2,XT,MLE,XHLE,XRTE,TBLE,TBTE,TBLMTE,XCMT,
XLSM1,XLSM2,SSMAX,DAI,MTE,MTR
COMMON /BLK5/ XHLE1,XHTE1,H3,MNN
IF(X.LT.XHLE1) GO TO 4
IF(MTE.LG.1.AND.X.GT.XLSM2) GO TO 4
IF(MTE.NE.1.AND.X.GT.XRTE1) GO TO 4
RR2=RR1*(X-2.*H)
RR1=RR0*(X+H)
RF1=RR1*(X+H)
RF2=RR2*(X+2.*H)
RF3=RR3*(X+3.*H)
RF4=RR4*(X+4.*H)
UNUM=XI*(4+H)*RR3+H*RR2-H*RR1-UN1*RR0+RF4,RF3,RF2,RF1+H*RF4
RETURN
END
4 RESORT(4,5,CMP1(X))
INDX=2*SIZEPI(X)/I
D4ADJ=12*SIZEPI(X)-JPIX*DNDX1/P
RETURN
END

```

```

D4ADY001
D4ADY002
D4ADY003
D4ADY004
D4ADY005
D4ADY006
D4ADY007
D4ADY008
D4ADY009
D4ADY010
D4ADY011
D4ADY012
D4ADY013
D4ADY014
D4ADY015
D4ADY016
D4ADY017
D4ADY018
D4ADY019

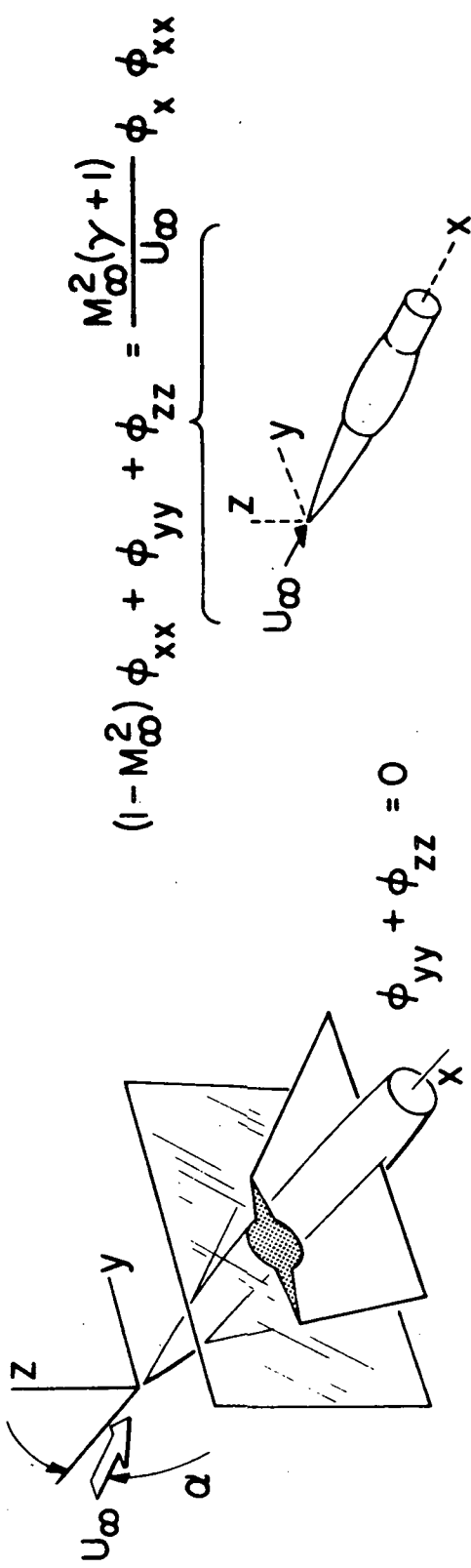
SIMP3001
SIMP3002
SIMP3003
SIMP3004
SIMP3005
SIMP3006
SIMP3007
SIMP3008
SIMP3009
SIMP3010
SIMP3011
SIMP3012
SIMP3013
SIMP3014
SIMP3015
SIMP3016
SIMP3017
SIMP3018
SIMP3019
SIMP3020
SIMP3021
SIMP3022
SIMP3023
SIMP3024
SIMP3025
SIMP3026
SIMP3027
SIMP3028
SIMP3029
SIMP3030
SIMP3031
SIMP3032
SIMP3033

FUNCTION U4ADY(X)
DOUBLE PRECISION K12,K11,RF1,RF2,UNUM
COMMON /BLK3/ DN,UN1,UN2,XT,MLE,XHLE,XRTE,TBLE,TBTE,TBLMTE,XCMT,
XLSM1,XLSM2,SSMAX,DAI,MTE,MTR
COMMON /BLK5/ XHLE1,XHTE1,H3,MNN
IF(X.LT.XHLE1) GO TO 4
IF(MTE.LG.1.AND.X.GT.XLSM2) GO TO 4
IF(MTE.NE.1.AND.X.GT.XRTE1) GO TO 4
RR2=RR1*(X-2.*H)
RR1=RR0*(X+H)
RF1=RR1*(X+H)
RF2=RR2*(X+2.*H)
RF3=RR3*(X+3.*H)
RF4=RR4*(X+4.*H)
UNUM=XI*(4+H)*RR3+H*RR2-H*RR1-UN1*RR0+RF4,RF3,RF2,RF1+H*RF4
RETURN
END
4 RESORT(4,5,CMP1(X))
INDX=2*SIZEPI(X)/I
D4ADJ=12*SIZEPI(X)-JPIX*DNDX1/P
RETURN
END

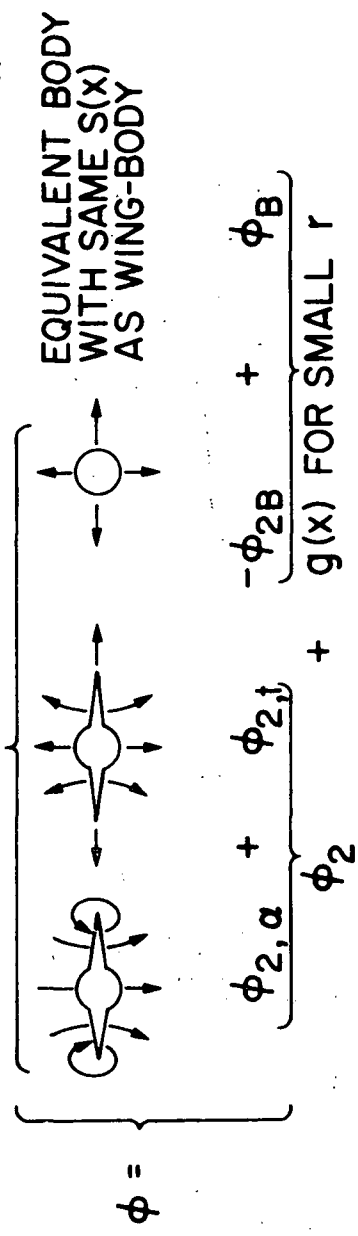
```

## REFERENCES

1. Steger, J. L. and Lomax, H.: Generalized Relaxation Methods Applied to Problems in Transonic Flow. Proc. 2nd Int. Conf. on Numerical Methods in Fluid Dynamics, Sept. 1970; Lecture Notes in Physics, 1971, pp. 193-197.
2. Garabedian, P. R. and Korn, D. G.: Numerical Design of Transonic Airfoils. Numerical Solution of Partial Differential Equations - II, Bert Hubbard, ed., Academic Press, Inc., 1971, pp. 253-271.
3. Murman, E. M. and Cole, J. D.: Calculation of Plane Steady Transonic Flows. AIAA J., Vol. 9, No. 1, Jan. 1971, pp. 114-121.
4. Murman, E. M. and Krupp, J. A.: The Numerical Calculation of Steady Transonic Flows Past Thin Lifting Airfoils and Slender Bodies. AIAA Paper No. 71-566, Presented at AIAA 4th Fluid and Plasma Dynamics Conf., Palo Alto, Calif., June 21-23, 1971
5. Bailey, F. R.: Numerical Calculation of Transonic Flow About Slender Bodies of Revolution. NASA TN D-6582, Dec. 1971.
6. Spreiter, J. R. and Stahara, S. S.: Calculative Techniques for Transonic Flows About Certain Classes of Airfoils and Slender Bodies. NASA CR-1722, 1971.
7. Stahara, S. S. and Spreiter, J. R.: Calculative Techniques for Transonic Flows About Certain Classes of Wing-Body Combinations. NEAR TR 36, Nov. 1971. NASA CR-2103, 1972.
8. Heaslet, M. A. and Spreiter, J. R.: Three-Dimensional Transonic Flow Theory Applied to Slender Wings and Bodies. NACA Rep. 1318, 1957.
9. Adams, M. C. and Sears, W. R.: Slender-Body Theory - Review and Extensions. J. Aero. Sci., Vol. 20, No. 2, 1953, pp. 85-98.
10. Stocker, P. M.: Supersonic Flow Past Bodies of Revolution with Thin Wings of Small Aspect Ratio. Aero. Quart., Vol. III, May 1951, pp. 61-79.

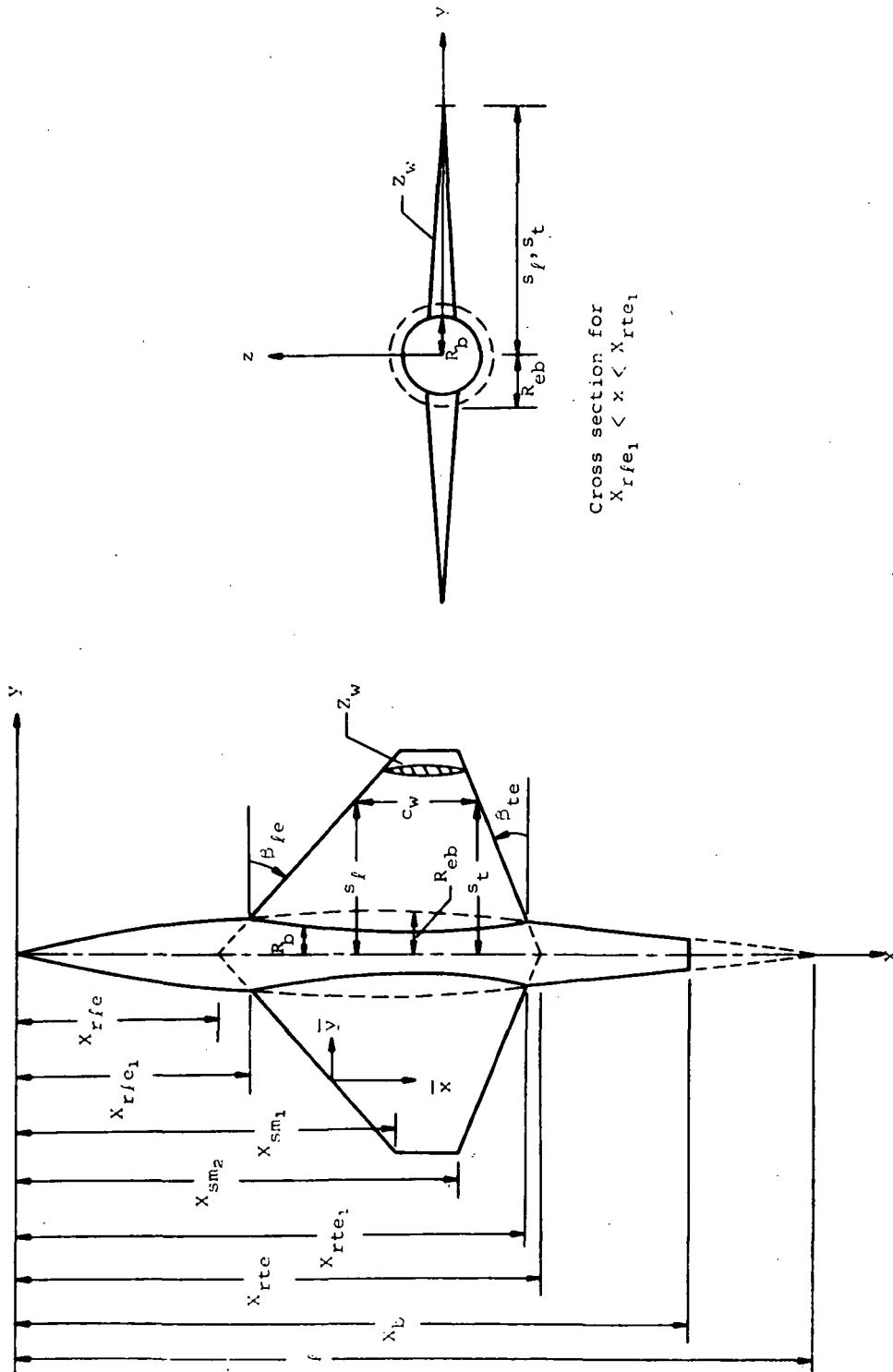


$$(1 - M_\infty^2) \phi_{xx} + \phi_{yy} + \phi_{zz} = \frac{M_\infty^2(\gamma + 1)}{U_\infty} \phi_x \phi_{xx}$$



$$C_p = -\frac{2}{U_\infty} (\phi_x + \alpha \phi_z) - \frac{1}{U_\infty^2} (\phi_y^2 + \phi_z^2)$$

Figure 1.- Transonic equivalence rule for slender wing-body combinations.



Cross section for  $x_{rfe1} < x < x_{rte1}$

Figure 2(a). - General configuration of finite thickness wing-indented circular body combinations with straight/sweptforward trailing edge planforms ( $\beta_{te} \leq 0$ ).

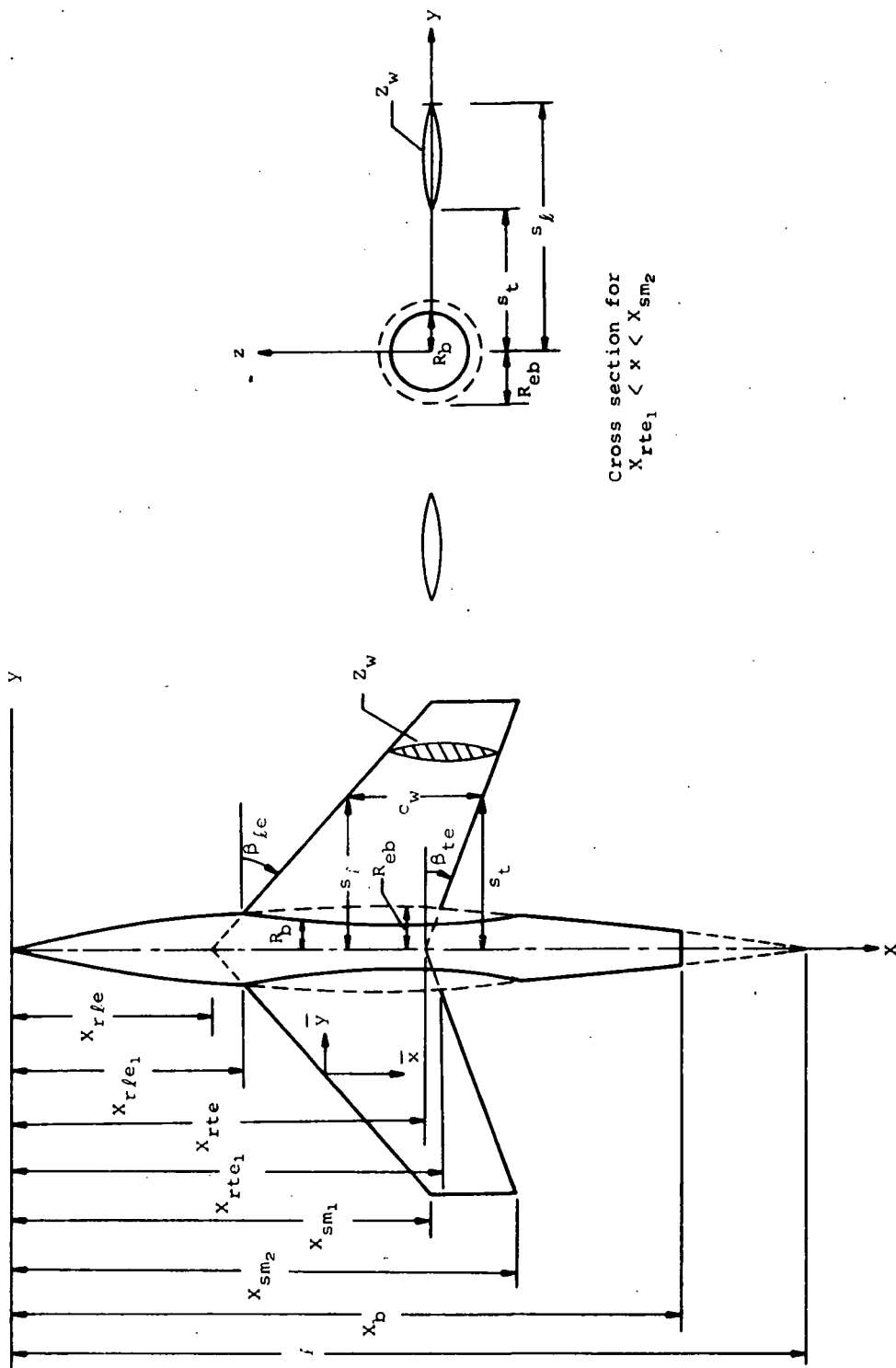
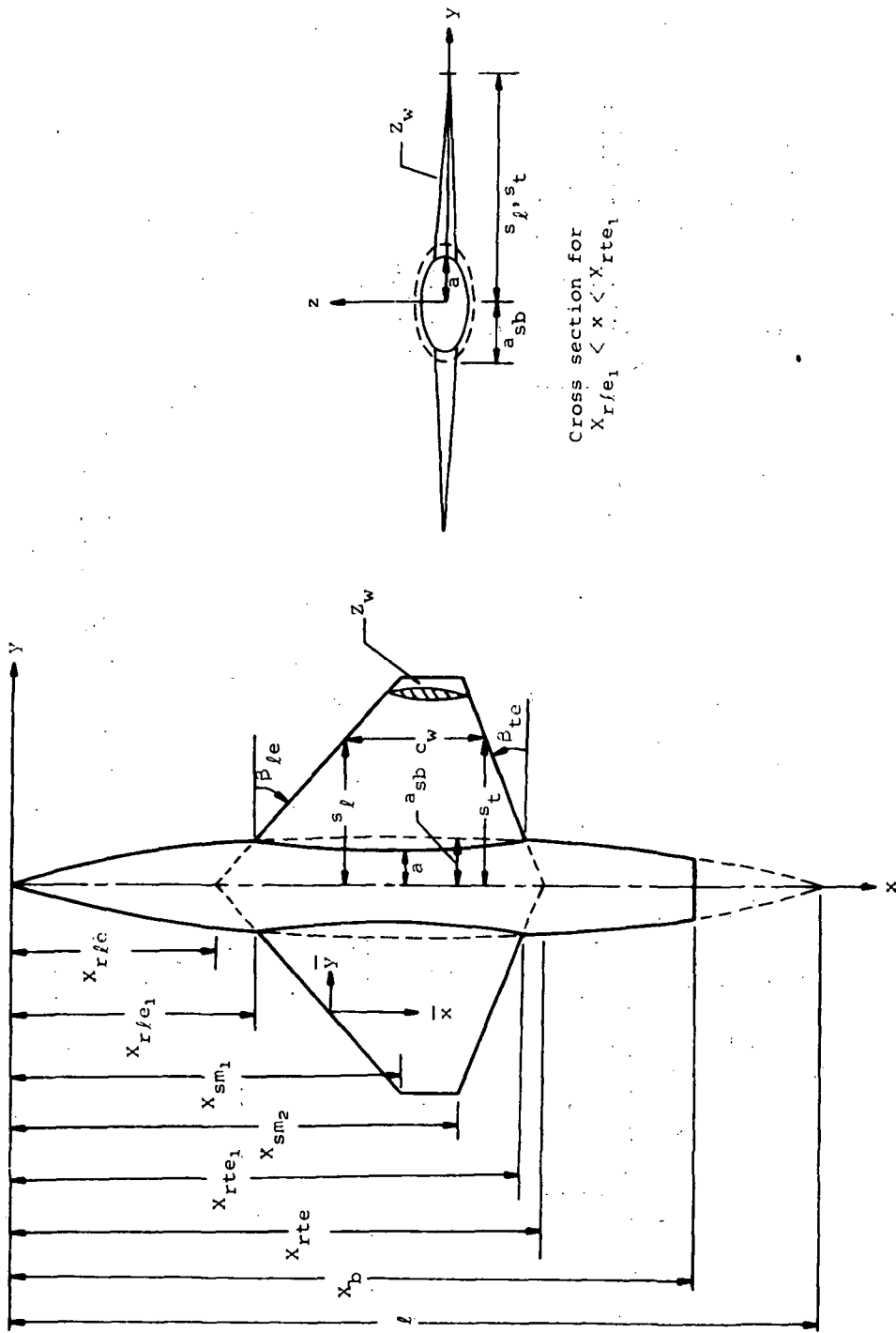


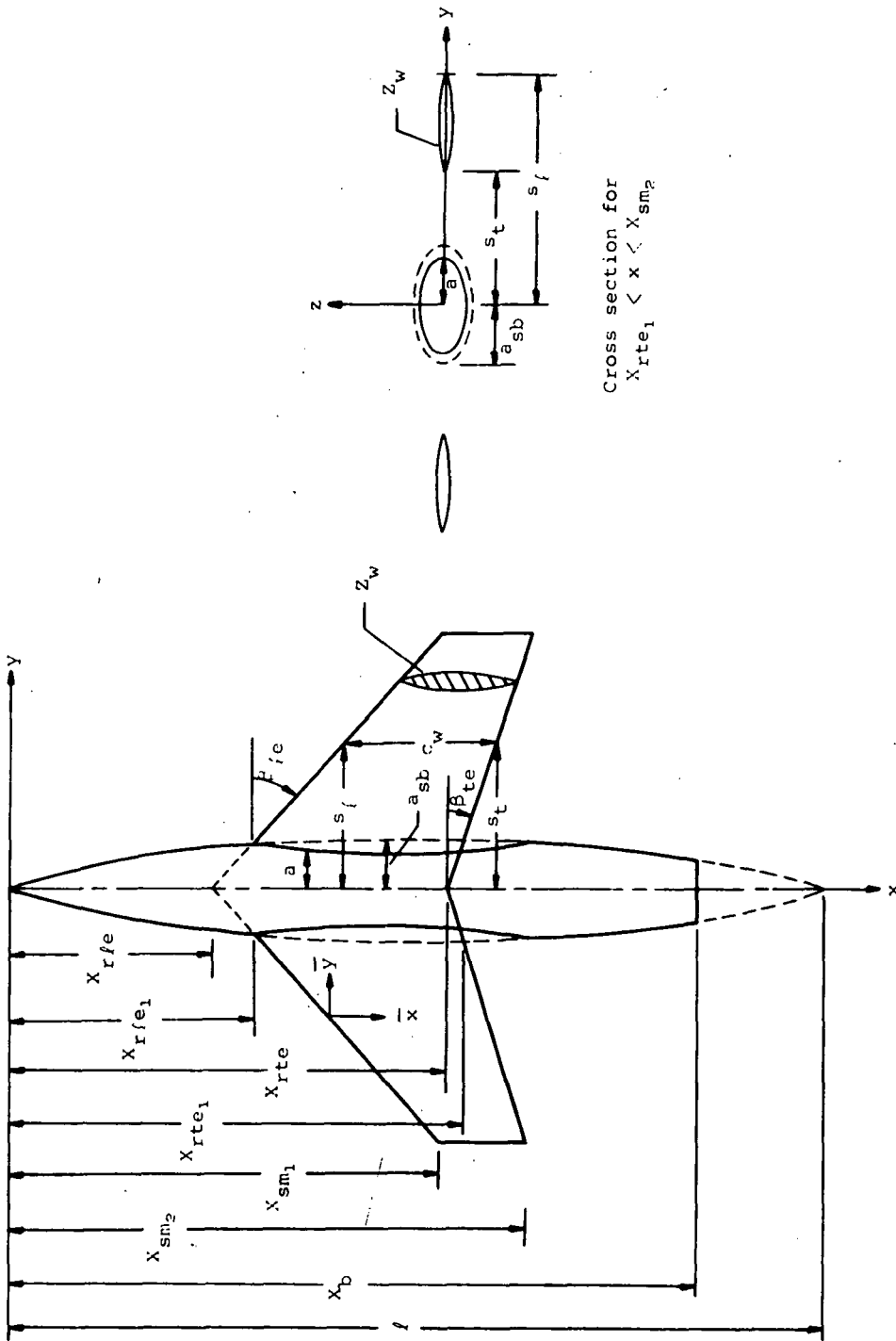
Figure 2(b) - General configuration of finite thickness wing-indented circular body combinations with sweptback trailing edge planforms ( $\beta_{te} > 0$ ).



Cross section for  
 $x_{r/e1} < x < x_{rte1}$

Figure 3(a).- General configuration of finite thickness wing-indented elliptic body combinations with straight/sweptforward trailing edge planforms ( $\beta_{te} \leq 0$ ).





Cross section for  
 $x_{rte1} < x < x_{sm2}$

Figure 3(b). - General configuration of finite thickness wing-indented elliptic body combinations with sweptback trailing edge planforms ( $\beta_{te} > 0$ ).

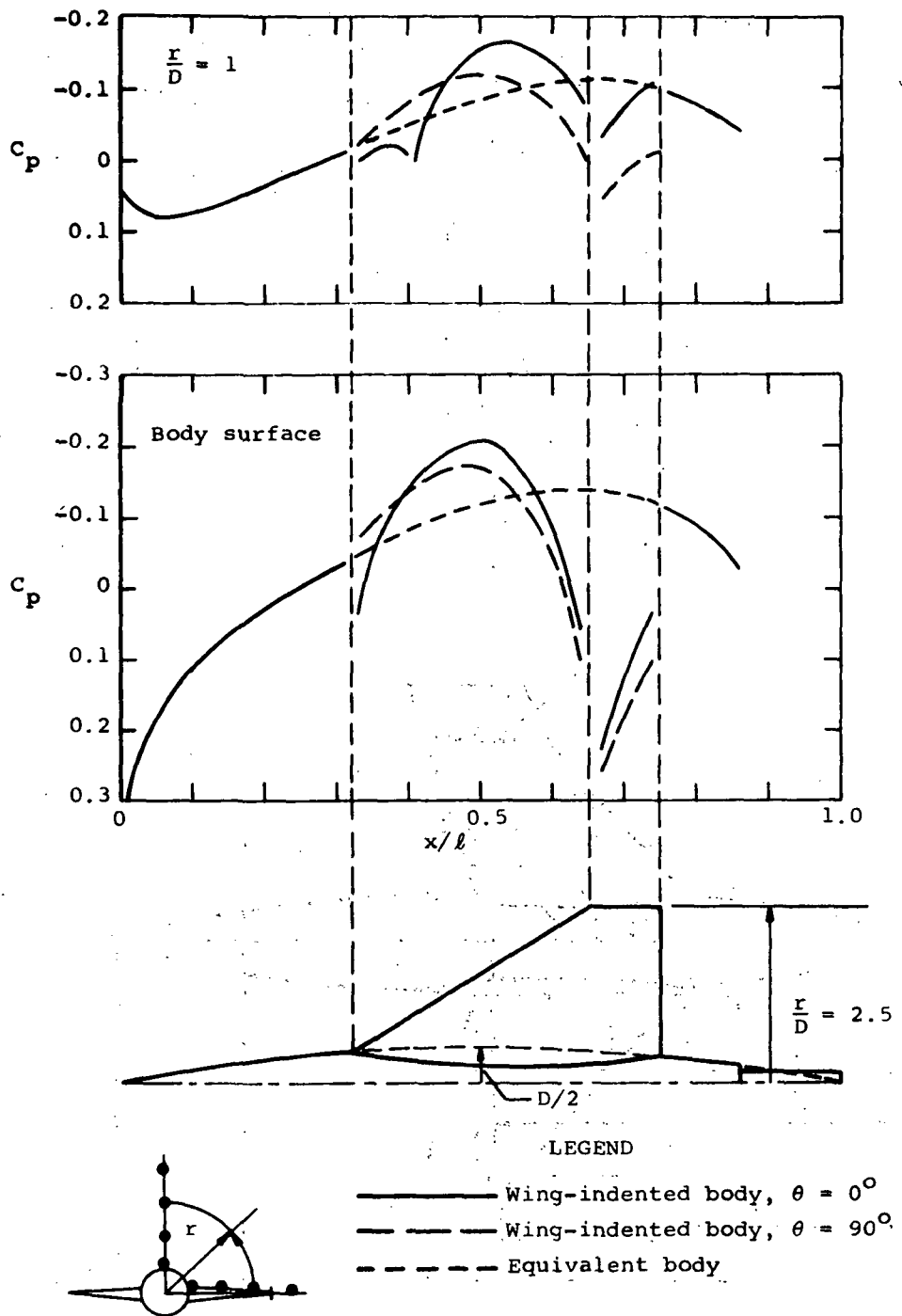


Figure 4.- Theoretical surface and flow field pressure distributions at  $M_\infty = 1$  for a nonlifting parabolic-arc profile wing--indented parabolic-arc body combination; equivalent body thickness ratio  $D/l = 0.1$ , wing aspect ratio  $AR = 1.7$ , thickness/chord ratio  $t/c_w = 0.04$ , planform taper ratio  $TR = 0.2$ , and with  $X_{rle}/l = 0.25$ ,  $C_{RT} = 0.50$ ,  $X_{b/l} = 0.86$ .

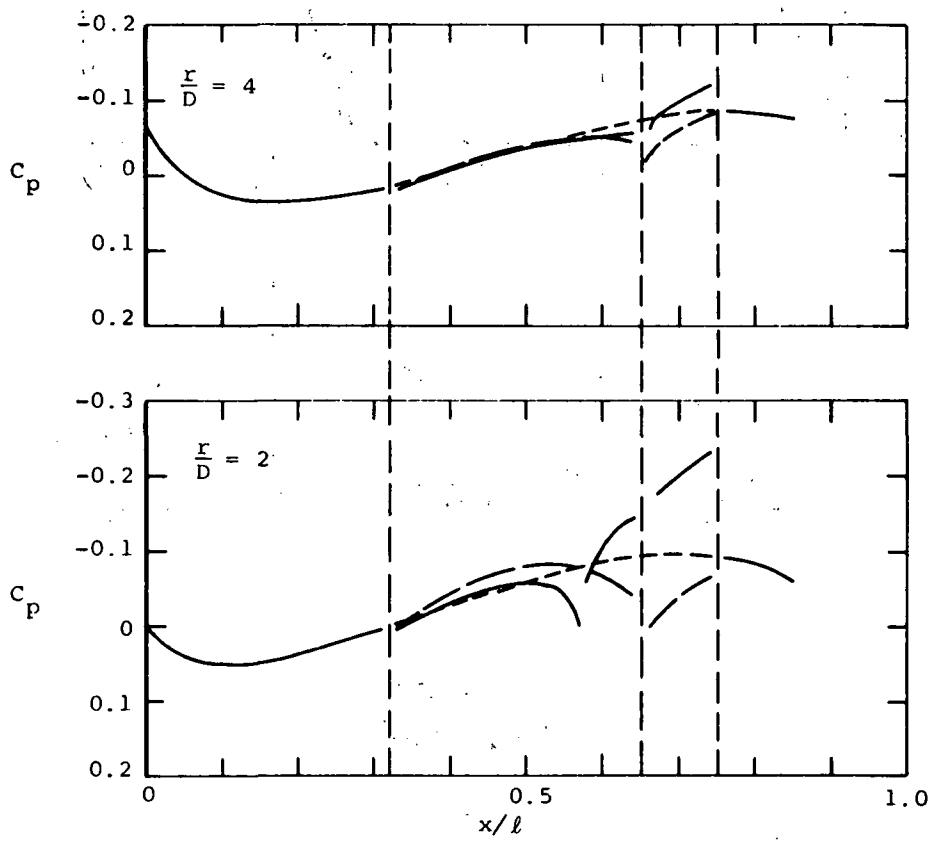


Figure 4.- Concluded

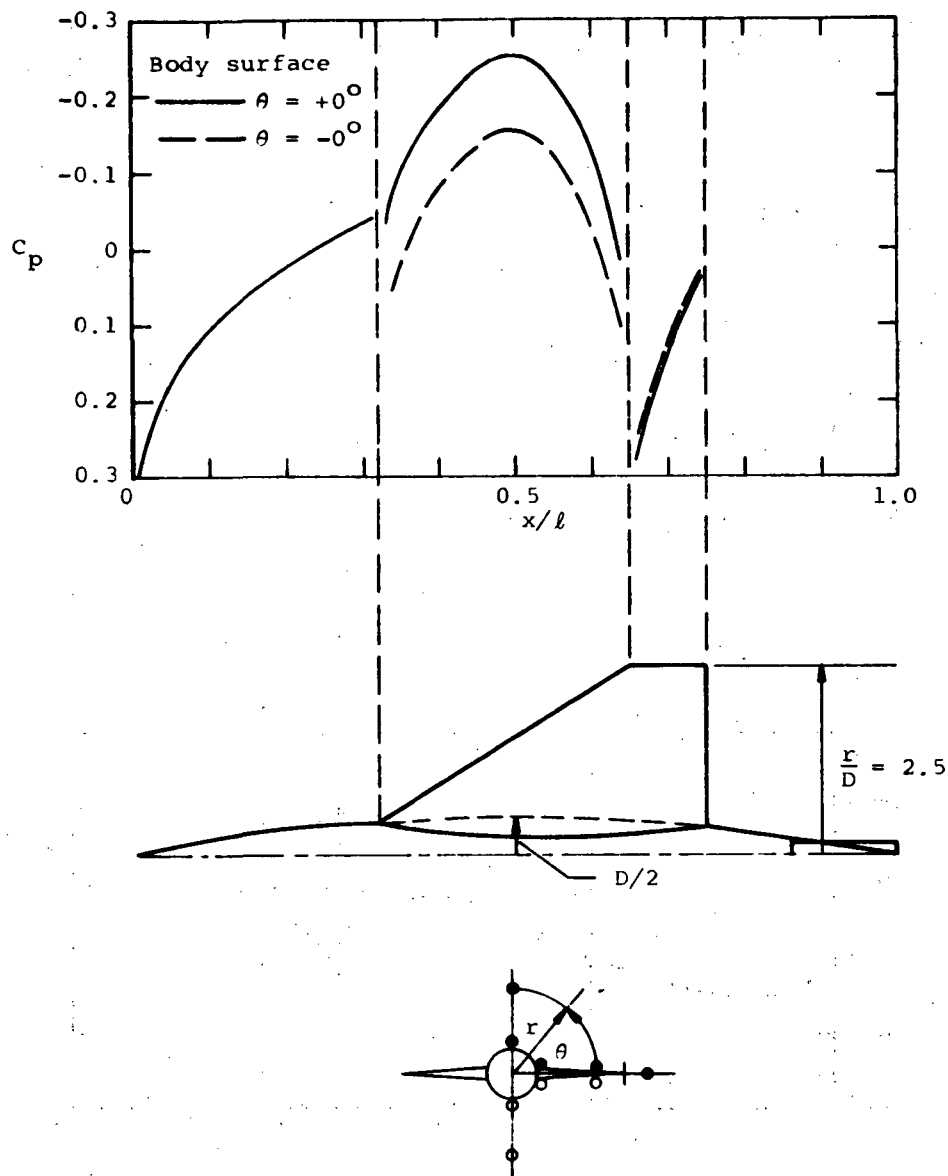


Figure 5.- Theoretical surface and flow field pressure distributions and loadings at  $M_\infty = 1$  and  $\alpha = 2^\circ$  for a parabolic-arc profile wing--indented parabolic-arc body combination; equivalent body thickness ratio  $D/l = 0.1$ , wing aspect ratio  $AR = 1.7$ , thickness/chord ratio  $t/c_w = 0.04$ , planform taper ratio  $TR = 0.2$ , and with  $x_{rle}/l = 0.25$ ,  $C_{R_T/l} = 0.5$ ,  $x_b/l = 0.86$ .

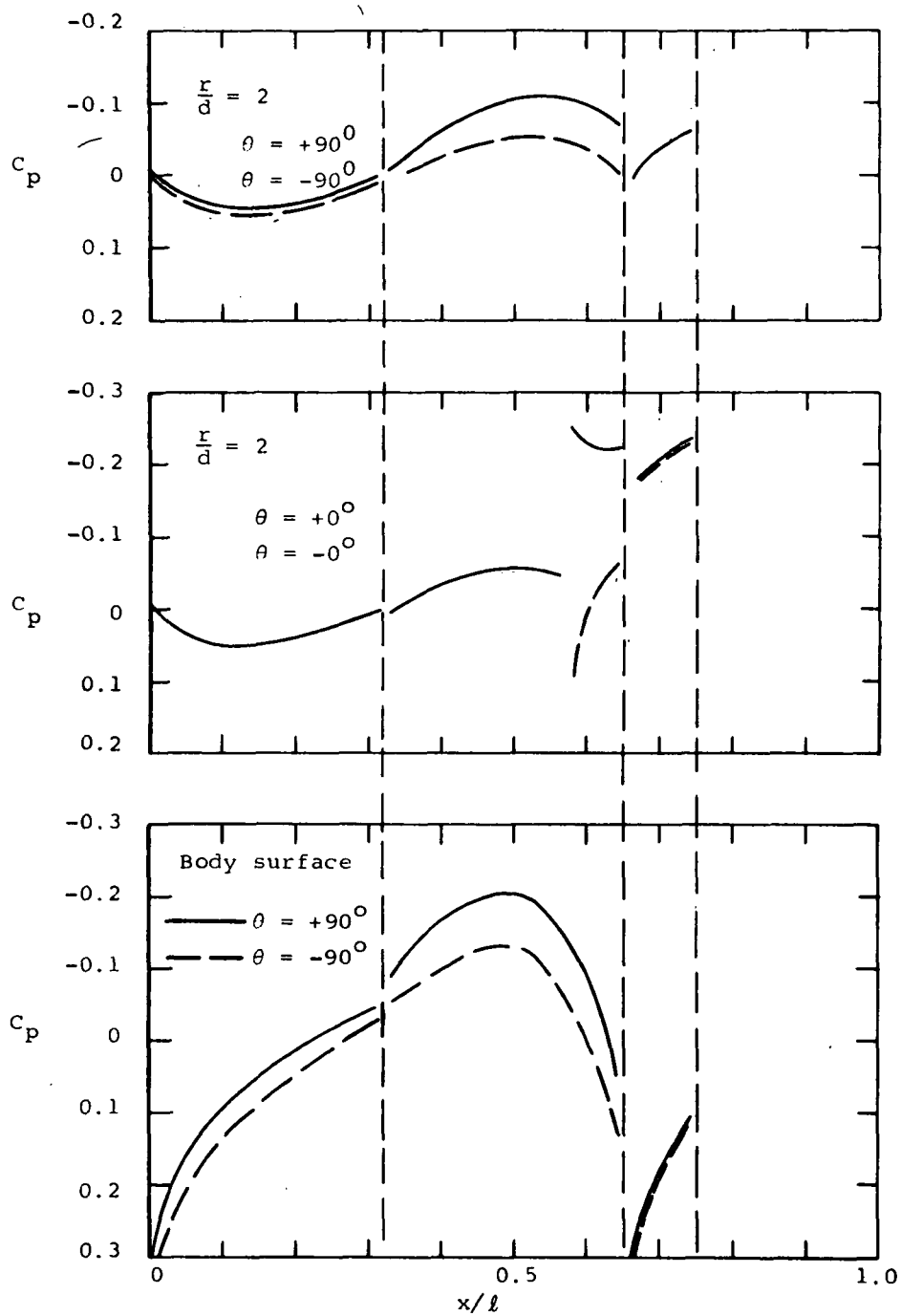


Figure 5.- Continued.

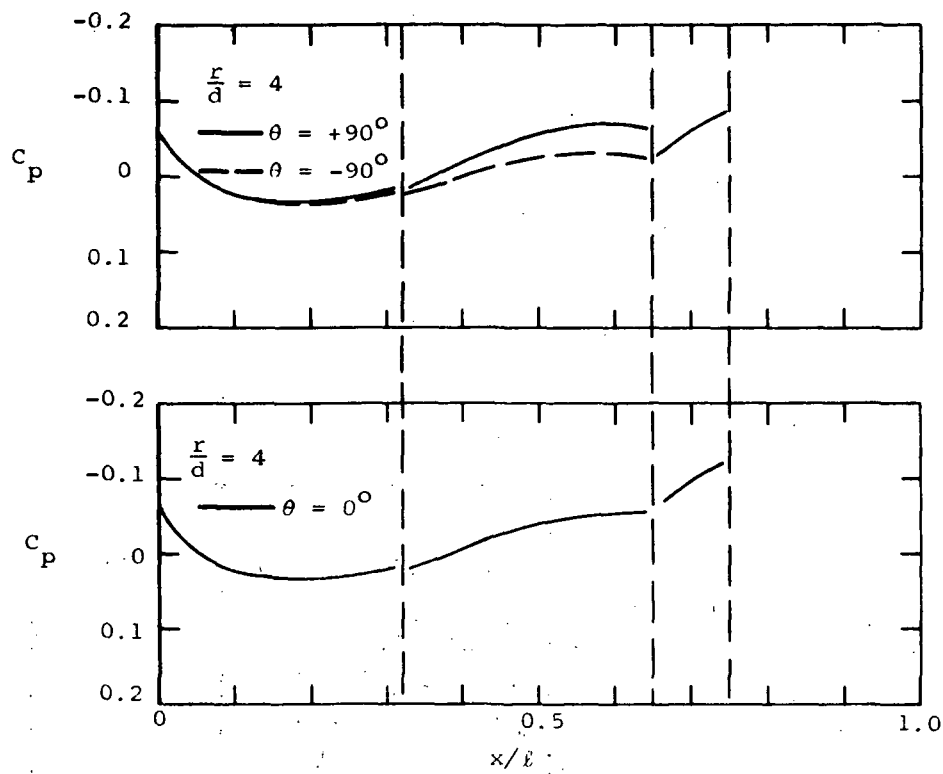


Figure 5.- Concluded.

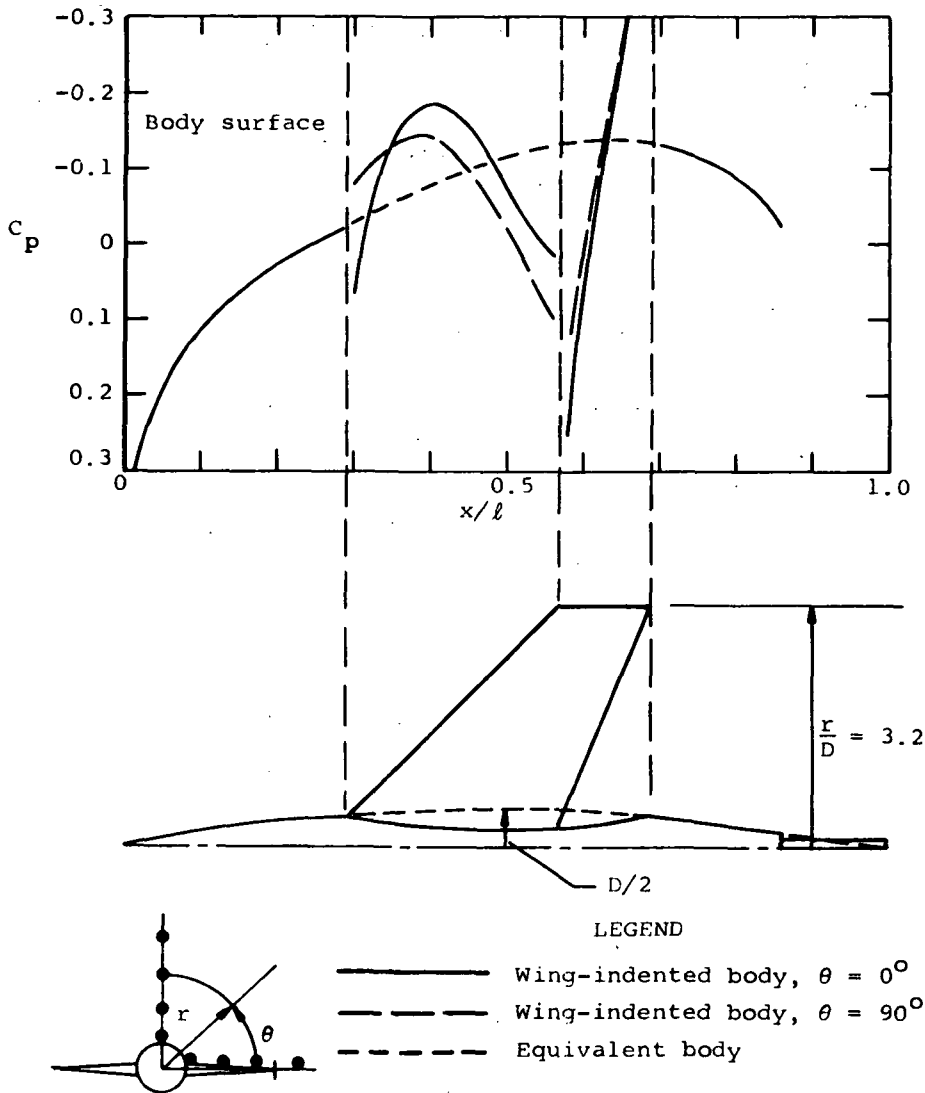


Figure 6.- Theoretical surface and flow field pressure distributions at  $M_\infty = 1$  for a nonlifting parabolic-arc profile wing--indented parabolic-arc body combination; equivalent body thickness ratio  $D/l = 0.1$ , wing aspect ratio  $AR = 2.8$ , thickness ratio  $t/c_w = 0.04$ , planform taper ratio  $TR = 0.4$ , and with  $x_{rle}/l = 0.25$ ,  $C_{TR} = 0.3$ ,  $x_{b/l} = 0.86$ .

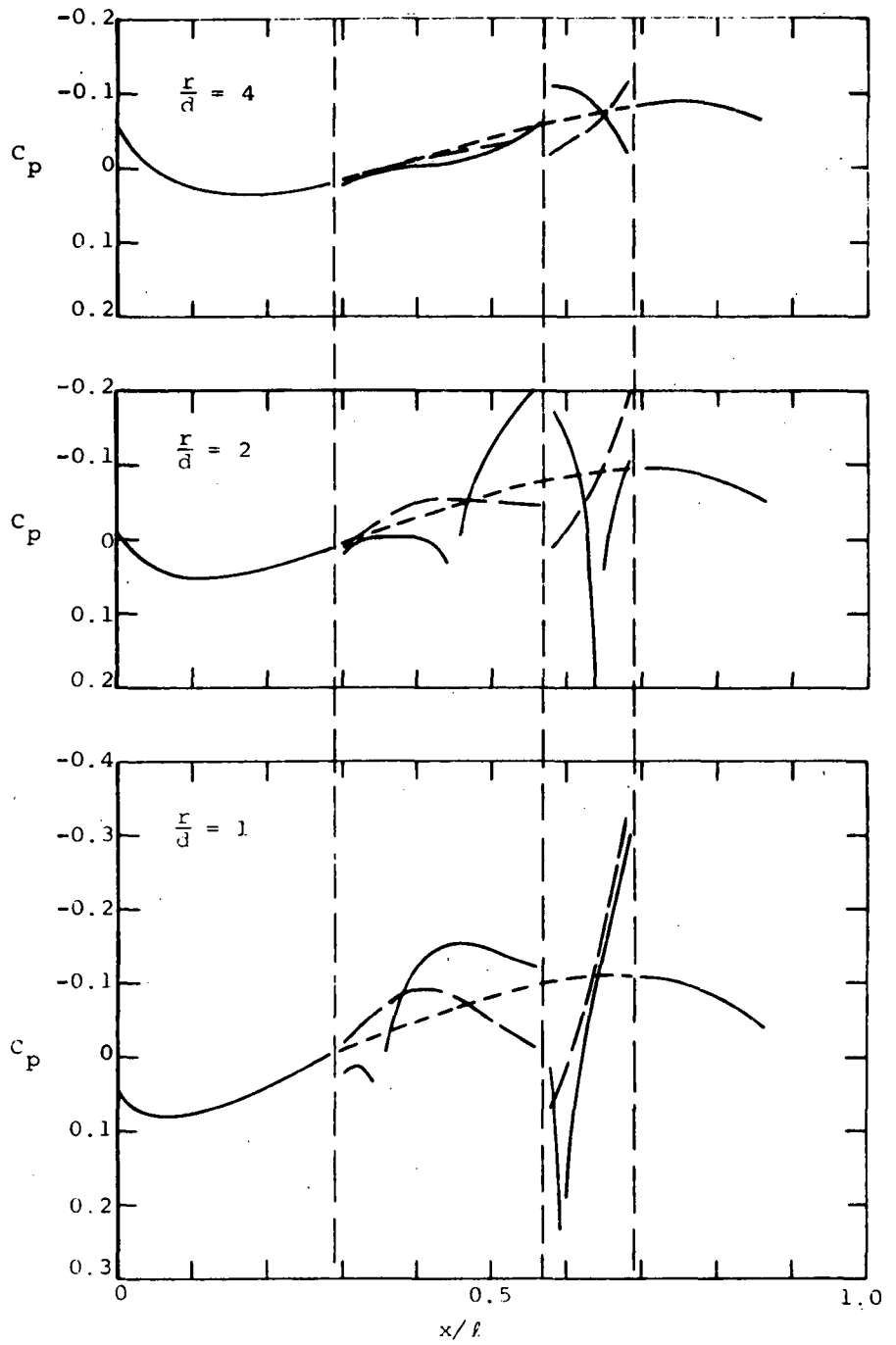


Figure 6.- Concluded.



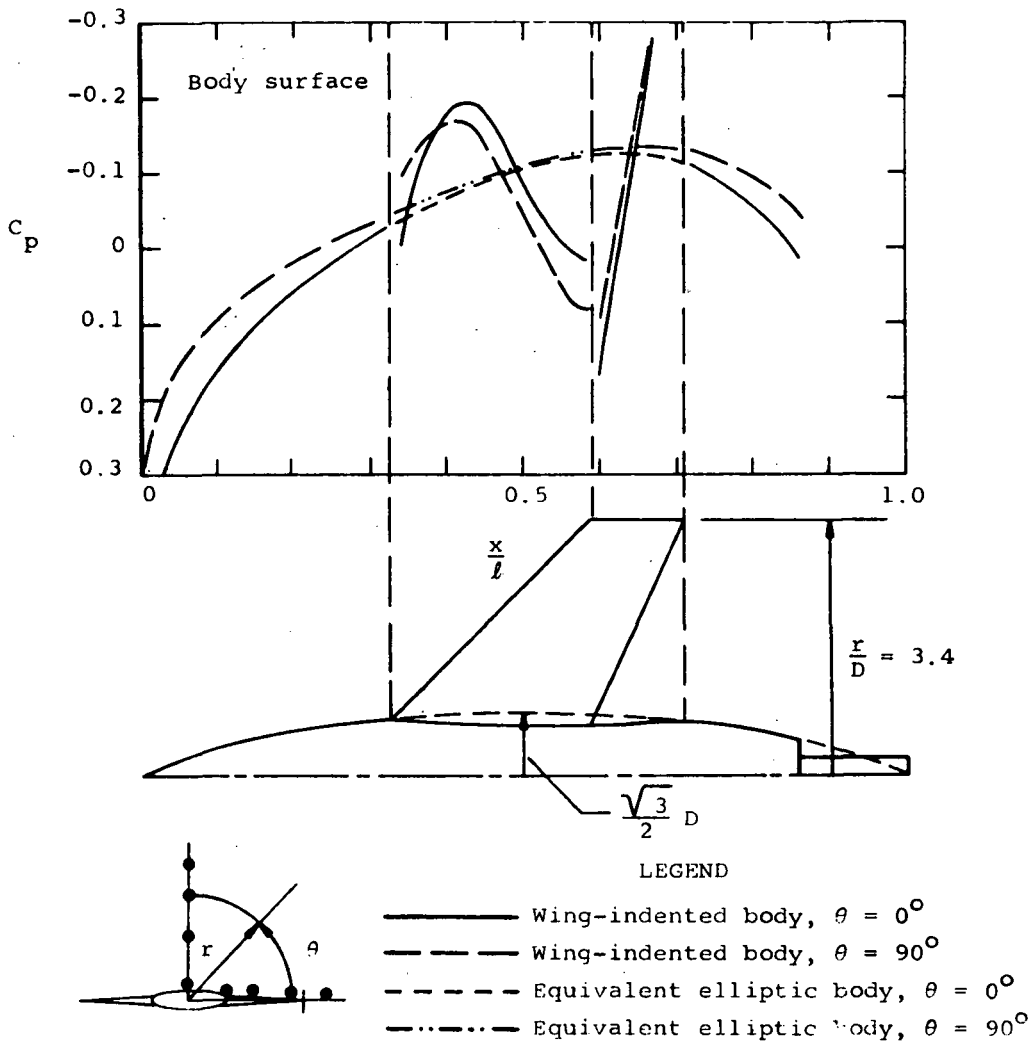


Figure 7.- Theoretical surface and flow field pressure distributions at  $M_\infty = 1$  for a nonlifting parabolic-arc profile wing-indented parabolic-arc body combination; having a body of elliptical cross section with  $\lambda = 3$ ; equivalent body thickness ratio  $D/l = 0.1$ , wing aspect ratio  $AR = 2.8$ , thickness ratio  $t/c_w = 0.04$ , planform taper ratio  $TR = 0.4$ , and with  $x_{rte}/l = 0.25$ ,  $C_{RT}/l = 0.3$ ,  $x_b/l = 0.86$ .

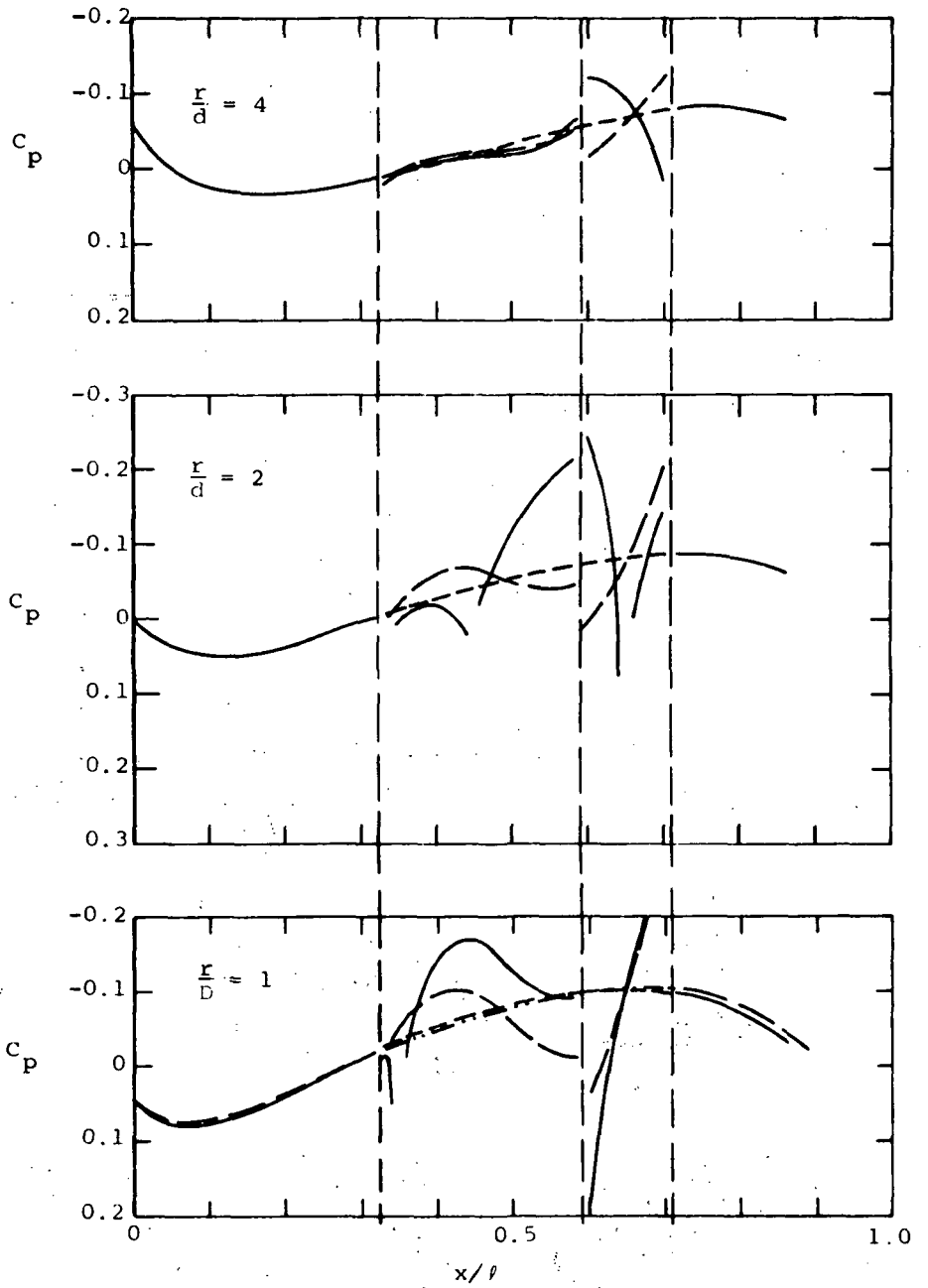


Figure 7.- Concluded.

STRANIN AMACH=1.,MOPT=1,TAUB=.1,TAUM=.04,XMTB=.5,XMTW=.5,ANGLE=58.,  
SSMAX=.25,XRLE=.25,TR=.2,CRT=.5,XLBASE=.86,XLOUTP=.05,4END

(a) Input.

CALCULATION OF SURFACE AND FLOW FIELD PRESSURE DISTRIBUTIONS  
FOR FLOW AT FREE STREAM MACH NUMBERS AT OR NEAR ONE, BELOW  
THE LOWER CRITICAL, OR ABOVE THE UPPER CRITICAL ABOUT A FINITE  
THICKNESS WING-INDENTED CIRCULAR BODY COMBINATION WITH THE  
EQUIVALENT BODY OF REVOLUTION EITHER USER-SPECIFIED OR HAVING  
ORDINATES R PROPORTIONAL TO X/L-(X/L)\*\*M OR 1-X/L-(1-X/L)\*\*M,  
THE WING HAVING A CONSTANT THICKNESS/CHORD RATIO, TAPER RATIO  
BETWEEN 0 AND 1, AND WITH ORDINATES Z PROPORTIONAL TO XRAR/C  
-(XBAR/C)\*\*M OR 1-XBAR/C-(1-XBAR/C)\*\*M BY USING THE TRANSONIC  
EQUIVALENCE RULE AND THE LOCAL LINEARIZATION METHOD

WING-BODY COMBINATION GEOMETRY AND FLOW FIELD CHARACTERISTICS

EQUIVALENT BODY THICKNESS RATIO = 0.10000E 00  
EQUIVALENT BODY MAXIMUM THICKNESS AT X/L = 0.50000E 00  
EXPONENT M FOR EQUIVALENT BODY ORDINATES = 0.20000E 01  
SEB\*\*(X) = 0 AT X/L = C.21132E 00  
WING MAX. THICKNESS AT XBAR/C = C.50000E 00  
WING THICKNESS/CHORD RATIO = C.40000E-01  
EXPONENT M FOR WING ORDINATES = C.20000E 01  
LEADING EDGE OF WING ROOT CHORD AT X/L = C.25000E 00  
TRAILING EDGE OF WING ROOT CHORD AT X/L = C.75000E 00  
PLANFORM TAPER RATIO = C.20000E 00  
LEADING EDGE PIERCES BODY AT X/L = 0.31960E 00  
TRAILING EDGE PIERCES BODY AT X/L = C.75000E 00  
BODY RISE AT X/L = 0.86000E 00  
LEADING EDGE SWEEP ANGLE (DEG) = C.58000E 02  
TRAILING EDGE SWEEP ANGLE (DEG) = 0.00000E 00  
LOCATION OF WING TIP LEADING EDGE AT X/L = C.65000E 00  
LOCATION OF WING TIP TRAILING EDGE AT X/L = 0.75000E 00  
NORMALIZED MAX. SEMISPAN SSMAX/L = C.25000E 00  
ANGLE OF ATTACK ALPHA (DEG) = 0.00000E 01  
RATIO OF SPECIFIC HEATS = C.14000E 01  
FREE STREAM MACH NUMBER = C.10000E 01

START OF INTEGRATION FROM SEB\*\*(X) = 0 TO NCGE

X/L	RBODY/L	THETA(DEG)	CP(BODY)	CP(R/D)= 1.00	CP(R/D)= 2.00	CP(R/D)= 3.00	CP(R/D)= 4.00	CP(R/D)= 5.00	CP(R/D)= 6.00
0.2113	0.0333	0.0000	2.1307E-02	3.3159E-02	3.4270E-02	3.4476E-02	3.4548E-02	3.4582E-02	3.4600E-02
0.2113	0.0333	9.0000E 01	2.1307E-02	3.3159E-02	3.4270E-02	3.4476E-02	3.4548E-02	3.4582E-02	3.4600E-02
0.2003	0.0320	0.0000	2.8813E-02	3.8171E-02	3.7124E-02	3.6069E-02	3.5247E-02	3.4587E-02	3.4039E-02
0.2003	0.0320	9.0000E 01	2.8813E-02	3.8171E-02	3.7124E-02	3.6069E-02	3.5247E-02	3.4587E-02	3.4039E-02
0.1503	0.0255	0.0000	6.6652E-02	5.9471E-02	4.7472E-02	4.0071E-02	3.4755E-02	3.0613E-02	2.7221E-02
0.1503	0.0255	9.0000E 01	6.6692E-02	5.9471E-02	4.7472E-02	4.0071E-02	3.4755E-02	3.0613E-02	2.7221E-02
0.1003	0.0181	0.0000	1.1374E-01	7.5672E-02	5.0874E-02	3.6118E-02	2.5607E-02	1.7441E-02	1.0765E-02
0.1003	0.0181	9.0000E 01	1.1374E-01	7.5672E-02	5.0874E-02	3.6118E-02	2.5607E-02	1.7441E-02	1.0765E-02
0.0503	0.0096	0.0000	1.8138E-01	7.9464E-02	4.0133E-02	1.7038E-02	6.3612E-04	-1.2090E-02	-2.2450E-02
0.0503	0.0096	9.0000E 01	1.8138E-01	7.9464E-02	4.0133E-02	1.7038E-02	6.3612E-04	-1.2090E-02	-2.2450E-02
0.0043	0.0009	0.0000	3.7747E-01	4.6107E-02	-7.9117E-03	-3.9512E-02	-6.1932E-02	-7.9323E-02	-9.3533E-02
0.0043	0.0009	9.0000E 01	3.7747E-01	4.6107E-02	-7.9117E-03	-3.9512E-02	-6.1932E-02	-7.9323E-02	-9.3533E-02

START OF INTEGRATION FROM SEB\*\*(X) = 0 TO TAIL

X/L	RBODY/L	THETA(DEG)	CP(BODY)	CP(R/D)= 1.00	CP(R/D)= 2.00	CP(R/D)= 3.00	CP(R/D)= 4.00	CP(R/D)= 5.00	CP(R/D)= 6.00
0.2113	0.0333	0.0000	2.1307E-02	3.3159E-02	3.4270E-02	3.4476E-02	3.4548E-02	3.4582E-02	3.4600E-02
0.2113	0.0333	9.0000E 01	2.1307E-02	3.3159E-02	3.4270E-02	3.4476E-02	3.4548E-02	3.4582E-02	3.4600E-02
0.2503	0.0375	0.0000	-3.4545E-03	1.4950E-02	2.3030E-02	2.7311E-02	3.0278E-02	3.2559E-02	3.4413E-02
0.2503	0.0375	9.0000E 01	-3.4545E-03	1.4950E-02	2.3030E-02	2.7311E-02	3.0278E-02	3.2559E-02	3.4413E-02
0.3003	0.0420	0.0000	-3.1658E-02	-8.3207E-03	6.9848E-03	1.5600E-02	2.1656E-02	2.6337E-02	3.0154E-02
0.3003	0.0420	9.0000E 01	-3.1658E-02	-8.3207E-03	6.9848E-03	1.5600E-02	2.1656E-02	2.6337E-02	3.0154E-02
0.3503	0.0453	0.0000	-4.2752E-02	-1.1470E-02	-4.4772E-03	5.0147E-03	1.2459E-02	1.8439E-02	2.3466E-02
0.3503	0.0453	9.0000E 01	-4.2752E-02	-1.1470E-02	-4.4772E-03	5.0147E-03	1.2459E-02	1.8439E-02	2.3466E-02

Figure 8.- Sample input/output for a wing-body combination having a circular body and with  $TR \neq 0$ ,  $\beta_{co} \leq 0$ ,  $\alpha = 0$ .

0.4003	0.0463	0.0000	-1.3545E-01	-9.0759E-03	-2.6387E-02	-1.6436E-02	-5.8411E-03	2.7547E-03	9.9210E-03
0.4003	0.0463	9.0000E 01	-1.3421E-01	-7.9245E-02	-4.0477E-02	-2.1309E-02	-8.5757E-03	1.0043E-03	8.7054E-03
0.4503	0.0452	0.0000	-1.8585E-01	-1.0661E-01	-4.7339E-02	-3.4247E-02	-2.2217E-02	-1.2275E-02	-3.9321E-03
0.4503	0.0452	9.0000E 01	-1.6115E-01	-1.0676E-01	-6.3579E-02	-4.1061E-02	-2.6016E-02	-1.4901E-02	-5.6153E-03
0.5003	0.0421	0.0000	-2.0276E-01	-1.5242E-01	-5.4059E-02	-4.7542E-02	-3.5858E-02	-2.5902E-02	-1.7476E-02
0.5003	0.0421	9.0000E 01	-1.6633E-01	-1.1840E-01	-7.8063E-02	-5.5503E-02	-4.0206E-02	-2.8662E-02	-1.9387E-02

START OF SUPERSONIC CALCULATION

SUPERSONIC CALCULATION STARTS AT X/L = 0.54232E 00

X/L	RBODY/L	THETA(DEG)	CP(RCDY)	CP(R/D= 1.00)	CP(R/D= 2.00)	CP(R/D= 3.00)	CP(R/D= 4.00)	CP(R/D= 5.00)	CP(R/D= 6.00)
0.5503	0.0374	0.0000	-1.7406E-01	-1.6090E-01	-4.4047E-02	-5.5216E-02	-4.5729E-02	-3.7216E-02	-2.9553E-02
0.5503	0.0374	9.0000E 01	-1.3590E-01	-1.0833E-01	-8.0084E-02	-6.1958E-02	-4.9152E-02	-3.9346E-02	-3.1418E-02
0.6003	0.0319	0.0000	-7.6846E-02	-1.3388E-01	-1.0986E-01	-5.6845E-02	-5.0777E-02	-4.4920E-02	-3.9556E-02
0.6003	0.0319	9.0000E 01	-4.4981E-02	-6.8740E-02	-6.4622E-02	-5.6721E-02	-4.9885E-02	-4.4233E-02	-3.9450E-02
0.7003	0.0300	0.0000	1.3714E-01	-6.9617E-02	-2.0376E-01	-1.3049E-01	-9.9491E-02	-8.6103E-02	-7.8081E-02
0.7003	0.0300	9.0000E 01	1.8803E-01	2.0859E-02	-3.3187E-02	-5.4919E-02	-6.0142E-02	-6.1365E-02	-6.1009E-02
0.8003	0.0320	0.0000	-8.8124E-02	-7.8922E-02	-8.0057E-02	-8.1227E-02	-8.2102E-02	-8.2804E-02	-8.3386E-02
0.8003	0.0320	9.0000E 01	-8.8124E-02	-7.8922E-02	-8.0057E-02	-8.1227E-02	-8.2102E-02	-8.2804E-02	-8.3386E-02
0.8503	0.0255	0.0000	-3.9535E-02	-4.7040E-02	-5.9191E-02	-6.6680E-02	-7.2057E-02	-7.6247E-02	-7.9679E-02
0.8503	0.0255	9.0000E 01	-3.9535E-02	-4.7040E-02	-5.9191E-02	-6.6680E-02	-7.2057E-02	-7.6247E-02	-7.9679E-02

DRAG COEFFICIENT = 0.10440E 00

(b) Output.

Figure 8.- Concluded.

STRANIN AMACH=1.,MOPT=1,TAUB=-1,TAUW=.04,XMTB=.5,XMTW=.5,ANGLE=58.,  
SSMAX=.25,XRLB=.25,TR=.2,CRT=.5,XLBASE=.86,XLOUTP=.05,ALPHA=2.,END

(a) Input.

CALCULATION OF SURFACE AND FLOW FIELD PRESSURE DISTRIBUTIONS  
FOR FLOW AT FREE STREAM MACH NUMBERS AT OR NEAR ONE, BELOW  
THE LOWER CRITICAL, OR ABOVE THE UPPER CRITICAL ABOUT A FINITE  
THICKNESS WING-INDENTED CIRCULAR BODY COMBINATION WITH THE  
EQUIVALENT BODY OF REVOLUTION EITHER USER-SPECIFIED OR HAVING  
ORDINATES  $W$  PROPORTIONAL TO  $X/L-(X/L)^{**N}$  OR  $1-X/L-(1-X/L)^{**N}$ ,  
THE WING HAVING A CONSTANT THICKNESS/CHORD RATIO, TAPER RATIO  
BETWEEN 0 AND 1, AND WITH ORDINATES  $Z$  PROPORTIONAL TO  $XBAR/C$   
 $-(XBAR/C)^{**M}$  OR  $1-XBAR/C-(1-XBAR/C)^{**M}$  BY USING THE TRANSONIC  
EQUIVALENCE RULE AND THE LOCAL LINEARIZATION METHOD

WING-BODY COMBINATION GEOMETRY AND FLOW FIELD CHARACTERISTICS

EQUIVALENT BODY THICKNESS RATIO = C.10000E 00  
EQUIVALENT BODY MAXIMUM THICKNESS AT X/L = 0.50000E 00  
EXPONENT N FOR EQUIVALENT BODY ORDINATES = 0.20000E 01  
SER\*\*(X) = 0 AT X/L = C.21132E 00  
WING MAX. THICKNESS AT XBAR/C = C.50000E 00  
WING THICKNESS/CHORD RATIO = C.40000E-01  
EXPONENT M FOR WING ORDINATES = C.20000E 01  
LEADING EDGE OF WING ROOT CHORD AT X/L = C.25000E 00  
TRAILING EDGE OF WING ROOT CHORD AT X/L = C.75000E 00  
PLANFORM TAPER RATIO = 0.20000E 00  
LEADING EDGE PIERCES BODY AT X/L = C.31960E 00  
TRAILING EDGE PIERCES BODY AT X/L = C.75000E 00  
BODY BASE AT X/L = C.86000E 00  
LEADING EDGE SWEEP ANGLE (DEG) = C.58000E 02  
TRAILING EDGE SWEEP ANGLE (DEG) = 0.00000  
LOCATION OF WING TIP LEADING EDGE AT X/L = C.65000E 00  
LOCATION OF WING TIP TRAILING EDGE AT X/L = C.75000E 00  
NORMALIZED MAX. SPAN SPAN/SSMAX/L = C.25000E 00  
ANGLE OF ATTACK ALPHA (DEG) = 0.20000E 01  
RATIO OF SPECIFIC HEATS = 0.14000E 01  
FREE STREAM MACH NUMBER = 0.10000E 01

START OF INTEGRATION FROM SER\*\*(X) = C TO NUSE

X/L	RBODY/L	THETA(DEG)	CP(EFF)	CP(R/D) = 1.00(CP(R/D) = 2.00(CP(R/D) = 3.00(CP(R/D) = 4.00(CP(R/D) = 5.00(CP(R/D) = 6.00					
0.2113	0.0333	0.0000	1.7652E-02	3.2874E-02	3.4202E-02	3.4446E-02	3.4531E-02	3.4571E-02	3.4592E-02
0.2113	0.0333	9.0000E 01	6.4031E-03	2.5652E-02	3.0344E-02	3.1830E-02	3.2554E-02	3.2982E-02	3.3265E-02
0.2113	0.0333	-9.0000E 01	3.2649E-02	4.1178E-02	3.8331E-02	3.7182E-02	3.6576E-02	3.6202E-02	3.5949E-02
0.2003	0.0320	0.0000	2.5157E-02	3.7508E-02	3.7060E-02	3.6041E-02	3.5231E-02	3.4577E-02	3.4032E-02
0.2003	0.0320	9.0000E 01	1.3294E-02	3.3640E-02	3.3198E-02	3.3426E-02	3.3256E-02	3.2991E-02	3.2706E-02
0.2003	0.0320	-9.0000E 01	4.6768E-02	4.6177E-02	4.1173E-02	3.8768E-02	3.7269E-02	3.6204E-02	3.5385E-02
0.1503	0.0255	0.0000	6.3037E-02	5.9307E-02	4.7432E-02	4.0053E-02	3.4745E-02	3.0607E-02	2.7216E-02
0.1503	0.0255	9.0000E 01	4.8381E-02	5.2304E-02	4.3750E-02	3.7600E-02	3.2857E-02	2.9124E-02	2.5979E-02
0.1503	0.0255	-9.0000E 01	8.7441E-02	6.6945E-02	5.1233E-02	4.2577E-02	3.6634E-02	3.2115E-02	2.8472E-02
0.1003	0.0181	0.0000	1.1008E-01	7.5591E-02	5.0854E-02	3.6109E-02	2.5602E-02	1.7438E-02	1.0762E-02
0.1003	0.0181	9.0000E 01	9.2631E-02	6.9771E-02	4.7879E-02	3.4114E-02	2.4102E-02	1.6236E-02	9.757E-03
0.1003	0.0181	-9.0000E 01	1.3728E-01	8.1728E-02	5.3507E-02	3.5139E-02	2.7122E-02	1.8653E-02	1.1774E-02
0.0503	0.0096	0.0000	1.7773E-01	7.9442E-02	4.0126E-02	1.7035E-02	6.3473E-04	-1.2091E-02	-2.2451E-02
0.0503	0.0096	9.0000E 01	1.5740E-01	7.5877E-02	3.8340E-02	1.5840E-02	-2.6243E-04	-1.2805E-02	-2.3090E-02
0.0503	0.0096	-9.0000E 01	2.0771E-01	8.3076E-02	4.1938E-02	1.8240E-02	1.5375E-03	-1.1369E-02	-2.1850E-02
0.0043	0.0009	0.0000	3.7391E-01	4.6107E-02	-7.9117E-03	-3.9512E-02	-6.1932E-02	-7.9323E-02	-9.3533E-02
0.0043	0.0009	9.0000E 01	3.5100E-01	4.5750E-02	-8.0902E-03	-3.9031E-02	-6.2022E-02	-7.9395E-02	-9.3552E-02
0.0043	0.0009	-9.0000E 01	4.0637E-01	4.6465E-02	-7.7331E-03	-3.9393E-02	-6.1843E-02	-7.9252E-02	-9.3473E-02

START OF INTEGRATION FROM SER\*\*(X) = C TO TAIL

X/L	RBODY/L	THETA(DEG)	CP(EFF)	CP(R/D) = 1.00(CP(R/D) = 2.00(CP(R/D) = 3.00(CP(R/D) = 4.00(CP(R/D) = 5.00(CP(R/D) = 6.00					
0.2113	0.0333	0.0000	1.7652E-02	3.2874E-02	3.4202E-02	3.4446E-02	3.4531E-02	3.4571E-02	3.4592E-02
0.2113	0.0333	9.0000E 01	6.4031E-03	2.5652E-02	3.0344E-02	3.1830E-02	3.2554E-02	3.2982E-02	3.3265E-02
0.2113	0.0333	-9.0000E 01	3.2649E-02	4.1178E-02	3.8331E-02	3.7182E-02	3.6576E-02	3.6202E-02	3.5949E-02
0.2503	0.0375	0.0000	-7.1044E-03	1.4623E-02	2.2742E-02	2.7273E-02	3.0257E-02	3.2545E-02	3.4404E-02
0.2503	0.0375	9.0000E 01	-1.6181E-02	7.9276E-03	1.9235E-02	2.4746E-02	2.8343E-02	3.1005E-02	3.3116E-02
0.2503	0.0375	-9.0000E 01	1.1708E-02	2.2791E-02	2.8953E-02	2.9952E-02	3.2257E-02	3.4140E-02	3.5730E-02

Figure 9.- Sample input/output for a wing-body combination having a circular body and with  $TR \neq 0$ ,  $B_{le} \leq 0$ ,  $\alpha \neq 0$ .

0.3003	0.0420	0.0000	-2.5314E-02	-8.7861E-03	6.8748E-03	1.5552E-02	2.1629E-02	2.6320E-02	3.0162E-02
0.3003	0.0420	9.0000 01	-4.1592E-02	-1.4545E-02	3.6267E-03	1.1319E-02	1.9932E-02	2.4951E-02	2.8997E-02
0.3003	0.0420	-9.0000 01	-1.9288E-02	-1.3121E-03	1.0553E-02	1.7975E-02	2.3434E-02	2.7757E-02	3.1336E-02
0.3503	0.0453	0.01UPPER1	-1.0355E-01	-1.2315E-02	-4.6357E-03	4.9451E-03	1.2420E-02	1.8414E-02	2.3389E-02
0.3503	0.0453	0.01LOWER1	2.0472E-02	-1.2315E-02	-4.6357E-03	4.9451E-03	1.2420E-02	1.8414E-02	2.3389E-02
0.3503	0.0453	9.0000 01	-1.1530E-01	-5.8221E-02	-2.2168E-02	-5.5204E-03	5.0506E-03	1.2755E-02	1.8608E-02
0.3503	0.0453	-9.0000 01	-6.5025E-02	-2.0265E-02	-1.7149E-04	9.6057E-03	1.6523E-02	2.1981E-02	2.6918E-02
0.4003	0.0463	0.01UPPER1	-1.6853E-01	-1.7800E-02	-2.9744E-02	-1.6577E-02	-5.9150E-03	2.7077E-03	9.8886E-03
0.4003	0.0463	0.01LOWER1	-7.9930E-02	-1.7800E-02	-2.9744E-02	-1.6577E-02	-5.9150E-03	2.7077E-03	9.8886E-03
0.4003	0.0463	9.0000 01	-1.6544E-01	-1.0647E-01	-5.8079E-02	-3.3811E-02	-1.8184E-02	-6.7745E-03	2.1752E-03
0.4003	0.0463	-9.0000 01	-1.0004E-01	-5.0703E-02	-2.2359E-02	-8.5742E-03	1.1681E-03	8.8714E-03	1.5293E-02
0.4503	0.0452	0.01UPPER1	-2.3608E-01	-1.8094E-01	-4.8127E-02	-3.4507E-02	-2.2351E-02	-1.2358E-02	-3.5884E-03
0.4503	0.0452	0.01LOWER1	-1.3318E-01	-3.3905E-02	-4.8127E-02	-3.4507E-02	-2.2351E-02	-1.2358E-02	-3.5884E-03
0.4503	0.0452	9.0000 01	-1.9573E-01	-1.3825E-01	-8.5776E-02	-5.7354E-02	-3.8717E-02	-2.5058E-02	-1.4341E-02
0.4503	0.0452	-9.0000 01	-1.2414E-01	-7.3650E-02	-4.0675E-02	-2.4400E-02	-1.3094E-02	-4.1977E-03	3.2137E-03
0.5003	0.0421	0.01UPPER1	-2.9131E-01	-2.1180E-01	-5.7976E-02	-4.7998E-02	-3.6079E-02	-2.6035E-02	-1.7565E-02
0.5003	0.0421	0.01LOWER1	-1.5177E-01	-9.2198E-02	-5.7976E-02	-4.7998E-02	-3.6079E-02	-2.6035E-02	-1.7565E-02
0.5003	0.0421	9.0000 01	-2.0258E-01	-1.5245E-01	-1.0375E-01	-7.4991E-02	-5.5641E-02	-4.1356E-02	-3.0135E-02
0.5003	0.0421	-9.0000 01	-1.2763E-01	-8.2573E-02	-5.1443E-02	-3.5470E-02	-2.4446E-02	-1.5750E-02	-8.4837E-03

START OF SUPERSONIC CALCULATION

SUPERSONIC CALCULATION STARTS AT X/L = 0.54232E 00

X/L	RBODY/L	THETA(DEG)	CP(XCCY)	CP(X/D)	1.00(CP(X/D)	2.00(CP(X/D)	3.00(CP(X/D)	4.00(CP(X/D)	5.00(CP(X/D)	6.00(CP(X/D)
0.5503	0.0374	0.01UPPER1	-2.2116E-01	-2.1471E-01	-5.3007E-02	-5.5999E-02	-4.6073E-02	-3.7416E-02	-3.0085E-02	-2.4103E-02
0.5503	0.0374	0.01LOWER1	-1.2453E-01	-1.0559E-01	-5.3007E-02	-5.5999E-02	-4.6073E-02	-3.7416E-02	-3.0085E-02	-2.4103E-02
0.5503	0.0374	9.0000 01	-1.7361E-01	-1.4418E-01	-1.0851E-01	-8.4207E-02	-6.7067E-02	-5.4217E-02	-4.4079E-02	-3.6479E-02
0.5503	0.0374	-9.0000 01	-5.5743E-02	-7.0551E-02	-5.0508E-02	-3.9020E-02	-3.0796E-02	-2.4174E-02	-1.8940E-02	-1.4840E-02
0.6003	0.0319	0.01UPPER1	-1.2235E-01	-1.8426E-01	-2.2219E-01	-5.8233E-02	-5.1298E-02	-4.5209E-02	-4.0183E-02	-3.6037E-02
0.6003	0.0319	0.01LOWER1	-2.8904E-02	-6.1685E-02	6.0715E-04	-5.8233E-02	-5.1298E-02	-4.5209E-02	-4.0183E-02	-3.6037E-02
0.6003	0.0319	9.0000 01	-8.4287E-02	-1.0607E-01	-9.5302E-02	-8.1400E-02	-7.0081E-02	-6.1158E-02	-5.3986E-02	-4.8066E-02
0.6003	0.0319	-9.0000 01	-3.2376E-03	-2.9388E-02	-3.2612E-02	-3.1195E-02	-2.9127E-02	-2.6915E-02	-2.4707E-02	-2.2500E-02
0.7003	0.0300	0.01UPPER1	1.4021E-01	-6.7898E-02	-2.0739E-01	-1.3326E-01	-1.0027E-01	-8.6509E-02	-7.8337E-02	-7.1037E-02
0.7003	0.0300	0.01LOWER1	1.3651E-01	-6.9357E-02	-2.0202E-01	-1.3326E-01	-1.0027E-01	-8.6509E-02	-7.8337E-02	-7.1037E-02
0.7003	0.0300	9.0000 01	1.6740E-01	2.1638E-02	-3.7193E-02	-5.4065E-02	-5.9448E-02	-6.0799E-02	-6.0537E-02	-5.9448E-02
0.7003	0.0300	-9.0000 01	1.6110E-01	2.2186E-02	-3.7693E-02	-5.4774E-02	-6.0131E-02	-6.1445E-02	-6.1114E-02	-6.0131E-02

DRAG COEFFICIENT = 0.13419E 00  
LIFT COEFFICIENT = 0.17070E 01  
PITCHING MOMENT COEFFICIENT = -0.89056E 00

(b) Output.

Figure 9.- Concluded.

STRAN AMACH=1., MOPT=1, TAUB=.1, TAUM=.04, XMTB=.5, XMTM=.5, ANGLE=58.,  
 SSMAX=.25, XRLE=.25, TR=.2, CRT=.5, XLBASE=.86, XLOUT=.05, ALPHA=2., AL=3., &END

(a) Input.

CALCULATION OF SURFACE AND FLOW FIELD PRESSURE DISTRIBUTIONS FOR FLOW AT FREE STREAM MACH NUMBERS AT OR NEAR ONE, BELOW THE LOWER CRITICAL, OR ABOVE THE UPPER CRITICAL ANGLE: A FINITE THICKNESS WING-INDENTED BODY COMBINATION WITH THE BODY HAVING AN ELLIPTIC CROSS SECTION THAT MAINTAINS A CONSTANT RATIO OF MAJOR/MINOR AXES ALONG THE ENTIRE BODY LENGTH WITH THE EQUIVALENT BODY OF REVOLUTION EITHER USER-SPECIFIED OR HAVING CR-DINATES R PROPORTIONAL TO X/L-(X/L)\*\*N OR 1-X/L-(1-X/L)\*\*N, THE WING HAVING A CONSTANT THICKNESS/CHORD RATIO, TAPER RATIO BETWEEN 0 AND 1, AND WITH ORIGINATES Z PROPORTIONAL TO XBAR/C -(XBAR/C)\*\*M OR 1-XBAR/C-(1-XBAR/C)\*\*M BY USING THE TRANSCAT EQUIVALENCE RULE AND THE LOCAL LINEARIZATION METHOD

WING-BODY COMBINATION GEOMETRY AND FLOW FIELD CHARACTERISTICS

RATIO OF SEMI-MAJOR/SEMI-MINOR AXIS = C.30000E 01  
 EQUIVALENT BODY THICKNESS RATIO = C.10000E 00  
 EQUIVALENT BODY MAXIMUM THICKNESS AT X/L = C.50000E 00  
 EXPONENT N FOR EQUIVALENT BODY COORDINATES = C.20000E 01  
 SEB\*\*(X) = 0 AT X/L = C.21132E 00  
 WING MAX. THICKNESS AT XBAR/C = C.50000E 00  
 WING THICKNESS/CHORD RATIO = C.40000E-01  
 EXPONENT M FOR WING COORDINATES = C.20000E 01  
 LEADING EDGE OF WING ROOT CHORD AT X/L = C.25000E 00  
 TRAILING EDGE OF WING FOOT CHORD AT X/L = C.75000E 00  
 PLANFORM TAPER RATIO = C.20000E 00  
 LEADING EDGE PIERCES BODY AT X/L = C.38070E 00  
 TRAILING EDGE PIERCES BODY AT X/L = C.75000E 00  
 BODY BASE AT X/L = C.86000E 00  
 LEADING EDGE SWEEP ANGLE (DEG) = C.58000E 02  
 TRAILING EDGE SWEEP ANGLE (DEG) = C.C0000  
 LOCATION OF WING TIP LEADING EDGE AT X/L = C.65000E 00  
 LOCATION OF WING TIP TRAILING EDGE AT X/L = C.75000E 00  
 NORMALIZED MAX. SEMISPAN SSMAX/L = C.25000E 00  
 ANGLE OF ATTACK ALPHA (DEG) = C.20000E 01  
 RATIO OF SPECIFIC HEATS = C.14000E 01  
 FREE STREAM MACH NUMBER = C.10000E 01

START OF INTEGRATION FROM SEB\*\*(X) = 0 TO NOSE

X/L	HNOSE/L	THETA(DEG)	CP(LEZY)	CP(R/D= 1.00)	CP(R/D= 2.00)	CP(R/D= 3.00)	CP(R/D= 4.00)	CP(R/D= 5.00)	CP(R/D= 6.00)
0.2113	0.0577	0.0000	2.9697E-02	3.6854E-02	3.5139E-02	3.4458E-02	3.4762E-02	3.4718E-02	3.4695E-02
0.2113	0.0192	9.0000E 01	-4.9801E-03	1.9287E-02	2.7071E-02	2.9726E-02	3.1020E-02	3.1780E-02	3.2278E-02
0.2113	0.0192	-9.0000E 01	3.2254E-02	4.2027E-02	3.9859E-02	3.8496E-02	3.7659E-02	3.7114E-02	3.6733E-02
0.2003	0.0555	0.0000	3.6627E-02	4.2121E-02	3.8053E-02	3.6478E-02	3.5476E-02	3.4733E-02	3.4140E-02
0.2003	0.0185	9.0000E 01	6.7900E-04	2.3926E-02	2.9855E-02	3.1294E-02	3.1705E-02	3.1781E-02	3.1715E-02
0.2003	0.0185	-9.0000E 01	3.6332E-02	4.6873E-02	4.2658E-02	4.0060E-02	3.8338E-02	3.7105E-02	3.6162E-02
0.1503	0.0442	0.0000	8.4855E-02	6.3604E-02	4.8461E-02	4.0507E-02	3.5000E-02	3.0769E-02	2.7329E-02
0.1503	0.0147	9.0000E 01	2.5626E-02	4.4900E-02	4.0471E-02	3.5539E-02	3.1418E-02	2.7975E-02	2.5041E-02
0.1503	0.0147	-9.0000E 01	7.4731E-02	6.7384E-02	5.2603E-02	4.2751E-02	3.7610E-02	3.2941E-02	2.9185E-02
0.1003	0.0313	0.0000	1.4130E-01	7.6617E-02	5.1593E-02	3.6437E-02	2.5786E-02	1.7556E-02	1.0844E-02
0.1003	0.0104	9.0000E 01	6.6931E-02	6.5481E-02	4.5206E-02	3.2466E-02	2.2920E-02	1.5317E-02	9.0091E-03
0.1003	0.0104	-9.0000E 01	1.2441E-01	8.2594E-02	5.9140E-02	3.9140E-02	2.7939E-02	1.9338E-02	1.2362E-02
0.0503	0.0166	0.0000	2.1901E-01	8.0565E-02	4.0471E-02	1.7155E-02	7.0433E-04	-1.2047E-02	-2.2460E-02
0.0503	0.0055	9.0000E 01	1.2382E-01	7.2484E-02	3.6874E-02	1.4920E-02	-9.3070E-04	-1.3333E-02	-2.3570E-02
0.0503	0.0055	-9.0000E 01	1.8102E-01	8.4304E-02	4.2851E-02	1.6913E-02	2.0667E-03	-1.0935E-02	-2.1521E-02
0.0043	0.0015	0.0000	4.2662E-01	4.6119E-02	-7.9089E-03	-3.4510E-02	-6.1932E-02	-7.9323E-02	-9.3532E-02
0.0043	0.0005	9.0000E 01	3.6929E-01	4.5501E-02	-8.2121E-03	-3.4711E-02	-6.2082E-02	-7.5443E-02	-9.3632E-02
0.0043	0.0005	-9.0000E 01	3.7323E-01	4.6691E-02	-7.8170E-03	-3.4314E-02	-6.1784E-02	-7.9204E-02	-9.3434E-02

START OF INTEGRATION FROM SEB\*\*(X) = 0 TO TAIL

X/L	HNOSE/L	THETA(DEG)	CP(LEZY)	CP(R/D= 1.00)	CP(R/D= 2.00)	CP(R/D= 3.00)	CP(R/D= 4.00)	CP(R/D= 5.00)	CP(R/D= 6.00)
0.2113	0.0577	0.0000	2.9697E-02	3.6854E-02	3.5139E-02	3.4458E-02	3.4762E-02	3.4718E-02	3.4695E-02
0.2113	0.0192	9.0000E 01	-4.9801E-03	1.9287E-02	2.7071E-02	2.9726E-02	3.1020E-02	3.1780E-02	3.2278E-02
0.2113	0.0192	-9.0000E 01	3.2254E-02	4.2027E-02	3.9859E-02	3.8496E-02	3.7659E-02	3.7114E-02	3.6733E-02
0.2503	0.0650	0.0000	-3.3385E-04	1.7161E-02	2.3564E-02	2.7547E-02	3.0411E-02	3.2644E-02	3.4472E-02
0.2503	0.0217	9.0000E 01	-2.3538E-02	3.0961E-03	1.6355E-02	2.2843E-02	2.6929E-02	2.9884E-02	3.2190E-02
0.2503	0.0217	-9.0000E 01	6.6659E-03	2.4411E-02	2.8741E-02	3.1337E-02	3.3373E-02	3.5068E-02	3.6522E-02

Figure 10.- Sample input/output for a wing-body combination having an elliptical body and with TR ≠ 0, β<sub>0</sub> ≤ 0, α ≠ 0.

0.3003	0.0728	0.0000	-3.4176E-02	-9.3541E-03	6.8810E-03	1.5561E-02	2.1635E-02	2.4324E-02	3.0145E-02
0.3003	0.0243	9.0000E 01	-4.4569E-02	-1.6684E-02	1.6510E-03	1.1869E-02	1.8804E-02	2.4036E-02	2.8227E-02
0.3003	0.0248	-9.0000E 01	-1.6815E-02	1.6199E-03	1.2553E-02	1.9422E-02	2.4533E-02	2.8666E-02	3.2100E-02
0.3503	0.0789	0.0000	-6.3433E-02	-3.5815E-02	-1.0685E-02	1.7634E-03	1.0372E-02	1.6986E-02	2.2366E-02
0.3503	0.0263	9.0000E 01	-6.3134E-02	-1.4999E-02	-1.3465E-02	-5.9658E-04	8.4323E-03	1.5357E-02	2.0967E-02
0.3503	0.0269	-9.0000E 01	-4.3844E-02	-2.0633E-02	-4.7157E-03	5.5071E-03	1.3089E-02	1.9109E-02	2.4167E-02
0.4003	0.0830	0.0(UPPER)	-1.3338E-01	-7.7849E-03	-1.9949E-02	-8.7076E-03	2.3704E-04	7.4149E-03	1.3370E-02
0.4003	0.0830	0.0(LLOWER)	4.4417E-02	-7.7349E-03	-1.9949E-02	-8.7076E-03	2.3704E-04	7.4149E-03	1.3370E-02
0.4003	0.0271	9.0000E 01	-1.3518E-01	-7.8563E-02	-4.1570E-02	-2.2118E-02	-9.4300E-03	-1.1666E-04	7.2124E-03
0.4003	0.0277	-9.0000E 01	-7.8030E-02	-3.2890E-02	-1.2268E-02	-1.3539E-03	6.5047E-03	1.2771E-02	1.8018E-02
0.4503	0.0834	0.0(UPPER)	-2.2484E-01	-1.9656E-01	-5.3038E-02	-3.7551E-02	-2.4492E-02	-1.3921E-02	-5.1265E-03
0.4503	0.0834	0.0(LLOWER)	9.5429E-02	-4.7413E-02	-5.3038E-02	-3.7551E-02	-2.4492E-02	-1.3921E-02	-5.1265E-03
0.4503	0.0275	9.0000E 01	-1.5827E-01	-1.3547E-01	-8.6272E-02	-5.8245E-02	-3.9544E-02	-2.5715E-02	-1.4804E-02
0.4503	0.0279	-9.0000E 01	-1.2538E-01	-7.2552E-02	-4.2515E-02	-2.6271E-02	-1.4680E-02	-5.4707E-03	2.2317E-03
0.5003	0.0801	0.0(UPPER)	-2.6787E-01	-2.3975E-01	-7.2912E-02	-5.8920E-02	-4.4316E-02	-3.2241E-02	-2.2133E-02
0.5003	0.0801	0.0(LLOWER)	1.5022E-01	-1.1636E-01	-7.2912E-02	-5.8920E-02	-4.4316E-02	-3.2241E-02	-2.2133E-02
0.5003	0.0267	9.0000E 01	-2.3275E-01	-1.6946E-01	-1.1677E-01	-8.4960E-02	-6.3288E-02	-4.7152E-02	-3.4355E-02
0.5003	0.0267	-9.0000E 01	-1.5563E-01	-1.0022E-01	-6.5108E-02	-4.5939E-02	-3.2469E-02	-2.1853E-02	-1.3003E-02

START OF SUPERSONIC CALCULATION

SUPERSONIC CALCULATION STARTS AT X/L = 0.54232E 00

X/L	BODY/L	THETA(DEG)	CP(XCCY)	CP(X/D= 1.00)	CP(X/D= 2.00)	CP(X/D= 3.00)	CP(X/D= 4.00)	CP(X/D= 5.00)	CP(X/D= 6.00)
0.5503	0.0729	0.0(UPPER)	-2.4483E-01	-2.3568E-01	-6.7458E-02	-6.7246E-02	-5.4718E-02	-4.3983E-02	-3.4932E-02
0.5503	0.0729	0.0(LLOWER)	-1.3406E-01	-1.2342E-01	-6.7458E-02	-6.7246E-02	-5.4718E-02	-4.3983E-02	-3.4932E-02
0.5503	0.0243	9.0000E 01	-2.1875E-01	-1.6978E-01	-1.2470E-01	-9.6074E-02	-7.6019E-02	-6.0956E-02	-4.9027E-02
0.5503	0.0243	-9.0000E 01	-1.3938E-01	-9.5654E-02	-6.7159E-02	-5.1242E-02	-4.0027E-02	-3.1143E-02	-2.3682E-02
0.6003	0.0631	0.0(UPPER)	-1.3192E-01	-1.7966E-01	-2.2356E-01	-5.9157E-02	-5.2205E-02	-4.5961E-02	-4.0752E-02
0.6003	0.0631	0.0(LLOWER)	-2.8191E-02	-7.5253E-02	-2.4762E-04	-5.9157E-02	-5.2205E-02	-4.5961E-02	-4.0752E-02
0.6003	0.0210	9.0000E 01	-1.1992E-01	-1.1682E-01	-9.9784E-02	-8.4131E-02	-7.1967E-02	-6.2514E-02	-5.4461E-02
0.6003	0.0210	-9.0000E 01	-2.8163E-02	-4.0630E-02	-3.7462E-02	-3.4207E-02	-3.1237E-02	-2.8456E-02	-2.5839E-02
0.7003	0.0550	0.0(UPPER)	1.3230E-01	-3.9002E-02	-1.5151E-01	-1.2484E-01	-9.4236E-02	-8.2051E-02	-7.5077E-02
0.7003	0.0550	0.0(LLOWER)	1.2689E-01	-4.0953E-02	-1.8671E-01	-1.2489E-01	-9.4236E-02	-8.2051E-02	-7.5077E-02
0.7003	0.0183	9.0000E 01	1.5910E-01	2.1566E-02	-3.1702E-02	-4.8917E-02	-5.5222E-02	-5.7500E-02	-5.8083E-02
0.7003	0.0183	-9.0000E 01	1.6091E-01	2.1883E-02	-3.2230E-02	-4.9629E-02	-5.5919E-02	-5.8138E-02	-5.8657E-02

DRAG COEFFICIENT = C.12462E 00  
LIFT COEFFICIENT = C.17073E 01  
PITCHING MOMENT COEFFICIENT = -0.84940E 00

(b) Output.

Figure 10.- Concluded.



STRAN IN AMACH=1., MOPT=1, TAUB=.1, TAUW=.04, XMTB=.5, XMTW=.5, ANGLE=45.,  
 SSMAX=.3215, XRLB=.25, TR=.4, CRT=.4, XLBASE=.86, XLOUTP=.05, LEND

(a) Input.

CALCULATION OF SURFACE AND FLOW FIELD PRESSURE DISTRIBUTIONS  
 FOR FLOW AT FREE STREAM MACH NUMBERS AT OR NEAR ONE, BELOW  
 THE LOWER CRITICAL OR ABOVE THE UPPER CRITICAL ABOUT A FINITE  
 THICKNESS WING-IDENTIFIED CIRCULAR BODY COMBINATION WITH THE  
 EQUIVALENT BODY OF REVOLUTION EITHER USER-SPECIFIED OR HAVING  
 ORDINATES R PROPORTIONAL TO X/L-(X/L)\*\*N OR L-X/L-(L-X/L)\*\*N,  
 THE WING HAVING A CONSTANT THICKNESS/CHORD RATIO, TAPER RATIO  
 BETWEEN 0 AND 1, AND WITH ORDINATES Z PROPORTIONAL TO XBAR/C  
 -(XPAR/C)\*\*M OR L-XPAR/C-(L-XBAR/C)\*\*M BY USING THE TRANSCNIC  
 EQUIVALENCE RULE AND THE LOCAL LINEARIZATION METHOD

WING-BODY COMBINATION GEOMETRY AND FLOW FIELD CHARACTERISTICS

EQUIVALENT BODY THICKNESS RATIO = C.10000E 00  
 EQUIVALENT BODY MAXIMUM THICKNESS AT X/L = C.50000E 00  
 EXPONENT N FOR EQUIVALENT BODY ORDINATES = C.20000E 01  
 SEB\*\*(X) = 0 AT X/L = 0.21132E 00  
 WING MAX. THICKNESS AT XBAR/C = C.50000E 00  
 WING THICKNESS/CHORD RATIO = C.40000E-01  
 EXPONENT M FOR WING ORDINATES = 0.20000E 01  
 LEADING EDGE OF WING ROOT CHORD AT X/L = C.25000E 00  
 TRAILING EDGE OF WING ROOT CHORD AT X/L = C.55000E 00  
 PLANFORM TAPER RATIO = C.40000E 00  
 LEADING EDGE PIERCES BODY AT X/L = C.25129E 00  
 TRAILING EDGE PIERCES BODY AT X/L = C.57156E 00  
 BODY BASE AT X/L = C.86000E 00  
 LEADING EDGE SWEEP ANGLE (DEG) = C.45000E 02  
 TRAILING EDGE SWEEP ANGLE (DEG) = C.2375E 02  
 LOCATION OF WING TIP LEADING EDGE AT X/L = C.57156E 00  
 LOCATION OF WING TIP TRAILING EDGE AT X/L = C.69156E 00  
 NORMALIZED MAX. SEMISPAN SSMAX/L = C.32150E 00  
 ANGLE OF ATTACK ALPHA (DEG) = C.00000  
 RATIO OF SPECIFIC HEATS = 0.14000E 01  
 FREE STREAM MACH NUMBER = C.10000E 01

START OF INTEGRATION FROM SEB\*\*(X) = 0 TO NOSE

X/L	RBODY/L	THETA(DEG)	CP(BODY)	CP(R/D= 1.00)	CP(R/D= 2.00)	CP(R/D= 3.00)	CP(R/D= 4.00)	CP(R/D= 5.00)	CP(R/D= 6.00)
0.2113	0.0333	C.0000	2.1307E-02	3.3159E-02	3.4270E-02	3.4476E-02	3.4548E-02	3.4582E-02	3.4600E-02
0.2113	0.0333	9.0000E 01	2.1307E-02	3.3159E-02	3.4270E-02	3.4476E-02	3.4548E-02	3.4582E-02	3.4600E-02
0.2003	0.0320	0.0000	2.8813E-02	3.8171E-02	3.7124E-02	3.6069E-02	3.5247E-02	3.4587E-02	3.4039E-02
0.2003	0.0320	9.0000E 01	2.8813E-02	3.8171E-02	3.7124E-02	3.6069E-02	3.5247E-02	3.4587E-02	3.4039E-02
0.1503	0.0255	0.0000	6.6692E-02	5.9471E-02	4.7472E-02	4.0071E-02	3.4755E-02	3.0613E-02	2.7221E-02
0.1503	0.0255	9.0000E 01	6.6692E-02	5.9471E-02	4.7472E-02	4.0071E-02	3.4755E-02	3.0613E-02	2.7221E-02
0.1003	0.0181	0.0000	1.1374E-01	7.5672E-02	5.0874E-02	3.6118E-02	2.5607E-02	1.7441E-02	1.0765E-02
0.1003	0.0181	9.0000E 01	1.1374E-01	7.5672E-02	5.0874E-02	3.6118E-02	2.5607E-02	1.7441E-02	1.0765E-02
0.0503	0.0096	0.0000	1.8138E-01	7.9464E-02	4.0133E-02	1.7038E-02	6.3612E-04	-1.2090E-02	-2.2450E-02
0.0503	0.0096	9.0000E 01	1.8138E-01	7.9464E-02	4.0133E-02	1.7038E-02	6.3612E-04	-1.2090E-02	-2.2450E-02
0.0043	0.0009	0.0000	3.7747E-01	4.6107E-02	-7.9117E-03	-3.9512E-02	-6.1932E-02	-7.9323E-02	-9.3533E-02
0.0043	0.0009	9.0000E 01	3.7747E-01	4.6107E-02	-7.9117E-03	-3.9512E-02	-6.1932E-02	-7.9323E-02	-9.3533E-02

START OF INTEGRATION FROM SEB\*\*(X) = 0 TO TAIL

X/L	RBODY/L	THETA(DEG)	CP(BODY)	CP(R/D= 1.00)	CP(R/D= 2.00)	CP(R/D= 3.00)	CP(R/D= 4.00)	CP(R/D= 5.00)	CP(R/D= 6.00)
0.2113	0.0333	0.0000	2.1307E-02	3.3159E-02	3.4270E-02	3.4476E-02	3.4548E-02	3.4582E-02	3.4600E-02
0.2113	0.0333	9.0000E 01	2.1307E-02	3.3159E-02	3.4270E-02	3.4476E-02	3.4548E-02	3.4582E-02	3.4600E-02
0.2503	0.0375	0.0000	-3.4545E-03	1.4990E-02	2.3030E-02	2.7311E-02	3.0278E-02	3.2559E-02	3.4413E-02
0.2503	0.0375	9.0000E 01	-3.4545E-03	1.4990E-02	2.3030E-02	2.7311E-02	3.0278E-02	3.2559E-02	3.4413E-02
0.3003	0.0420	0.0000	6.4617E-02	2.2711E-02	1.9734E-02	2.3766E-02	2.7481E-02	3.0616E-02	3.3278E-02
0.3003	0.0420	9.0000E 01	-7.8405E-02	-1.1963E-02	1.1116E-02	1.9936E-02	2.5327E-02	3.2370E-02	3.2320E-02
0.3503	0.0440	0.0000	-1.4081E-01	1.0000E 06	-4.9488E-03	1.9090E-03	5.4154E-03	1.5928E-02	2.1505E-02
0.3503	0.0440	9.0000E 01	-1.3218E-01	-6.5572E-02	-2.4888E-02	-6.7934E-03	4.5358E-03	1.2803E-02	1.9335E-02
0.4003	0.0434	0.0000	-1.8553E-01	-1.2128E-01	-8.0282E-03	-9.6051E-03	-2.2625E-03	5.0103E-03	1.1470E-02
0.4003	0.0434	9.0000E 01	-1.4164E-01	-9.0492E-02	-4.6757E-02	-2.4610E-02	-1.0504E-02	-2.3866E-04	7.8218E-03

Figure 11.- Sample input/output for a wing-body combination having a circular body and with TR ≠ 0,  $\delta_{te} > 0$ ,  $\alpha = 0$ .

0.4503	C.0413	0.0000	-1.5553E-01	-1.5350E-01	1.0000E 06	-1.3361E-02	-5.5250E-C3	-3.4170E-03	2.4011E-03
0.4503	0.0413	9.0000E 01	-5.9678E-02	-8.2432E-02	-5.2027E-02	-3.2566E-02	-1.9330E-02	-9.9426E-03	-1.8102E-03
0.5003	0.0391	0.0000	-7.4455E-C2	-1.4372E-C1	-1.2943E-01	-1.6070E-02	-1.7618E-02	-1.4648E-02	-5.4307E-03
0.5003	0.0391	9.0000E 01	-1.5426E-02	-5.1925E-02	-6.5851E-02	-3.5565E-02	-2.5932E-02	-1.8148E-02	-1.1739E-C2

START OF SUPERSONIC CALCULATION

SUPERSONIC CALCULATION STARTS AT X/L = 0.54232E 00

X/L	R6UDY/L	THETA(DEG)	CP(RODY)	CP(R/D= 1.00)CP(R/D= 2.00)CP(R/D= 3.00)CP(R/D= 4.00)CP(R/D= 5.00)CP(R/D= 6.00)
0.5503	0.0390	0.0000	5.1569E-03	-1.2736E-01 -1.4753E-01 1.0000E 06 -4.5947E-C2 -3.8540E-02 -3.1144E-02
0.5503	0.0390	9.0000E 01	7.1914E-02	-1.5654E-02 -4.5427E-02 -4.4275E-02 -1.8527E-02 -7.2306E-02 -2.6442E-02
0.6003	0.0418	0.0000	5.6515E-C2	1.9414E-01 -1.3863E-01 -2.1714E-01 -1.0602E-01 -7.6655E-C2 -6.1098E-02
0.6003	0.0418	9.0000E 01	1.8844E-02	1.5786E-02 -1.2692E-02 -2.6594E-02 -3.1319E-02 -3.1867E-02 -1.0599E-02
0.6503	0.0439	0.0000	-2.6776E-C1	-1.5102E-01 3.9488E-02 -1.2196E-01 -6.9199E-02 -6.0871E-C2 -5.5779E-02
0.6503	0.0439	9.0000E 01	-2.7797E-01	-1.7927E-01 -1.1552E-01 -6.4898E-02 -7.6059E-02 -6.7084E-02 -6.0440E-02
0.7003	0.0420	0.0000	-1.3105E-01	-1.0776E-01 -9.2537E-02 -8.3971E-02 -7.7950E-C2 -7.3247E-02 -6.5502E-C2
0.7003	0.0420	9.0000E 01	-1.3105E-01	-1.0776E-01 -9.2537E-02 -8.3971E-02 -7.7950E-C2 -7.3247E-02 -6.5502E-C2
0.7503	0.0375	0.0000	-1.1609E-01	-9.7726E-02 -8.9751E-C2 -8.5572E-02 -8.2649E-C2 -8.0403E-02 -7.8576E-02
0.7503	0.0375	9.0000E 01	-1.1609E-01	-9.7726E-02 -8.9751E-C2 -8.5572E-02 -8.2649E-C2 -8.0403E-02 -7.8576E-02
0.8003	0.0320	0.0000	-8.8124E-02	-7.8922E-02 -6.0097E-02 -8.1727E-02 -8.2102E-02 -8.2804E-02 -8.3386E-02
0.8003	0.0320	9.0000E 01	-8.8124E-02	-7.8922E-02 -6.0097E-02 -8.1727E-02 -8.2102E-02 -8.2804E-02 -8.3386E-02
0.8503	0.0255	0.0000	-3.9535E-C2	-4.7040E-02 -5.9191E-02 -6.6680E-02 -7.2057E-C2 -7.6247E-C2 -7.6474E-C2
0.8503	0.0255	9.0000E 01	-3.9535E-02	-4.7040E-02 -5.9191E-02 -6.6680E-02 -7.2057E-C2 -7.6247E-C2 -7.6474E-C2

DRAG COEFFICIENT = 0.1044E 00

(b) Output.

Figure 11. - Concluded.

6TRANIN AMACH=1. ,MOPT=1,TAUB=.1,TAUM=.04,XMTB=.5,XMTW=.5,ANGLE=45.,  
 SSMAX=.338,XRLE=.25,TR=.4,CRT=.4,XLBASE=.86,XLOUTP=.05,AL=3.,6END

(a) Input.

CALCULATION OF SURFACE AND FLOW FIELD PRESSURE DISTRIBUTIONS  
 FOR FLOW AT FREE STREAM MACH NUMBERS AT OR NEAR ONE, BELOW  
 THE LOWER CRITICAL, OR ABOVE THE UPPER CRITICAL ABOUT A FINITE  
 THICKNESS WING-INCENTED BODY COMBINATION WITH THE BODY HAVING  
 AN ELLIPTIC CROSS SECTION THAT MAINTAINS A CONSTANT RATIO OF  
 MAJOR/MINOR AXES ALONG THE ENTIRE BODY LENGTH WITH THE EQUI-  
 VALENT BODY OF REVOLUTION EITHER USER-SPECIFIED OR HAVING CO-  
 ORDINATES R PROPORTIONAL TO X/L-(X/L)\*\*N OR 1-X/L-(1-X/L)\*\*N,  
 THE WING HAVING A CONSTANT THICKNESS/CHORD RATIO, TAPER RATIO  
 BETWEEN 0 AND 1, AND WITH COORDINATES Z PROPORTIONAL TO XBAR/C  
 -(XBAR/C)\*\*M OR 1-XBAR/C-(1-XBAR/C)\*\*M BY USING THE TRANSONIC  
 EQUIVALENCE RULE AND THE LOCAL LINEARIZATION METHOD

WING-BODY COMBINATION GEOMETRY AND FLOW FIELD CHARACTERISTICS

RATIO OF SEMIMAJOR/SEMIMINOR AXIS = C.30000E 01  
 EQUIVALENT BODY THICKNESS RATIO = C.10000E 00  
 EQUIVALENT BODY MAXIMUM THICKNESS AT X/L = C.50000E 00  
 EXPONENT N FOR EQUIVALENT BODY COORDINATES = C.20000E 01  
 SEB\*\*(X) = 0 AT X/L = C.21132E 00  
 WING MAX. THICKNESS AT XBAR/C = C.50000E 00  
 WING THICKNESS/CHORD RATIO = C.40000E-01  
 EXPONENT M FOR WING COORDINATES = C.20000E 01  
 LEADING EDGE OF WING ROOT CHORD AT X/L = C.25000E 00  
 TRAILING EDGE OF WING ROOT CHORD AT X/L = C.55000E 00  
 PLANFORM TAPER RATIO = C.40000E 00  
 LEADING EDGE PIERCES BODY AT X/L = C.22613E 00  
 TRAILING EDGE PIERCES BODY AT X/L = C.53919E 00  
 BODY BASE AT X/L = C.86000E 00  
 LEADING EDGE SWEEP ANGLE (DEG) = C.45000E 02  
 TRAILING EDGE SWEEP ANGLE (DEG) = C.25054E 02  
 LOCATION OF WING TIP LEADING EDGE AT X/L = C.58800E 00  
 LOCATION OF WING TIP TRAILING EDGE AT X/L = C.70800E 00  
 NORMALIZED MAX. SEMISPAN SSMAX/L = C.33800E 00  
 ANGLE OF ATTACK ALPHA (DEG) = C.00000  
 RATIO OF SPECIFIC HEATS = C.14000E 01  
 FREE STREAM MACH NUMBER = C.10000E 01

START OF INTEGRATION FROM SEB\*\*(X) = 0 TO ACSE

X/L	RBODY/L	THETA(DEG)	CP(BCY)	CP(R/D)= 1.00	CP(R/D)= 2.00	CP(R/D)= 3.00	CP(R/D)= 4.00	CP(R/D)= 5.00	CP(R/D)= 6.00
0.2113	0.0577	C.0000	4.7974E-02	3.7658E-02	3.5267E-02	3.4421E-02	3.4797E-02	3.4740E-02	3.4710E-02
0.2113	0.0142	9.0000E 01	1.2418E-02	3.0253E-02	3.3360E-02	3.4053E-02	3.4306E-02	3.4426E-02	3.4451E-02
0.2003	0.0555	C.0000	5.7104E-02	4.2837E-02	3.8188E-02	3.6535E-02	3.5508E-02	3.4754E-02	3.4154E-02
0.2003	0.0185	9.0000E 01	1.8787E-02	3.5020E-02	3.6160E-02	3.5623E-02	3.4953E-02	3.4423E-02	3.3929E-02
0.1503	0.0442	0.0000	1.0313E-01	6.3994E-02	4.8544E-02	4.0543E-02	3.5020E-02	3.0782E-02	2.7338E-02
0.1503	0.0147	9.0000E 01	5.0911E-02	5.5879E-02	4.6461E-02	3.9611E-02	3.4495E-02	3.0446E-02	2.7104E-02
0.1003	0.0313	0.0000	1.5958E-01	7.8793E-02	5.1634E-02	3.8454E-02	2.5796E-02	1.7562E-02	1.0848E-02
0.1003	0.0104	9.0000E 01	3.4420E-02	7.2880E-02	5.0134E-02	3.5786E-02	2.5419E-02	1.7321E-02	1.0681E-02
0.0503	0.0166	0.0000	2.3788E-01	8.0611E-02	4.0418E-02	1.7164E-02	7.0711E-04	-1.2045E-02	-2.2459E-02
0.0503	0.0095	9.0000E 01	1.3160E-01	7.8353E-02	3.9851E-02	1.6912E-02	5.6524E-04	-1.2136E-02	-2.2522E-02
0.0043	0.0015	0.0000	4.4493E-01	4.6119E-02	-7.5088E-03	-3.5510E-02	-6.1932E-02	-7.9323E-02	-9.3532E-02
0.0043	0.0005	9.0000E 01	3.4004E-01	4.6096E-02	-7.9147E-03	-3.5513E-02	-6.1933E-02	-7.9324E-02	-9.3533E-02

START OF INTEGRATION FROM SEB\*\*(X) = 0 TO TAIL

X/L	RBODY/L	THETA(DEG)	CP(BCY)	CP(R/D)= 1.00	CP(R/D)= 2.00	CP(R/D)= 3.00	CP(R/D)= 4.00	CP(R/D)= 5.00	CP(R/D)= 6.00
0.2113	0.0577	C.0000	4.7974E-02	3.7658E-02	3.5267E-02	3.4421E-02	3.4797E-02	3.4740E-02	3.4710E-02
0.2113	0.0142	9.0000E 01	1.2418E-02	3.0253E-02	3.3360E-02	3.4053E-02	3.4306E-02	3.4426E-02	3.4451E-02
0.2503	0.0650	C.0000	1.7543E-02	1.8326E-02	2.3756E-02	2.7627E-02	3.0455E-02	3.2671E-02	3.4452E-02
0.2503	0.0217	9.0000E 01	-8.6543E-03	1.3264E-02	1.3264E-02	2.7017E-02	3.0109E-02	3.2449E-02	3.4337E-02
0.3003	0.0728	C.0000	-1.5815E-02	-7.5935E-03	7.1287E-03	1.5662E-02	2.1651E-02	2.6359E-02	3.0170E-02
0.3003	0.0243	9.0000E 01	-3.2910E-02	-5.0892E-03	6.9124E-03	1.5553E-02	2.1627E-02	2.6317E-02	3.0140E-02
0.3503	0.0784	C.0000	-2.1022E-02	1.0000E 06	1.3079E-03	7.1848E-03	1.3604E-02	1.9148E-02	2.3851E-02
0.3503	0.0261	9.0000E 01	-1.1342E-01	-4.7325E-02	-1.4910E-02	1.2753E-04	9.6454E-03	1.6616E-02	2.2133E-02

Figure 12.- Sample input/output for a wing-body combination having an elliptical body and with  $TR \neq 0$ ,  $\beta_{co} > 0$ ,  $\alpha = 0$ .

0.4003	0.0793	0.0000	-1.8332E-01	-1.4009E-01	-1.7435E-02	-1.6409E-02	-7.2054E-03	-1.3027E-03	0.7467E-03
0.4003	0.0794	0.0000E 01	-1.6231E-01	-9.8191E-02	-5.1754E-02	-3.0159E-02	-1.4855E-02	-1.5634E-03	5.4780E-03
0.4503	0.0793	0.0000	-1.7841E-01	-1.6717E-01	1.0000E 00	-2.0053E-02	-1.4561E-01	-7.5241E-03	-6.2437E-04
0.4503	0.0794	0.0000E 01	-1.7435E-01	-1.6297E-02	-1.0297E-02	-4.0049E-02	-2.5278E-02	-1.4013E-02	-6.0541E-03
0.5003	0.0712	0.0000	-1.3068E-02	-1.1000E-01	-1.2231E-01	-1.1252E-02	-1.6521E-02	-1.2476E-02	-7.8672E-03
0.5003	0.0717	0.0000E 01	-4.5503E-02	-5.8194E-02	-4.7049E-02	-3.4734E-02	-2.4955E-02	-1.7319E-02	-1.1117E-02

START OF SUPERSONIC CALCULATION

SUPERSONIC CALCULATION STARTS AT X/L = 0.54232E 00

X/L	P30DY/L	THETA(DEG)	CP(X/CY)	CP(Y/D)	1.001CP(Y/D)	2.001CP(Y/D)	3.001CP(Y/D)	4.001CP(Y/D)	5.001CP(Y/D)	7.001
0.5503	0.0662	0.0000	-1.7670E-03	-9.7047E-02	-1.7818E-01	1.0000E 00	-1.4534E-02	-1.1435E-02	-2.1591E-02	
0.5503	0.0627	0.0000E 01	4.9924E-02	-2.1245E-01	-1.1073E-02	-3.8001E-02	-4.3153E-02	-2.8077E-02	-3.3316E-02	
0.6003	0.0767	0.0000	1.6845E-01	2.7114E-01	-2.4000E-01	-3.1069E-01	-1.1037E-01	-4.3937E-02	-5.5643E-02	
0.6003	0.0636	0.0000E 01	5.2130E-01	5.2479E-01	5.4772E-01	-1.5577E-02	-1.4471E-02	-2.7133E-02	-2.7110E-02	
0.6503	0.0738	0.0000	-1.5205E-01	-1.0202E-01	5.4140E-02	-2.1544E-01	-1.4045E-02	-7.4065E-02	-6.4270E-02	
0.6503	0.0626	0.0000E 01	-1.6550E-01	-1.0851E-01	-8.0352E-02	-6.9336E-02	-6.2852E-02	-5.7995E-02	-5.3849E-02	
0.7003	0.0726	0.0000	-4.7124E-01	-3.9774E-01	-1.4115E-01	9.4802E-02	1.835CE-02	-2.3764E-02	-3.8054E-02	
0.7003	0.0622	0.0000E 01	-4.9149E-01	-3.1079E-01	-2.0443E-01	-1.5415E-01	-1.2397E-01	-1.0524E-01	-9.2879E-02	
0.7503	0.0647	0.0000	-5.4607E-02	-1.4354E-02	-8.5079E-02	-8.5253E-02	-9.2471E-02	-8.0284E-02	-7.4459E-02	
0.7503	0.0616	0.0000E 01	-1.2134E-01	-9.9409E-02	-9.0414E-02	-8.5469E-02	-8.2870E-02	-8.0513E-02	-7.8654E-02	
0.8003	0.0554	0.0000	-5.9736E-02	-7.4748E-02	-7.5031E-02	-8.0760E-02	-7.1841E-02	-6.2637E-02	-6.3270E-02	
0.8003	0.0185	0.0000E 01	-5.8217E-02	-8.2044E-02	-8.1064E-02	-8.1674E-02	-8.2357E-02	-8.2968E-02	-8.3501E-02	
0.8503	0.0441	0.0000	-2.9815E-03	-4.2523E-02	-5.8121E-02	-6.6209E-02	-7.1753E-02	-7.6076E-02	-7.9582E-02	
0.8503	0.0147	0.0000E 01	-5.5352E-02	-5.0620E-02	-6.0200E-02	-6.7134E-02	-7.2317E-02	-7.6414E-02	-7.9755E-02	

DRAW COEFFICIENT = 0.54817E-01

(b) Output.

Figure 12.- Concluded.

NATIONAL AERONAUTICS AND SPACE ADMINISTRATION  
WASHINGTON, D.C. 20546

OFFICIAL BUSINESS  
PENALTY FOR PRIVATE USE \$300

FIRST CLASS MAIL

POSTAGE AND FEES PAID  
NATIONAL AERONAUTICS AND  
SPACE ADMINISTRATION  
451



POSTMASTER: If Undeliverable (Section 1099, Postal Manual) Do Not Return

*"The aeronautical and space activities of the United States shall be conducted so as to contribute . . . to the expansion of human knowledge of phenomena in the atmosphere and space. The Administration shall provide for the widest practicable and appropriate dissemination of information concerning its activities and the results thereof."*

—NATIONAL AERONAUTICS AND SPACE ACT OF 1958

## NASA SCIENTIFIC AND TECHNICAL PUBLICATIONS

**TECHNICAL REPORTS:** Scientific and technical information considered important, complete, and a lasting contribution to existing knowledge.

**TECHNICAL NOTES:** Information less broad in scope but nevertheless of importance as a contribution to existing knowledge.

**TECHNICAL MEMORANDUMS:** Information receiving limited distribution because of preliminary data, security classification, or other reasons. Also includes conference proceedings with either limited or unlimited distribution.

**CONTRACTOR REPORTS:** Scientific and technical information generated under a NASA contract or grant and considered an important contribution to existing knowledge.

**TECHNICAL TRANSLATIONS:** Information published in a foreign language considered to merit NASA distribution in English.

**SPECIAL PUBLICATIONS:** Information derived from or of value to NASA activities. Publications include final reports of major projects, monographs, data compilations, handbooks, sourcebooks, and special bibliographies.

**TECHNOLOGY UTILIZATION PUBLICATIONS:** Information on technology used by NASA that may be of particular interest in commercial and other non-aerospace applications. Publications include Tech Briefs, Technology Utilization Reports and Technology Surveys.

*Details on the availability of these publications may be obtained from:*

**SCIENTIFIC AND TECHNICAL INFORMATION OFFICE**

**NATIONAL AERONAUTICS AND SPACE ADMINISTRATION**

Washington, D.C. 20546